12-2016

# Formation of Bioactive-Carrier Hollow Solid Lipid Micro- and Nanoparticles

Junsi Yang
*University of Nebraska-Lincoln*, junsiyang@huskers.unl.edu

# FORMATION OF BIOACTIVE-CARRIER HOLLOW SOLID LIPID MICRO- AND NANOPARTICLES

by

Junsi Yang

A THESIS

Presented to the Faculty of

The Graduate College at the University of Nebraska

In Partial Fulfillment of Requirements

For the Degree of Master of Science

Major: Food Science and Technology

Under the Supervision of Professor Ozan N. Ciftci

Lincoln, Nebraska

December, 2016

# FORMATION OF BIOACTIVE-CARRIER HOLLOW SOLID LIPID MICRO- AND NANOPARTICLES

Junsi Yang, M.S.

University of Nebraska, 2016

Advisor: Ozan N. Ciftci

In recent years, bioactive lipids (e.g., carotenoids, phytosterols, and tocopherols) have attracted a lot of interest to develop health and wellness promoting foods and beverages. However, bioactive lipids are water-insoluble and degrade easily during processing and storage, making their addition into foods and beverages challenging.

The main objective of this thesis was to develop a novel green process to form bioactive lipid-carrier hollow solid lipid micro- and nanoparticles using supercritical carbon dioxide (SC-$CO_2$). Specific objectives were to develop hollow solid lipid micro- and nanoparticles using SC-$CO_2$ technology, and to load the hollow solid lipid micro- and nanoparticles with essential oil to develop food grade free-flowing powder antibacterial. Hollow solid lipid micro- and nanoparticles were formed from fully hydrogenated soybean oil (FHSO) using a novel process based on atomization of $CO_2$-expaneded lipid. Hollow spheres ($d_{50\%}$= 278 nm) were obtained using 50 μm nozzle diameter and 200 bar expansion pressure. Shell thickness of the particles decreased with increasing pressure and nozzle diameter. Polymorphism of the particles changed from β to α by decreasing the nozzle diameter. Melting point of FHSO decreased from 69 °C to 57 °C above 120 bar in $CO_2$, and onset melting temperature of the particles was 50 °C due to nanosize.

Peppermint essential oil was successfully loaded into the hollow particles using the same process to develop food grade antibacterials. The highest loading efficiency of 47.5% was achieved at 50% initial essential oil concentration at 50 μm nozzle diameter and 200 bar expansion pressure. The release of the loaded essential oil depended on initial essential oil concentration, which was affected by the physical strength of the solid lipid shell. Essential oil-loaded particles obtained at 50% initial essential oil concentration caused 3 log decrease in growth of *Pseudomonas fluorescens* compared to 2 log decrease with free essential oil.

Hollow solid lipid micro- and nanoparticles are promising bioactive-carriers with high loading capacity. Solid lipid shell protects the loaded bioactive from environmental conditions, and provides slow release. The free-flowing powder makes handling and storage convenient, and the simple and clean process makes the scaling up more feasible.

FOR MY PARENTS, AND LUQI

# ACKNOWLEDGMENTS

I would like to sincerely express my gratitude to my advisor, Dr. Ozan N. Ciftci, for his support, encouragement, guidance and patience throughout my M.S. program. Without him, I would never have completed my research projects, and most importantly, gained knowledge and critical thinking, as well as experienced and learned to be more mature as a graduate student. He is not only my advisor, but also my valuable friend. I would also thank Dr. Randy Wehling and Dr. George Cavender as my committee members for their helpful suggestions and support on my research and study. I appreciate that I have had the opportunity to get to know both of them.

I would like to thank our collaborator, Dr. Bob Hutkins, for his help, guidance, and suggestions on the microbiology part in my research. I would also like to thank his graduate student, Car Reen Kok, for her teaching and assistance when I conducted the specific experiments. I appreciate their efforts and treasure the experience working with them.

I would like to thank all my laboratory colleagues, Henok Belayneh, Ali Ubeyitogullari, Lisbeth Vallecilla Yepez, Josh Gudeman, Steven Kaiser, and Liyang Xie for their all-the-time support, collaboration, many helps on experiments and data analysis, and friendship. Thank them, my lab mates who helped my projects done giving their valuable time and effort.

I would like to express my thanks to UNL Office of Research and Economic Development for financial support, and ConAgra Foods for instrument support and providing lipid samples.

I gratefully appreciate the care, support and love from my family and friends throughout my M.S. studies at University of Nebraska-Lincoln.

## Table of Contents

## List of Figures

## Organization

This Thesis is organized as follows: introduction and thesis objectives (Chapter 1), a literature review (Chapter 2) followed by manuscripts describing two research projects (Chapter 3 and 4), and summary, conclusions, and recommendations (Chapter 5). All chapters have been formatted using guidelines for *Food Research International.* References can be found at the end of each chapter.

# CHAPTER 1. INTRODUCTION AND THESIS OBJECTIVES

## 1.1. Introduction

The growing demand for "natural" products along with the increase in diet-related illnesses such as obesity, diabetes, cardiovascular disease, inflammation, and cancer have led the food industry prioritize the development of health and wellness promoting foods using bioactive compounds. Health and wellness promoting foods refer to those that extend far beyond basic nutrition for the intended population, but could provide its unique characteristics and thus impart desirable physiological effects and associated health benefits. However, many of these bioactive compounds are lipophilic, resulting in poor water solubility that requires extra processes such as emulsification to make their addition into water possible, and have poor absorption through gastrointestinal (GI) tract and limited bioavailability (Ting, Jiang, Ho, & Huang, 2014). Moreover, many of these lipophilic bioactives are chemically sensitive; meaning they degrade easily in the presence of oxygen, light, and heat during processing and storage. Therefore, effectively including lipophilic bioactives into foods and beverages has been a major challenge for the food industry.

The food industry has been searching for solutions to enrich foods with lipophilic bioactive compounds while ensuring stability, bioavailability, and controlled release at the appropriate target, as well as confirming accepted fractional influence on the organoleptic and qualitative properties (Đorđević et al., 2015). The most common solution to incorporate lipophilic bioactives into foods has been encapsulation where the bioactive is entrapped in a matrix, which provides protection from environmental

conditions, and allows modification of the physical properties to improve solubility compatibilities between bioactive compounds and the established food matrix (Dube, Ken, Nicolazzo, & Ian, 2010; Helgason, Awad, Kristbergsson, McClements, & Weiss, 2009; Hentschel, Gramdorf, Müller, & Kurz, 2008). From a technological point of view, there are some desirable characteristics required to achieve an efficient delivery system for bioactive compounds: (1) it must consist of only food grade materials; (2) it must be economic and easy to scale up; (3) it must protect the sensitive bioactives from degradation; (4) it should possess high loading capacity and longer retention before targeted release; and (5) it should maximize the uptake of encapsulated bioactives and enhance the bioavailability of the compound (McClements, Decker, Park, & Weiss, 2009; Đorđević et al., 2015).

Lipids are promising delivery vehicles for lipophilic bioactives mainly due to their biocompatibility (Dolatabadi, Valizadeh, & Hamishehkar, 2015; Severino et al., 2012). Additionally, lipid-based carriers should be able to target delivery inside the body through either active (e.g., by incorporating antibodies) or passive (e.g., based on particle size) mechanism (Mozafari & Mortazavi, 2005; Mozafari, 2006). Moreover, several studies have reported that encapsulation of bioactive compounds through lipid-based carrier systems may improve their therapeutic potential by facilitating intracellular delivery and prolonging their retention time inside the cell (Suntres, 2011; Çağdaş, Sezer, & Bucak, 2014).

Solid lipid nanoparticles have been developed as one of the latest generation of drug carriers, and recently they have been proposed as the new generation of lipophilic bioactive-carriers for food applications. However, they have limited bioactive loading

capacity, and tend to expel the loaded bioactive during crystallization due to their solid lipid core. Moreover, current solid lipid nanoparticles are currently produced using an energy-intensive high-pressure homogenization method that generates liquid products. This thesis reports the development of free-flowing powder hollow solid lipid micro- and nanoparticles that will overcome the low loading capacity and bioactive expelling problems using a novel green process based on supercritical carbon dioxide (SC-$CO_2$) technology. The resultant powder formula makes the handling, transportation and storage convenient, while the nanosize particles make the addition of lipophilic bioactives into beverages possible, and the green process does not use hazardous or toxic solvents and limits environmental pollution.

### 1.2. Hypothesis

It was hypothesized that atomization of a $CO_2$-expanded lipid mixture through a nozzle can form hollow solid lipid micro- and nanoparticles. It was also hypothesized that atomization of a $CO_2$-expanded mixture of solid lipid and essential oil through a nozzle can form essential oil-loaded hollow solid lipid micro- and nanoparticles, and further, the solid lipid shell provides slow release of the loaded essential oil, which results in improved antibacterial activity.

### 1.3. Thesis objectives

The main objective was to develop a novel green process to form bioactive lipid-carrier hollow solid lipid micro- and nanoparticles using SC-$CO_2$. The specific objectives were to:

***1)*** Develop hollow solid lipid micro- and nanoparticles using a green process based on SC-$CO_2$ technology; and

***2)*** Load the hollow solid lipid micro- and nanoparticles with essential oil to develop food grade free-flowing powder antibacterials.

### 1.4. References


Çağdaş, M., Sezer, A. D., & Bucak, S. (2014). Liposomes as potential drug carrier systems for drug delivery. In A. D. Sezer (Ed.), *Application of nanotechnology in drug delivery* (pp. 1-50). Retrieved from http://www.intechopen.com/books.

Dolatabadi, J. E. N., Valizadeh, H., & Hamishehkar, H. (2015). Solid lipid nanoparticles as efficient drug and gene delivery systems: Recent breakthroughs. *Advanced Pharmaceutical Bulletin, 5,* 151-159.

Đorđević, V., Balanč, B., Belščak-Cvitanovič, A., Lević, S., Trifković, K., Kalušević, A., Kostić, I., Komes, D., Bugarski, B., & Nedović, V. (2015). Trends in encapsulation technologies for delivery of food bioactive compounds. *Food Engineering Reviews, 7,* 452-490.

Dube, A., Ken, N., Nicolazzo, J. A., & Ian, L. (2010). Effective use of reducing agents and nanoparticle encapsulation in stabilizing catechins in alkaline solution. *Food Chemistry, 122,* 662-667.

Helgason, T., Awad, T. S., Kristbergsson, K., McClements, D. J., & Weiss, J. (2009). Effect of surfactant surface coverage on formation of solid lipid nanoparticles (SLN). *Journal of Colloid and Interface Science, 334,* 75-81.

Hentschel, A., Gramdorf, S., Müller, R. H., & Kurz, T. (2008). β-carotene-loaded nanostructured lipid carriers. *Journal of Food Science, 73,* 1-6.

McClements, D. J., Decker, E. A., Park, Y., & Weiss, J. (2009). Structural design principles for delivery of bioactive components in nutraceuticals and functional foods. *Critical Reviews in Food Science and Nutrition, 49,* 577-606.

Mozafari, M. R. (2006). Bioactive entrapment and targeting using nanocarrier technologies: an introduction. In M. R. Mozafari (Ed.), *Nanocarrier technologies* (pp. 1-16). Netherlands: Springer.

Mozafari, M. R., & Mortazavi, S. M. (2005). *Nanoliposomes: from fundamentals to recent developments.* Oxford: Trafford.

Severino, P., Andreani, T., Macedo, A. S., Fangueiro, J. F., Santana, M. H. A., Silva, A. M., & Souto, E. B. (2012). Current state-of-art and new trends on lipid nanoparticles (SLN and NLC) for oral drug delivery. *Journal of Drug Delivery, 10,* 1-10.

Suntres, Z. (2011). Liposomal antioxidants for protection against oxidant-induced damage. *Journal of Toxicology, 2011,* 1-16.

Ting, Y., Jiang, Y., Ho, C., & Huang, Q. (2014). Common delivery systems for enhancing *in vivo* bioavailability and biological efficacy of nutraceuticals. *Journal of Functional Foods, 7,* 112-128.

# CHAPTER 2. LITERATURE REVIEW

## 2.1. Bioactive compounds

Bioactive compounds are extra nutritional constituents that typically occur in small quantities in foods (Kris-Etherton et al., 2002). They are being intensively studied to evaluate their effects on health. Clinical studies have demonstrated that intaking bioactive compounds as part of consumers' daily diet may exert tangible health benefits (Stewart & Kleihues, 2003). Moreover, increases in dietary-intake-related illnesses such as obesity, type-2 diabetes, cardiovascular disease and cancer have led the food industry prioritize the development of health and wellness promoting foods using bioactive compounds.

Bioactive lipids (e.g., carotenoids, omega-3 fatty acids, tocopherols, and phytosterols) are a group of lipophilic bioactives that are water-insoluble and widely differ in their molecular, physicochemical and physiological properties. Carotenoids have been proposed to exhibit several potential health benefits: lutein and zeaxanthin to decrease age-related macular degeneration and cataracts (Stringham & Hammond, 2005), and lycopene to decrease the risk of prostate cancer (Basu & Imrhan 2007). Omega-3 fatty acids, particularly, eicosapentaenoic acid (EPA, 20:5) and docosahexaenoic acid (DHA, 22:6) decrease the risks of cardiovascular disease, fight diseases affected by immune response disorders, and mental disorders, as well as benefit infant development (Fidler, Sauerwald, Pohl, Demmelmair, & Koletzko, 2000; Makrides & Gibson, 2000; Hibbeln, Nieminen, Blasbalg, Riggs, & Lands, 2006; Jensen, 2006). Tocopherols have

the potential to decrease the risks of coronary heart disease, cancer, and urinary tract disease (McClements, Decker, & Weiss, 2007). Phytosterols could decrease the risk of coronary heart disease by reducing total and low-density lipoprotein cholesterol in humans through inhibiting the absorption of dietary cholesterol (Wong, 2001; Ostlund, 2004).

However, there are some problems associated with the efficient utilization of these lipophilic bioactives by both consumers and food industry: 1) they may not be possible to intake with diet properly; 2) they are tightly bound to the food matrix and water-insoluble, resulting poor bioavailability; and 3) they are chemically unstable, meaning they degrade easily during processing and storage. Therefore, effectively incorporating lipophilic bioactives into foods and beverages has been a major challenge.

To enrich foods with lipophilic bioactive compounds while ensuring stability, bioavailability, controlled release, and accepted organoleptic and qualitative properties, the food industry came up with a common solution: to entrap lipophilic bioactives in a matrix as delivery system (Đorđević et al., 2015). The matrix provides the protection of the encapsulated bioactive from environmental conditions such as temperature, oxygen, pH, and allows modification of the physical properties to improve solubility compatibilities between bioactive compounds and the established food matrix (Dube et al., 2010; Helgason et al., 2009; Hentschel et al., 2008). With a suitable delivery system, the *in vivo* fate of the bioactive compound is no longer determined by only its properties but by those of the delivery system (McClements et al., 2007).

Lipids have attracted much attention as delivery vehicles for lipophilic bioactives because they are digestible, often facilitate the absorption of bioactive in the small

intestine, could entrap material with different solubilities and can be produced using food grade lipids on an industrial scale (Dolatabadi et al., 2015; Severino et al., 2012; Anandharamakrishnan, 2013; Mozafari & Mortazavi, 2005).

### 2.2. Lipid-based delivery systems

Recent developments of lipid-based delivery systems for efficiently incorporating various lipophilic bioactives include emulsions, liposomes, solid lipid nanoparticles (SLN), and nanostructured lipid carriers (NLC). In this section, these lipid-based delivery systems are described in terms of their production methods, applications and features, and advantages and limitations.

#### 2.2.1. Emulsions

Emulsions are colloidal delivery systems, basically consist of oil phase, water phase and surfactant, and can be classified based on particle size into macroemulsions (~ μm), microemulsions (5-100 nm) and nanoemulsions (20-300 nm). Macroemulsions and nanoemulsions are kinetically stable but thermodynamically unstable, tend to break down during storage. Nanoemulsions are more resistant to oxidation than microemulsions, which are thermodynamically stable, low viscous, easy to prepare but always require higher concentrations of a surfactant typically with a co-surfactant, therefore, microemulsions has not been established certain food grade systems for delivery these lipophilic bioactives (Đorđević et al., 2015).

#### 2.2.1.1. Production methods

Emulsions are typically produced using mechanical (high-energy) or non-mechanical method. Mechanical (high-energy) methods include high-pressure homogenization (HPH), microfluidization, and ultrasonication. In addition, solvent diffusion method is one example of non-mechanical techniques to produce nanoemulsions (Tadros, Izquierdo, Esquena, & Solans, 2004; Unger et al., 2004).

High-pressure homogenizers push the coarse dispersion of the mixture with high pressure in the range of 35-345 bar through a narrow gap (a few microns). Due to the acceleration of fluid over a very short distance with very high velocity (over 1000 km/h), very high shear stress and cavitation forces disrupt the particles down to the submicron range (Fathi, Mozafari, & Mohebbi, 2012). A recent example of the technology was when Yuan, Gao, Mao, and Zhao (2008) formed β-carotene O/W nanoemulsions. They found that the chemical stability of the nanoemulsions decreased with increasing temperature but increased with pressure (up to 100 bar) and cycle numbers (up to 3). Moreover, β-carotene showed great stability with less loss in the first four weeks of storage at room temperature.

In microfluidization, a high-pressure (up to 1380 bar) to force the liquid dispersions through an interaction chamber in which microchannels are placed, and very fine particles in submicron range are produced. The emulsification mechanism is based on shear and cavitation forces. The operating pressure and number of passes play important roles in particle size of the obtained nanoemulsion (Constantinides, Chaubal, & Shorr, 2008; Maa & Hsu, 1999).

Emulsification by the ultrasonication method is attributed to bubble cavitation. The ultrasonic waves result in sequential formation, growth and collapse of microscopic vapor bubbles in the liquid. Consequently, the collapse of these cavities provides sufficient energy to increase surface area of droplets (Patil & Pandit, 2007).

Comparing these three high-energy mechanical methods, the use of HPH and ultrasonication may cause degradation or denaturation of the sensitive molecules being encapsulated, whereas the microfluidization was found to be more effective due to the smaller droplet diameters and less droplet diameter growth during storage (Fathi et al., 2012).

Nanoemulsions can also be obtained using solvent diffusion method (Tadros et al., 2004; Unger et al., 2004). Typically, the oil phase consists of oil carrier, lipophilic surfactant and hydrophilic organic solvent, and the aqueous phase consists of hydrophilic surfactant and water. Fine O/W emulsion can be produced by passing through a high-pressure homogenizer, then the solvent is removed by evaporation (Jaiswal, Gupta, & Kreuter, 2004; Mainardes & Evangelista, 2005). However, one limitation of this technique is the use of large amount of organic solvent; therefore, high energy and expensive equipment is required to remove organic solvent before completion of final product. In general, application of the low energy methods is limited in food sectors due to the need of organic solvent in those methods (Fathi et al., 2012).

#### 2.2.1.2. Applications and features

Emulsions have been used to encapsulate and deliver various lipophilic bioactives. For example, omega-3 fatty acids have been entrapped into food products

such as milk, yogurt, ice cream, and meat patties to protect omega-3 from oxidation (McClements & Decker, 2000; Chee et al., 2005, 2007; Sharma, 2005; Lee, Faustman, Djordjevic, Faraji, & Decker, 2006; Belhaj, Arab-Tehrany, & Linder, 2010). Application of emulsions as delivery systems of functional components, including lutein (Losso, Khachatryan, Ogawa, Godber, & Shih, 2005), lycopene (Ribeiro et al., 2003; 2006), β-carotene (Santipanichwong & Suphantharika, 2007; Yuan et al., 2008), curcumin (Wang et al., 2008), α-tocopherol (Cheong, Tan, Man, & Misran, 2008), and phytosterol (Leong et al., 2011) have been reported. For those bioactives which are crystalline at ambient temperatures, they are used either at levels below their saturation concentration in the carrier oil, or the lipid phase is melted before homogenization, thus decreasing the problems associated with emulsion formation and/or stability (McClements et al., 2007).

#### 2.2.1.3. Advantages and limitations

Emulsions are currently being used as delivery systems in various industries, including pharmaceuticals, cosmetics, and foods. They can provide a number of potential advantages to carry and deliver nutraceutical and functional food components, for example, it is possible to incorporate active ingredients that are water-soluble, water-insoluble, and amphiphilic at the same time within the same delivery system (McClements et al., 2007, 2009; McClements, 2005). Additionally, the heterogeneous structure offers an opportunity to develop novel techniques for controlling the chemical stability of encapsulated bioactives (Coupland & McClements, 1996; McClements & Decker, 2000).

Nevertheless, several limitations have restricted the prevalence of emulsions as delivery system, and therefore, more sophisticated structured systems are needed. The major problem is that emulsions are vulnerable to degradation when exposed to environmental conditions change, such as temperature and pH. In addition, emulsions are not physically stable in the liquid state, causing phase separation during storage. Moreover, rapid release of entrapped functional components due to the smaller size and the liquid state of the carrier, low stability in gastric condition, and long-term instability during storage are the major disadvantages (Benichou, Aserin, & Garti, 2002; Dickinson, 2003; Drusch, 2007; McClements et al., 2009; Fathi et al., 2012). Furthermore, emulsions are liquid products. In order to obtain a dry formulation, they must be dried to make handling, transportation, and utilization in some applications more convenient (Soottitantawat, Yoshii, Furuta, Ohkawara, & Linko, 2003; Desai & Park, 2005; Klinkesorn, Sophanodora, Chinachoti, McClements, & Decker, 2005; Vega & Roos, 2006).

### 2.2.2. Liposomes

Liposomes are microscopic vesicles composed of a membrane, usually phospholipid bilayers, surrounding an aqueous medium. Liposomes have been widely used for targeted drug delivery, but increasing interest for the delivery of the functional compounds has emerged in the recent decade. The mechanism of liposome formation is based on the unfavorable interactions between amphiphilic compounds (primarily phospholipids) and water molecules (Goyal et al., 2005; Jesorka & Orwar, 2008). Due to the special structure consisting of both lipid phase and water phase, liposomes can be

utilized to encapsulate water-soluble, lipid-soluble, and amphiphilic materials. Furthermore, liposomes are efficient in entrapping and stabilizing bioactives against environmental conditions and providing better protection (Mozafari & Khosravi-Darani, 2007). Similar to emulsions, liposome formation is based on the interaction of hydrophilic and lipophilic interactions between phases of lipid/lipid and lipid/water (Goyal et al., 2005).

#### 2.2.2.1. Production methods

Mechanical and non-mechanical methods have been developed to produce liposomes. Mechanical techniques include HPH, microfluidization, sonication, and extrusion. Non-mechanical techniques include reversed-phase evaporation and lipid hydration followed by vortex or manual stirring (Lasch, Weissing, & Brandl, 2003; Schroeder, Kost, & Barenholz, 2009). It has been shown that ultrasonic cavitation induced mechanical shear is an ideal method as it results in having particle size distribution in a narrower range than other methods (Maulucci et al., 2005; Moran et al., 2006).

#### 2.2.2.2. Applications and features

In the recent decade, liposomes have been investigated as delivery systems for enzymes (Jahadi et al., 2012, Smith, Jaime-Fonseca, Grover, & Bakalis, 2010), proteins (Sun-Waterhouse & Wadhwa, 2013), vitamins (Gonnet, Lethuaut, & Boury, 2010), flavors (Nedovic, Kalusevic, Manojlović, Petrovic, & Bugarski, 2013; Yoshida, Yokota, Foglio, Rodrigues, & Pinho, 2010), minerals (Evens et al., 2012), antioxidants (Isailović

et al., 2013; Kerdudo, Dingas, Fernandez, & Faure, 2014; Rashidinejad, Birch, Sun-Waterhouse, & Everett, 2014), and antimicrobials (Boualem, Subirade, Desjardins, & Saucier, 2013; Malheiros, Sant'Anna, Barbosa, Brandelli, & Franco, 2012). Liposomes have been also used to entrap polyphenolic compounds (Kerdudo et al., 2014; Pravilović, Radunović, Bošković-Vragolović, Bugarski, & Pjanović, 2014). Encapsulation of material in liposomes could help protect against environmental changes (Augustin & Hemar, 2009).

#### 2.2.2.3. Advantages and limitations

Large-scale production and delivery of both water-soluble and lipid-soluble ingredients are the predominate perks. Nevertheless, rapid release of the encapsulated bioactive due to the smaller size and the liquid state of the carrier, low stability in gastric condition, and long-term instability during storage are the major disadvantages associated with liposomes (Fathi et al., 2012). Moreover, liquid state, high expenses and time-consuming manufacturing processes limit the application of liposomes in food systems (Đorđević et al., 2015).

### 2.2.3. Solid lipid nanoparticles

SLN have attracted increasing attention as delivery systems of drugs and lipophilic food bioactives in the recent decade, but their potential for food applications has not been fully explored yet (Awad et al., 2008; Gallarate, Trotta, Battaglia, & Chirio, 2009; Taylor, Gaysinsky, Davidson, Bruce, & Weiss, 2007; Varshosaz et al., 2010). SLN are particles in the submicron range and composed of solid lipid, dispersed in water or

aqueous surfactant solution. The solid lipid matrixes are typically mono-, di- or triacylglycerol, with the lipophilic bioactives being a part of the lipid matrix (Jenning, Thünemann, & Gohla, 2000). Different from emulsions, SLN are submicron-sized particles in which the liquid oil is replaced by solid fat at room temperature or at body temperature, which could provide better protection of encapsulated material and achieve controlled release due to lower mobility in solid fat rather than in liquid oil (Pardeshi et al., 2012).

#### 2.2.3.1. Production methods

##### 2.2.3.1.1. High-pressure homogenization

HPH is a basic technique which enables the large-scale production of SLN. The lipid contents vary depending on different applications using HPH, typically are in the range of 5-10% but could go higher (up to 40%) forming lipid nanodispersions (Anandharamakrishnan, 2013).

In hot HPH method, firstly the solid lipid is melted at 5-10 °C above its melting point, then bioactive is dispersed in the lipid phase along with an aqueous surfactant under the same temperature. After premixing and forming a coarse free-emulsion, the mixture is passed through a high-pressure homogenizer above the lipid melting point and result in a hot O/W nanoemulsion. Cooling down to the room temperature leads to the solidification of the obtained nanoemulsion and the formation of SLN (Fathi et al., 2012; Anandharamakrishnan, 2013; Shin, Kim, & Park, 2015). Lyophilization could also be applied to initiate recrystallization of the lipid (Müller, Mäder, & Gohla, 2000).

The advantages of hot HPH technique include: 1) easy to scale up; 2) short production time; and 3) controlled smaller particle size with narrow size distribution. However, hot HPH has some limitations. Due to the loss of the lipophilic bioactive to the water phase, hot HPH may not efficiently incorporate these compounds into the solid matrix. Secondly, for those heat sensitive functional compounds such as enzyme and fish oil, hot HPH cannot be applied to obtain ideal particles. Finally, since most surfactant have low cloud point, which is the temperature above which an aqueous solution of a water-soluble surfactant becomes turbid, the presence of high temperatures may reduce the emulsifying capability and impact particle stability (Fathi et al., 2012).

Cold HPH has been proposed to address these problems. Similar to the first step in hot HPH, the bioactive is incorporated into a melted lipid. Then, the mixture is cooled down either in liquid nitrogen or dry ice, and grounded by a powder mill with particle size of 50-100 μm. The grounded powder are dispersed in an aqueous cold surfactant solution at room temperature and premix together. Finally, the lipid suspension is homogenized at or below room temperature to produce SLN (Pardeshi et al., 2012). For this cold HPH technique, special care must be employed since the temperature may rise during milling and homogenization (10-20 °C per cycle) (Fathi et al., 2012; Weiss et al., 2008). Cold HPH enables processing heat sensitive or water-soluble food compounds. Additionally, crystallization process is controllable and desired crystal structure could be successfully formed by rapid cooling procedure. However, a major drawback of this cold HPH technique could be larger particle size and broader size distribution, and therefore do not possess a uniform dissolution when masticated and digested (Weiss et al., 2008).

An example of the technology was performed by Schubert and Müller-Goymann (2005), who incorporated bovine serum albumin (BSA) in solid hydrogenated palm oil nanoparticles using HPH technique. They found that the addition of lecithin up to 30% (w/w) in the lipid posed a concentration-dependent decrease of particle size to 100 nm. In addition, Sun et al. (2013) developed curcumin-loaded SLN using hot HPH method with liquid lipid propylene glycol monocaprylate. They obtained curcumin-loaded SLN which had a mean particle size of 153 nm and achieved 90% encapsulation efficiency. They also reported that the SLN delivery could improve the dispersity and chemical stability of curcumin, elongate their antitumor activity and cellular uptake, and further enhance the bioavailability.

**2.2.3.1.2. Microemulsion formation**

Microemulsion formation is another method to produce SLN. This method is based on the dilution of a microemulsion in water that leads to precipitation of the lipid phase, thus forming particles (Gasco, 1997). Typically, microemulsions are produced by stirring an optically transparent lipid mixture at 65-70 °C which is normally composed of high melting fatty acid (stearic acid), emulsifier and water. Then, the hot microemulsion is dispersed in cold water under stirring, with the volume ratio of the hot microemulsion to cold water usually are in the range of 1:25 to 1:50 (Flanagan & Singh, 2006). Finally, the excess water is removed by either by ultrafiltration or lyophilization to condense the particle concentration (Weiss et al., 2008). Tiyaboonchai, Tungpradit, and Plianbangchang (2007) produced curcuminoid-loaded SLN at 75 °C. Under optimum processing conditions, lyophilized curcuminoid-loaded SLN had spherical shape with a

mean particle size of 450 nm and encapsulation efficiency of 70%, and *in vitro* release was prolonged for up to 12 h. Moreover, lyophilized curcuminoid-loaded SLN showed good physical and chemical stability over the 6-month storage period. Low mechanical energy input and theoretical stability are the advantages of microemulsions method; however, extremely sensitive to changes in the processing parameters, labor intensive work, and low nanoparticle concentrations are its limitations (Ekambaram, Sathali, & Priyanka, 2012).

#### 2.2.3.1.3. Ultrasonication

SLN can also be prepared by ultrasonication. For smaller particle size, a combination of high-speed homogenization and ultrasonication is required. Nayak, Tiyaboonchai, Patankar, Madhusudhan, and Souto (2010) produced curcuminoid-loaded SLN by combining high-speed homogenization and ultrasonication. The particles had spherical shape with sizes ranging between 120 and 250 nm. The encapsulation efficiency was between 80-94% and the loading capacity was between 1-3%. The advantages of this method include reduced shear stress and the need for only simple equipment (Ekambaram et al., 2012). Potential metal contamination, large particle size due to low dispersion quality, and physical instability (e.g., particle growth during storage) are the major concerns with the technique (Ekambaram et al., 2012; Üner, 2006). Moreover, lipid concentration tends to be low (<1%) and the surfactant concentration is comparatively high (Wissing, Kayser, & Müller, 2004).

#### 2.2.3.1.4. Solvent emulsification-evaporation or -diffusion

This technique is based on SLN dispersions by precipitation in O/W emulsions. During this procedure, addition of water to the organic solution with lipophilic material under mechanical agitation would result in coacervation and formation of lipid nanoparticles (Quintanar-Guerrero, Allémann, Fessi, & Doelker, 1999). Avoidance of heat is the most important advantage of this method. However, in this technique, because of the limited solubility of the lipid in organic solvents, it usually needs dilution of the suspension, therefore, the particle concentration (up to 15%) is lower than the one obtained by HPH technique. Additionally, solvent residues may pose toxicological problems (Trotta, Debernardi, & Caputo, 2003).

### 2.2.3.2. Applications and features

Three models of incorporating bioactive components into SLN have been proposed: homogeneous matrix model, bioactive-enriched shell model and bioactive-enriched core model. Production method and formulation components (lipid, lipophilic bioactive and surfactant) play important role in determining the SLN model. A homogeneous matrix will likely be formed when cold homogenization method is used and very lipophilic bioactives are incorporated using hot homogenization method. In this case, dissolution of the homogeneous matrix dictates the bioactive release. A bioactive-enriched shell model could be produced if phase separation happens during cooling of the liquid lipid to a solid. On the other hand, a bioactive-enriched core model might be formed if the bioactives solidify first and as a result, the shell would have less bioactives

when it begins solidifying. Passive diffusion governs this type of SLN model to release the loaded bioactive (Fathi et al., 2012).

To ensure the physical stability of SLN, zeta potential is commonly used to quantify surface charge (Bunjes, 2005; Lim & Kim, 2002). Charged particles possessing high zeta potential are less likely to suffer nanoparticle aggregation due to electric expulsion (Mehnert & Mader, 2001). It is also important to recognize that, after oral administration, due to the ionic strength and strong pH changes in GI tract, nanoparticles are likely to destabilize and this can lead to aggregation and size growth. However, Zimmermann and Müller (2001) demonstrated that by having SLN with larger than 8-9 mV zeta potential and in combination with steric stabilization, it is possible to produce stable SLN in GI environment. Loading capacity of SLN could be greatly affected by solubility of bioactive in melted lipid, structures of the solid lipid matrix and polymeric state of the lipid material (Fathi et al., 2012). The additions of solubilizers such as mono- and diacylglycerols could help boost bioactive solubility in lipid and therefore increase loading capacity. Crystallization of the lipid nanoparticles is different than the bulk lipid material. For bulk lipid, it tends to recrystallize in β' form and rapidly transformed to β form, whereas for lipid nanoparticles, it at least partially recrystallizes in α form (Westesen, Siekmann, & Koch, 1993). In order to produce SLN with delayed polymorphic form from α to β, changing fat type or using surfactant with hydrocarbon tails that crystallize before lipid could help preventing nanoparticle aggregation and storing at low temperatures (Awad et al., 2008; Helgason et al., 2009). To keep it physically and chemically stable, lyophilization with cryo-protective agents has been demonstrated as an effective technique (Mehnert & Mader, 2001). Generally, for the

production of SLN, relatively high melting-point lipids (melting point >70 °C) is recommended (Mehnert & Mader, 2001).

Patel and Martin-Gonzalez (2011) encapsulated ergocalciferol (vitamin $D_2$) in tripalmitin SLN stabilized by Tween 20 using hot HPH technique. The particle size of ergocalciferol-loaded SLN gradually decreased from 120 nm to 65 nm with increasing ergocalciferol content up to 20% (w/w). They also observed that the turbidity of SLN dispersions reduced noticeably with increasing ergocalciferol loading, indicating it could be useful for fortification of clear water-based drink. Qian, Decker, Xiao, and McClements (2012) have encapsulated β-carotene and studied the effect of lipid compositions on formulations. They found out that liquid lipid nanoparticles showed better stability to β-carotene than SLN, and suggested that cocoa butter and hydrogenated palm oil mixtures were too well packed and led to the expulsion of β-carotene.

#### 2.2.3.3. Advantages and limitations

SLN are delivery systems for drugs and bioactives alternative to emulsions and liposomes due to their advantages (Cavalli, Gasco, Chetoni, Burgalassi, & Saettone, 2002; Illing & Unruh, 2004; Müller et al., 1995): 1) most lipids and surfactants used in preparation have “Generally Recognized As Safe” (GRAS) status (Code of Federal Regulations, Food and Drugs, 2001); 2) stable formulations can be developed; 3) SLN production using HPH technique is highly reproducible (Gohla & Dingler, 2001; Tabatt, Sameti, Olbrich, Müller, & Lehr, 2004); 4) possibility of large-scale production (Gohla & Dingler, 2001; Tabatt et al., 2004); 5) effective protection of bioactives against chemical

degradation; and 6) more controlled release of encapsulated compounds due to the solid matrix.

Nevertheless, there are several disadvantages associated with SLN, including: 1) poor loading capacity due to solid lipid core and limited solubility of the active ingredient in the lipid phase; 2) expulsion of the loaded active ingredient after liquid-to-solid phase transition during storage; and 3) burst release which is due to the presence of active ingredient in the outer shell (Tabatt et al., 2004; Fathi et al., 2012).

### 2.2.4. Nanostructured lipid carriers

NLC are colloidal carriers featured as a solid lipid core with a mixture of both solid and liquid lipids with mean particle size falling into nanometer range (Anandharamakrishnan, 2013). NLC are considered as a modified version of SLN and the second generation of lipid nanoparticles (Müller, Radtke, & Wissing, 2002). In general, NLC possess the advantages of SLN, including low toxicity, biodegradation, protection, slow release, and elimination of organic solvents use, but also be able to overcome the limitations of SLN by creating a less ordered lipid matrix with many imperfections, which could allow for a higher loading capacity and decrease the risk of expelling of bioactives during storage (Fathi et al., 2012; Tamjidi, Shahedi, Varshosaz, & Nasirpour, 2013; Pardeshi et al., 2012). Due to the improved stability, high loading capacity and controlled release, NLC are widely used in the pharmaceutical field (Naseri, Valizadeh, & Zakeri-Milani, 2015).

There are several requirements needed for creating a suitable lipid blend for NLC (Tamjidi et al., 2013). Firstly, the solubility of the active compound in lipid matrix is

essential, as this influences loading capacity and the subsequent usefulness of the NLC (Jaspart, Piel, Delattre, & Evrard, 2005; Kasongo, Pardeike, Müller, & Walker, 2011). Secondly, the liquid and solid lipids should be spatially incompatible, meaning the oil molecules should not be participated in the solid crystalline matrix of solid lipid and the crystals of solid lipid should not be dissolved in the liquid lipid. Moreover, it is a prerequisite that the liquid and solid lipids used to form NLC are miscible at specific concentration; this means that macroscopic phase separation should not be occurred at a temperature below melting point of fat (Kasongo et al., 2011; Radtke & Müller, 2001). Thirdly, stability of the lipid phase should be confirmed, particularly as it relates to oxidation and lipolysis stability (Tamjidi et al., 2013). Fourth, the lipid phase should be biodegradable and able to easily produce NLC in the nanometer range, normally with a low viscosity or interfacial tension (Walstra, 2003). Finally, accepted toxicological profile of the lipid should be met to produce NLC (Tamjidi et al., 2013). Typically, lipids used to prepare NLC are mono-, di- and triacylglycerols, fatty acids and waxes (Tamjidi et al., 2013).

#### 2.2.4.1. Production methods

Compared to emulsions and liposomes, NLC can retain the encapsulated compound better and also prevent particles from coalescing by solid lipid matrix (Üner, 2006). As a matter of fact, the addition of a certain nanostructure could enhance the encapsulation load of bioactives and limit the expulsion phenomenon (Chen, Han, Cai, & Tang, 2010; Müller et al., 2002). NLC can be produced by simply mixing solid and liquid lipids, together with surfactants, leading to a less perfect solid with imperfections or

amorphous type (Üner, 2006; Shin et al., 2015; Anandharamakrishnan, 2013). Similar to SLN, NLC can be manufactured through HPH (either cold or hot), microemulsion formation, ultrasonication, high shear homogenization, or/and solvent emulsification-evaporation methods (Üner, 2006; Gasco, 1993; Trotta et al., 2003). It is also reported that the particle size is smaller compared to SLN (Fang, Fang, Liu, & Su, 2008).

#### 2.2.4.2. Applications and features

NLC are an advanced delivery system and appeared to possess the advantages associated with emulsions, liposomes and SLN, but at the same time, overcome some of the problems of SLN such as limited loading capacity and expulsion during storage (Westesen & Siekmann, 1997; Pardeshi et al., 2012). Lacatusu, Badea, Ovidiu, Bojin, and Meghea (2012) loaded lutein in NLC with omega-3 fatty acids as a liquid oil and carnauba wax and glycerol stearate as solid lipid. They reported that the particle size was below 200 nm and the loading efficiency reached up to 89%. In addition, a high blocking effect and oxygen scavenging of 98% was also demonstrated. Curcumin-loaded NLC were also studied for intragastric administration (Fang et al., 2012). Their results proposed that NLC are promising delivery system for improving solubility of water-insoluble bioactives such as curcumin. Additionally, β-carotene was successfully entrapped in NLC by HPH technique with Tween 80 as emulsifier (Hentschel et al., 2008). The mean diameter was 144 to 249 nm, and the particle size decreased as the emulsifier concentration increased. During the storage period, the mean particle size was around 0.3 μm of 9 weeks at 20 °C and 30 weeks at 4-8 °C. Furthermore, the addition of tocopherol improved the stability of β-carotene-loaded NLC.

### 2.2.4.3. Advantages and limitations

Compared to conventional carriers, NLC have some distinct advantages. Firstly, they can increase the solubility of the bioactive materials since the solubility of lipophilic bioactive compounds tends to be higher in liquid oils than in solid fats (Tamjidi et al., 2013). Secondly, NLC have the ability to enhance storage stability due to reduced mobility in the solid phase and could improve permeability and bioavailability of the bioactive materials (Tamjidi et al., 2013; Pardeshi et al., 2012). Finally, with the addition of liquid oil in the solid fat, NLC could increase payload capacity compared to SLN (Jenning et al., 2000; Westesen & Siekmann, 1997).

The major disadvantage associated with NLC is the occurrence of partial coalescence. This phenomenon would happen if lipid particles are partly crystalline, then, a crystal from one particle can penetrate into the liquid oil portion during a contact or collision which causes the particles to stick together, and may lead to a decrease in NLC stability to aggregation or gelation (Tamjidi et al., 2013). Various factors that could influence partial coalescence have been discussed elsewhere (McClements, 2005; Walstra, 2003). Based on those discussions, the types of lipids and emulsifiers, the ratio of solid to liquid lipid and the particle size pose significant influences on partial coalescence. If nanoparticles have amorphous structure with no presence of any crystal, then we would not expect any partial coalescence in NLC to occur (Tamjidi et al., 2013).

## 2.3. Supercritical fluid (SCF) technology

### 2.3.1. Introduction

A supercritical fluid (SCF) is defined as a fluid for which both pressure and temperature are above its critical point (Fig. 2.1), namely $P_c$ and $T_c$, respectively (Subramaniam, Rajewski, & Snavely, 1997; Nalawade, Picchioni, & Janssen, 2006). When pressure and temperature are very close to the critical point, the fluid reveals unique physical properties that are significantly different from its normal behavior, in which it is neither liquid nor gas but possesses the properties of both (Montes, Gordillo, Pereyra, & Martinez de la Ossa, 2011). SCF shows a density similar to a liquid, and appreciable for solvent power, while the gas-like viscosity and diffusivity facilitate increased rates of mass transfer (Pasquali, Bettini, & Giordano, 2008). SCF is dense but highly compressible, in particular near the supercritical region. The density of SCF can be easily tuned by small changes in pressure within the critical region, and consequently the solvent power can be affected (Subramaniam et al., 1997; Nalawade et al., 2006; Montes et al., 2011; Brunner, 2005). The special combination of gas-like viscosity, diffusivity, and compressibility and liquid-like density of a SCF makes it excellent for various applications such as solvents, antisolvent, or solute in polymer and lipid processing: e.g. polymer modification, polymer blending, polymer synthesis, lipid extraction and particle formation (Nalawade et al., 2006; Cooper, 2000; Tomasko et al., 2003; Temelli, 2009; Fahim et al., 2014; Knez & Weidner, 2003; Yeo & Kiran, 2005). Moreover, elimination of organic solvents to improve product quality makes SCF another wonderful candidate for different roles in various applications (Nalawade et al., 2006).

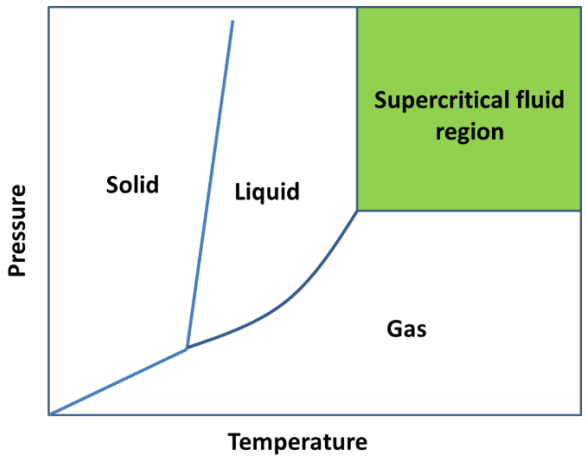


**Figure 2.1.** Phase diagram of supercritical fluids.

When processing with SCF, the driving potential for heat and mass transfer is dictated by the difference from the equilibrium state (Brunner, 2005). The equilibrium state provides information on: 1) the solvent power (capacity) of a supercritical solvent; 2) the amount of solvent and the equilibrium composition of these phases; 3) the selectivity of a solvent; and 4) the dependence of solvent properties on conditions of state (p, T) (Brunner, 2005). If capacity and selectivity are known for a solvent, then a good guess could be made about whether a separation problem can be solved with SCF (Brunner, 2005). The solubility of a low volatile substance in SCF (solvent) increases at constant pressure up to a temperature slightly below the $T_c$ of the solvent; however, further increase in temperature at "low" pressures (below 100 bar) lead to a decrease in solubility in SCF. The same dependence of the solubility and temperature higher than $T_c$ can also be observed. At "low" pressures, solubility decreases with increasing temperature since density of SCF decreases rapidly with increasing temperature at near-

critical pressures. Nevertheless, at “high” pressures, density changes with temperature are far more moderate, and solubility increases with temperature (Brunner, 2005).

### 2.3.2. Supercritical carbon dioxide (SC-$CO_2$) technology

Among many substances that can be used as SCF, carbon dioxide ($CO_2$) has been most commonly and widely used in pharmaceutical, chemical and food industries (Subramaniam et al., 1997). It is a clean and versatile solvent and a promising alternative to noxious and toxic organic solvents. Since $CO_2$ has a relatively lower critical temperature and pressure (31.1 °C, 74 bar), it can achieve a more gentle processing condition, avoiding the degradation of heat liable compounds. In addition, $CO_2$ is a generally regarded as safe (GRAS) substance, is chemically inert, non-flammable, inexpensive, and environmental friendly (Ciftci & Temelli, 2014; Vemavarapu, Mollan, Lodaya, & Needham, 2005; Nalawade et al., 2006). Moreover, many polymers and lipids possess melting point depression and volumetric expansion in the presence of $CO_2$, allowing for relatively low temperature processing (Ciftci & Temelli, 2014; Nalawade et al., 2006). Pressurized $CO_2$ has a substantial impact on the properties of components with which they are mixed, including increasing solubility, affecting phase behavior, drastically decreasing the viscosity of condensed phases and surface tension of liquid which enables mixtures to move freely in small pores and tiny structures (Brunner, 2010).

The solvent power of SC-$CO_2$ can be summarized by a few rules (Brunner, 2005; Del Valle & Aguilera, 1988): 1) it dissolves non-polar or slightly polar compounds; 2) the solvent power for low molecular weight compounds is high and decreases with increasing molecular weight; 3) SC-$CO_2$ has high affinity with oxygenated organic

compounds of medium molecular weight; 4) free fatty acids and their glycerides exhibit low solubility; 5) pigments are even less soluble; 6) water has a low solubility (<0.5%, w/w) at temperatures below 100 °C; 7) proteins, polysaccharides, sugars and mineral salts are insoluble; and 8) SC-$CO_2$ is capable of separating compounds that are less volatile, have a higher molecular weight and/or more polar as pressure increases.

SC-$CO_2$ is a good solvent for many non-polar low molecular weight compounds and a few polymers; but it is a generally very poor solvent for high molecular weight polymers under controllable conditions (Nalawade et al., 2006).

### 2.4. Particle formation using supercritical fluid (SCF) technology

SCF, especially $CO_2$, and their potential use for process development have gained the industries' interest in the recent decades. SCF have been adopted as a green and effective alternative to organic solvents to produce particles (Yeo & Kiran, 2005). Some extraction processes such as decaffeination and extraction of bioactives have already become commercialized. Particle formation may likely be the next commercialized application using SCF technology (Yeo & Kiran, 2005).

The unique properties, such as gas-like diffusivities, liquid-like densities, continuously adjustable solvent power/selectivity and the easiness of complete removal at the end of the process, make SCF particularly more attractive than conventional methods including freeze drying, spray-cooling, spray-drying, air micronization, coacervation, recrystallization from the liquid solution and sublimation, due to it is lack of contamination of the extracts, residues and environment (Fahim et al., 2014; Thereza, Gomes, Santos, & Meireles, 2012; Reverchon & Adami, 2006; Hakuta, Hayashi, & Arai,

2003). In some precipitation methods, organic solvent is completely eliminated, while in others organic solvent is used, but in greatly reduced amounts, which can be removed thoroughly due to their high solubility in SCF, therefore avoiding potential of product contamination (Martín & Cocero, 2008; Hakuta et al., 2003). Several techniques use the sudden changes of properties by adjusting pressure and temperature to achieve homogeneous supersaturation, leading to fine powder production with a narrow particle size distribution (Martín & Cocero, 2008; Priamo et al., 2013; Hakuta et al., 2003). Better control of particle size, size distribution and morphology can be obtained by SCF technology than the current methods to form solid lipid particles such as cold HPH and ultrasonication. Different morphologies can be easily obtained by adjusting process parameters including pressure, temperature, nozzle diameters, depressurization rate, and the amount of dissolved $CO_2$ (Nalawade et al., 2006). Furthermore, if a SCF with a relatively lower critical temperature is used, such as $CO_2$, the process could be conducted in a mild condition, thus prevent the compounds from thermal degradation (Martín & Cocero, 2008; Hakuta et al., 2003).

Particle formation using SCF technology can be divided into three groups depending on their role in the processing: a) SCF as a solvent: Rapid Expansion of Supercritical Solutions (RESS); b) SCF as a solute: Particles from Gas-Saturated Solutions (PGSS); and c) SCF as antisolvent: Gas Anti-solvent (GAS), and Supercritical Anti-solvent (SAS).

### 2.4.1. Rapid Expansion of Supercritical Solutions (RESS)

In this process, SCF is a solvent. The active substance is firstly dissolved in a SCF and becomes saturated at a fixed temperature and pressure, and then a sudden depressurization takes place in a nozzle, which sprays particles containing active substance at a high velocity, creating high supersaturation, due to rapid decrease in the solvent power and temperature (Martín & Cocero, 2008; Hakuta et al., 2003; Priamo et al., 2013; Fahim et al., 2014).

The advantages of RESS process for fine particle formation include: 1) it allows high supersaturations which are transmitted rapidly and homogeneously to the whole fluid, leading to forming particles in small size and narrow size distribution (Martín & Cocero, 2008); 2) it can be conducted under relatively mild temperature (typically below 80 °C), and is thus suitable for heat sensitive active substance (Martín & Cocero, 2008); and 3) it eliminates the use of organic solvents (Martín & Cocero, 2008; Fahim et al., 2014). However, there is a major limitation of the RESS process: it can only apply to substances with high solubility in the SCF, mainly non-polar compounds or volatile polar compounds such as ethanol, while non-soluble compounds such as acids could not be processed (Jung & Perrut, 2001; Reverchon, 1999; Martín & Cocero, 2008). Additionally, the production capacity may be limited; however, the benefit of elimination of organic solvent is sacrificed by the addition of a cosolvent to alleviate this problem (Martín & Cocero, 2008). Furthermore, the extremely fast precipitation could lead to difficulty in controlling the loading and morphology of the particles (Yeo & Kiran, 2005).

In the recent two decades, several groups have studied the RESS process for particle formation, such as pharmaceuticals including carbamazepine (Gosselin, Thibert, Preda, & McMullen, 2003), griseofulvin (Hu, Johnston, & Williams III, 2004), ibuprofen (Kayrak, Akman, & Hortacsu, 2003), and functional food compounds such as phytosterols (Jiang, Chen, & Zhao, 2003; Türk & Lietzow, 2004). Türk and Bolten (2010) reported the formation of submicron particles of naproxen by using the RESS process with the particle size in a range of 0.56-0.82 μm. Mishima et al. (2000) encapsulated protein in polymer. They dissolved protein and polymer both in SC-$CO_2$ with or without a cosolvent. The mixed solution is then depressurized through a nozzle to form microparticles. Oliveira, Pinto, and Dariva (2005) investigated formation of polypropylene microparticles from solution mixture with *n*-butane. They demonstrated that the concentration of polymer has a profound effect on particle morphology, relatively lower polymer concentrations favored particle formation with reduced agglomeration.

### 2.4.2. Particles from Gas-Saturated Solutions (PGSS)

In contrast to RESS, the PGSS process takes advantage of the SCF as a solute rather than a solvent since the solubilities of compressed gases in liquids and solids are usually much higher than those of such liquids and solids in the compressed gases (Fahim et al., 2014; Martín & Cocero, 2008). In the PGSS process, the SCF is firstly dissolved in a melted solid or a liquid suspended solution, and then the gas-saturated solution is suddenly depressurized and expanded through a nozzle from supercritical conditions to ambient pressure, leading to the precipitation of the fine particles as the dissolved SCF leaves the system in gas form (Željko, 2006; Martín & Cocero, 2008). This process is in

particular suitable for substances such as polymers, oils and fat, in which SCF not only has a large solubility but also leads to a considerable reduction in melting point, viscosity and interfacial tension (Martín & Cocero, 2008; Fahim et al., 2014; Martín & Weidner, 2010; Weidner, 2009). Again, the driving force is the sudden pressure drop and intense cooling effect produced by the escape of SCF. PGSS process can only be applied to substances for which the antisolvent effect of SCF is small, because otherwise, the solute would precipitate and not expand in the vessel (Martín & Cocero, 2008).

The advantages of PGSS process for particle formation include: 1) low SCF consumption and a reduced operating pressure due to the high solubility of SCF in melted solid or liquid suspended solution (Priamo et al., 2012; Jung & Perrut, 2001); 2) elimination of organic solvents (Tabernero, Del Valle, & Galán, 2012); 3) lower cost compared to other processes (Fahim et al., 2014), and 4) ease of adaptation to large scale production (Yeo & Kiran, 2005). However, the major disadvantage of PGSS process is the difficulty producing submicron-sized particles and poor control of particle size (Fahim et al., 2014; Weidner, 2009).

Up to date, more than 100 substances have been powderized with the PGSS process, including polymers, waxes and resins, natural products (extracts from spices, phospholipids, methanol) and fat derivatives (fatty acids, diglycerides, fatty alcohols, cocoa butter) (Weidner, 2009; Münüklü, 2005; Jung & Perrut, 2001). The atomization in the PGSS process can be improved by using a second gas such as air as an addition in the expansion vessel, generating the Gas-assisted Melting Atomization process (GAMA) (Salmaso, Elvassore, Bertucco, & Caliceti, 2009). Another application of the PGSS process is PGSS-drying, which dries aqueous solution into powder form (Priamo et al.,

2012; Thereza et al., 2012). This technique promotes the mass transfer between the SCF and the aqueous solution, and then the mixture is depressurized (Tabernero et al., 2012). Recently, Varona, Kareth, Martín, and Cocero (2010) used this technique to encapsulate lavandin oil in starches by removing water from an O/W emulsion stabilized with N-octenyl succinic anhydride starches as surfactants. Gitin, Varona, and Cocero (2011) encapsulated garlic essential oil by PGSS process where polyethylene glycol (PEG) was used as a carrier. They reported that the particle size was within 71-206 μm, and the encapsulation efficiency was 26-49%.

### 2.4.3. Gas Anti-solvent (GAS)

GAS is devised to recrystallize solid materials that are not soluble in SCF (Tabernero et al., 2012). The SCF is used in batch mode in this process (Yeo & Kiran, 2005; Fahim et al., 2014). The technique is especially suitable for polymers and fats and oils because most them are not soluble in SCF or gases (Yeo & Kiran, 2005). The molten solid is firstly dissolved in conventional liquid organic solvent as in SAS, and the solution is then introduced into the SCF from the bottom by a filter by a disperser, at a predetermined constant rate and temperature, leading to a rapid volume expansion of organic solvent (Fahim et al., 2014; Martín & Cocero, 2008; Yeo & Kiran, 2005; Franceschi et al., 2008). As a result, the solvent power of the conventional organic solvent decreases and supersaturation in which the gas concentration in solution increases with pressure and in turn causes precipitation of the particles (Fahim et al., 2014; Martín & Cocero, 2008; Yeo & Kiran, 2005). In this process, the antisolvent gas does not have to be at supercritical condition (Yeo & Kiran, 2005). After the solute material has

completely precipitated out, fresh antisolvent SCF or gases is used to flush the system to remove away the solvent (Jung & Perrut, 2001; Yeo & Kiran, 2005).

The advantages of GAS process include: 1) ability to load a large amount of solute material at one time; 2) flexibility in choosing organic liquid solvent that has less operational problems compared to other techniques; and 3) the potential to obtain solvent-free particles in micron and submicron sizes (Fahim et al., 2014; Knez & Weidner, 2003; Silva & Meireles, 2014). However, the major drawback is the possible toxic solvent residue (Fahim et al., 2014; Knez & Weidner, 2003; Silva & Meireles, 2014). Moreover, there is a lack of control over particle size, which prevents the formation of mono dispersed particles (Fahim et al., 2014).

Some of the most remarkable applications among varieties of materials processed with SC-$CO_2$ as antisolvent are pharmaceuticals, polymers, superconductor precursors, and natural substances and colorants (Martín & Cocero, 2008). Kim et al. (2011) formed cyclotetramethylenetetranitramine particles using GAS process, and the particle size was within 1-133 μm. However, studies that address the mechanism and kinetics of particle formation in the GAS process are scarce (Martín & Cocero, 2008).

### 2.4.4. Supercritical Anti-solvent (SAS)

In SAS process, SCF acts as an antisolvent, saturates the liquid solvent that reduces the solubility of a solute dissolved into a conventional liquid solvent, resulting in precipitation of solute. Due to the phase behavior of SCF with many solvents, the solution expands and its viscosity is reduced, and therefore solubility of the active substance in the liquid phase decreases (Fahim et al., 2014; Hakuta et al., 2003). Upon

depressurization, the expanded solution becomes supersaturated, thus forcing the active substance to deposit as micron-sized particles (Hakuta et al., 2003; Reverchon, Adami, Caputo, & De Marco, 2008). There are different types of SAS techniques where the substance is firstly dissolved in a conventional solvent (dichloromethane, methanol, ethanol, dimethylsulfoxide, etc.) and then leads to the precipitation of the particles (Fahim et al., 2014). Indeed, SAS process is a modified GAS process in a continuous or semi-continuous operation.

The advantages of SAS process include: 1) it controls of the particle morphology on a very wide range from nanoparticles to microparticles; 2) is amenable to continuous processing which is suitable for large scale production of micro- and nanoparticles; and 3) freshly precipitated particles can be easily collected and the SCF with organic solvent can be drained continuously from the system (Fahim et al., 2014). Nevertheless, the major limitation of SAS process is the usage of organic solvents which may have toxic residual solvent in the final product (Fahim et al., 2014). In addition, longer washing period is required due to agglomeration and aggregation of the particles in the nozzle (Jung & Perrut, 2001; Yeo & Kiran, 2005; Byrappa, Ohara, & Adschiri, 2008).

The use of SCF as antisolvent can usually be performed at pressure lower than 100 bar and temperature slightly above the $T_c$ of SCF. Falk, Randolph, Meyer, Kelly, and Manning (1997) produced composite microspheres by the SAS process. In their study, a homogeneous solution of the solutes and polymers were sprayed, thus co-precipitation of polymers and solutes occurred where both composite microspheres and microcapsules were formed. Young, Johnston, Mishima, and Tanaka (1999) produced the lysozyme with a biodegradable polymer by precipitating with a vapor-over-liquid antisolvent, and

the obtained particles were in a range of 1-10 μm. There are only few reports on the use of GAS for food and food ingredients. Generally, SAS process has been demonstrated to have industrial potential not only for drugs or polymers, but also for food applications (Weber, Beutin, Tschernjaew, & Kummel, 1997; Rantakylä, 2004; Thiering, Dehghani, & Foster, 2001).

### 2.5. Lipid particle formation using supercritical carbon dioxide (SC-$CO_2$)

The need for incorporation of lipophilic bioactive compounds into food and beverages to improve bioactive solubility and bioavailability, leading to improved food quality and health benefits, has led the development of lipid-based particle formation in food industry. Lipids are promising delivery vehicles for lipophilic bioactives due to their biocompatibility and enhanced absorption (Dolatabadi et al., 2015; Severino et al., 2012). Contrary to larger lipid particles, micro- and nano- lipid particles could help prevent separations of bioactives from solidifying lipid matrix and bioactives can be evenly dispersed in the matrix, therefore maintaining integrity in case of degradation due to thermal or mechanical stress (Müller et al., 2002). In addition, because of the extremely small size, nanocarriers have shown advantages including improvement of the aqueous solubility, enhancement of residence time in GI regions, better physicochemical stability in GI tract, intracellular delivery and transcellular delivery (Oehlke et al., 2014).

The utilization of solid lipids rather than liquid oils has advantages of achieving controlled bioactive release and bioactive stability against thermal and mechanical stress (Dolatabadi et al., 2015; Scalia, Young, & Traini, 2015), thus SLN have become one of the most promising lipid-based delivery system for bioactives and drugs. Nevertheless, to

some extent, current conventional methods producing SLN have restricted the full potential of developing an efficient delivery system. Safety concerns due to solvent use in solvent emulsification/evaporation method; bioactive instability in hot homogenization and high shear homogenization methods, and potential metal contamination and particle physical instability in ultrasonication method are the limitations of the current methods (Beh, Mammucari, & Foster, 2012; Ekambaram et al., 2012).

SC-$CO_2$ technology could address these problems by decreasing the melting temperature of the solid lipids, thus making particle formation under moderate conditions to process heat sensitive bioactives (Ciftci & Temelli, 2014). SC-$CO_2$ has a substantial impact on the properties of components with which they are mixed, including increasing solubility, affecting phase behavior, drastically decreasing the viscosity of condensed phases and surface tension of liquid (Brunner, 2010), thus used to optimize process parameters to generate ideal particles with preferred size and morphology (Hakuta et al., 2003; Knez & Weidner, 2003; Nalawade et al., 2006; Mishima, 2008). Moreover, increasing operating pressure within a specific range under the critical low temperature obtained by melting study could enhance the solubility of either $CO_2$ or lipids in the other one, which in turn affect the supersaturation of the solute in the solvent and the mass transfer of that solvent, which are both substantial for micronization and formation of composite particles (Yasuji, Takeuchi, & Kawashima, 2007).

Understanding the melting behavior of solid lipids in pressurized $CO_2$ is important for the production of solid lipid particles using SC-$CO_2$ (Ciftci & Temelli, 2014). Fundamentals concerning melting point depression, phase behavior and volumetric expansion have been explored to design particle formation process for

controlling the micronization (Knez & Weidner, 2003). Salmaso et al. (2009) reported that the melting temperature of the protein lipid mixture decreased to 35-40 °C under 150 bar $CO_2$ pressure. Moreover, Ciftci and Temelli (2014) reported a positive correlation between the melting point depression and volumetric expansion of the solid lipids in pressurized $CO_2$.

Lipid particle formation using SC-$CO_2$ is a fairly new research area. Badens, Magnan, and Charbit (2001) formed microparticles with size ranging from 1 to 40 μm from soy lecithin by the SAS process with ethanol as cosolvent. Using the same SAS process, Kunastitchai, Pichert, Sarisut, and Müller (2006) generated liposomes in a dry and reconstitutable form. In addition, Dos Santos, Richard, Pech, Thies, and Benoit (2002) coated protein particles of BSA with two commercial lipids, either Gelucire® 50-02 or Dynasan® 114, by depressurizing the suspension of BSA particles in SC-$CO_2$ solution of lipids. Gelucire® 50-02 consisted of a mixture of glycerides and fatty acid esters, whereas Dynasan® 114 only had trimyristin. The protein release of the particles coated with both lipids were more controllable than that of the uncoated protein. However, particles coated with trimyristin experienced an initial burst release of about 70% in 30 min at 37 °C due to the crystallization, leading to a rather homogeneous coating, whereas a prolonged release has been achieved over a 24 h period from particles coated with Gelucire® 50-02. Moreover, Mandžuka and Knez (2008) determined the Solid-Liquid-Gas equilibrium data in 50-600 bar for monostearate/$CO_2$ and tristearate/$CO_2$, and formed particles using batch PGSS micronization. Micronizations of monostearate and tristearate were performed in pressure range of 60-210 bar at 70 and 80 ºC, and at 60 and 70 ºC, respectively. The average size of monstearate and tristearate

particles were 10-40 μm depending on pre-expansion pressure and temperature. Particles after micronization had irregular and porous shape. Polymorphic form remained the same but the degree of crystallinity for both was lower when compared to original samples. Using SCF assisted emulsion/diffusion method, which was proposed to improve the classical emulsification/diffusion by the addition of a continuous SCF processing step to eliminate organic solvent, Campardelli et al. (2013) produced lipid nanoparticles of stearic acid. They tested different formulations for stearic acid nanoparticles and processed by supercritical continuous extraction at 80 bar and 25 ºC/or 45 ºC (liquid/gas ratio of 0.1). The mean particle size was 33 and 41 nm, respectively, achieving one order of magnitude smaller than the ones obtained by conventional emulsion/diffusion method, and the supercritical flow did not damage the particles. Similar to the PGSS process, supercritical melting micronization (ScMM) process was adopted by Lubary, De Loos, Ter Horst, and Hofland (2011) to produce microparticles from milk fat. Both anhydrous milk fat (AMF) and a diacylglycerol-based modified milk fat (D-AMF) had the ability to dissolve 30% (w/w) $CO_2$ in up to 130 bar and 25-70 ºC, and melting point depression was observed in both systems with pressurized $CO_2$. The AMF particles were composed of mainly the β' polymorph, regardless of morphology, whereas D-AMF seemed to crystallize predominately as α polymorph. Furthermore, Bertucco, Caliceti, and Elvassore (2007) reported a similar process for the formation of SLN using Gas-assisted Melting Atomization (GAMA). In their process, molten mixture was pressurized with $CO_2$, and then a semisolid or liquid mixture was created with a second gas (air) which did not completely dissolve into the mixture, and then the mixture was expanded with evaporation of $CO_2$ to form solid lipid micro- and nanoparticles.

SC-$CO_2$ technology, specifically the PGSS process, has been reported to achieve loading of lipophilic bioactives in the solid lipid particles (Salmaso et al., 2009; Vezzù et al., 2010). Pedro et al. (2016) produced curcumin-loaded solid lipid particles by the PGSS technique. The lipid matrix studied was tristearin + soy phosphatidylcholine (PC)/dimethylsulfoxide (DMSO) + curcumin, with ratios from 65.6:1 to 3:1. The loading yield was found to be in the range of 30-87% (w/w) drug/lipid. Curcumin-loaded solid lipid particles were more homogeneous in size with low DMSO feed, whereas the formulation with the highest DMSO feed yielded a bimodal particle size distribution with significant aggregation. The PGSS process was found to be properly set-up to produce solid lipid particles without degrading drugs. De Paz, Martín, and Cocero (2012a) formulated β-carotene with soybean lecithin by PGSS-drying process. They firstly prepared organic-on-water β-carotene emulsions and aqueous β-carotene suspensions, and then precipitated the lecithin by PGSS-drying to obtain the β-carotene-encapsulated lecithin particles. The particle size ranged from 10-500 μm, constituted by fused spherical particles less than 10 μm. The encapsulation efficiency was up to 60%. By hydrating these particles, β-carotene-loaded multilamellar liposomes of 1-5 μm were able to be obtained. In the same year, the same group formulated β-carotene with poly-(ε-caprolactones) by PGSS process (De Paz, Martín, Duarte, & Cocero, 2012b). The particle size was in the range of 270-650 μm with a β-carotene content up to 340 ppm when using polycaprolactone with molecular weight of 10000 g/mol, whereas the decreased to 110-130 μm when using polycaprolactone with molecular weight of 4000 g/mol. They also investigated the effects operating conditions on the particle formation. Bigger particles were obtained when the pressure and temperature were 150 bar and 50 ºC, compared to

the particles obtained at 110 bar and 70 ºC. Moreover, García-González et al. (2010) investigated the encapsulation efficiency of solid lipid hybrid particles prepared using the PGSS technique and loaded with different polarity active agents. The lipid hybrid contained a glyceryl monostearate (Lumulse® GMS-K), and a waxy triglyceride (Cutina® HR). All experiments were performed at 130 bar and 71 °C based on the previous measurements of lipid melting points. Solid lipid particles were loaded with silanized $TiO_2$ and caffeine, glutathione or ketoprofen in 6-7% (w/w) for the mineral filler and 4.5, 5.6 and 16.1% (w/w) for the active agents. They found that hydrophilic drugs, such as caffeine and glutathione, had a limited interaction with the lipophilic matrix and thus a limited capacity to be encapsulated. On the contrary, hydrophobic ketoprofen was entrapped in the lipidic particles as a molecular dispersion, and this formulation can be used for a sustained release ($t_{2h}$ = 20%). Furthermore, Sampaio de Sousa, Simplício, De Sousa, and Duarte (2007) produced caffeine-loaded solid lipid particles of glyceryl monostearate using the PGSS technique at 130 bar and 61 °C and had a mean particle size $D_{[3,2]}$ of 5.49 µm. The particles were loaded with 140 mg of caffeine/g particle.

## 2.6. Conclusions

Development of bioactive-carriers to improve the solubility, stability and bioavailability of lipophilic bioactives has become a target for food industry to produce health and wellness promoting foods and beverages. Lipids are especially preferred in formulation of dietary controlled delivery systems, due to their biocompatibility, enhancement of the absorption of bioactive in the GI tract, and targeted delivery. Production of the bioactive-carrier hollow solid lipid micro- and nanoparticles using SC-

$CO_2$ is a relatively new area. Hollow solid lipid micro- and nanoparticles have the advantages of SLN such as better protection of the loaded bioactive but higher loading capacity and minimized or no bioactive expelling due to hollow structure using a simple and green process.

## 2.7. References


Anandharamakrishnan, C. (2013). Bioactive entrapment using lipid-based nanocarrier technology. In: Techniques for Nanoencapsulation of Food Ingredients (pp. 17-28). SpringerBriefs in Food, Health, and Nutrition.

Augustin, M. A., & Hemar, Y. (2009). Nano- and micro-structured assemblies for encapsulation of food ingredients. *Chemical Society Reviews, 38,* 902-912.

Awad, T. S., Helgason, T., Kristbergsson, K., Decker, E. A., Weiss, J., & McClements, D. J. (2008). Effect of cooling and heating rates on polymorphic transformations and gelation of tripalmitin solid lipid nanoparticle (SLN) suspensions. *Food Biophysics, 3,* 155-162.

Badens, E., Magnan, C., & Charbit, G. (2001). Microparticles of soy lecithin formed by supercritical processes. *Biotechnology and Bioengineering, 72,* 194-204.

Basu, A., & Imrhan, V. (2007). Tomatoes versus lycopene in oxidative stress and carcinogenesis: conclusions from clinical trials. *European Journal of Clinical Nutrition, 61,* 295-303.

Beh, C. C., Mammucari, R., & Foster, N. R. (2012). Lipid-based drug carrier systems by dense gas technology: A review. *Chemical Engineering Journal, 188,* 1-14.

Belhaj, N., Arab-Tehrany, E., & Linder, M. (2010). Oxidative kinetics of salmon oil in bulk and in nanoemulsion stabilized by marine lecithin. *Process Biochemistry, 45,* 187-195.

Benichou, A., Aserin, A., & Garti, N. (2002). Protein-polysaccharide interactions for stabilization of food emulsions. *Journal of Dispersion Science and Technology, 23,* 93-123.

Bertucco, A., Caliceti, P., & Elvassore, N. (2007). Patent No. WO2007028421 A1.

Boualem, K., Subirade, M., Desjardins, Y., & Saucier, L. (2013). Development of an encapsulation system for the protection and controlled release of antimicrobial nisin at meat cooking temperature. *Journal of Food Research, 2,* 36-45.

Brunner, G. (2010). Applications of supercritical fluids. *Annual Review of Chemical Biomolecular Engineering, 1,* 321-342.

Brunner, G. (2005). Supercritical fluids: technology and application to food processing. *Journal of Food Engineering, 67,* 21-33.

Bunjes, H. (2005). Characterization of solid lipid nano and microparticles. In: *Lipospheres in drug targets and delivery.* CRC Press.

Byrappa, K., Ohara, S., & Adschiri, T. (2008). Nanoparticles synthesis using supercritical fluid technology - towards biomedical applications. *Advanced Drug Delivery Reviews, 60,* 299-327.

Campardelli, R., Cherain, M., Perfetti, C., Iorio, C., Scognamiglio, M., Reverchon E., & Porta, F. D. (2013). Lipid nanoparticles production by supercritical fluid assisted emulsion-diffusion. *Journal of Supercritical Fluids, 82,* 34-40.

Cavalli, R., Gasco, M. R., Chetoni, P., Burgalassi, S., & Saettone, M. F. (2002). Solid lipid nanoparticles (SLN) as ocular delivery system for tobramycin. *International Journal of Pharmaceutics, 238,* 241-245.

Chee, C. P., Djordjevic, D., Faraji, H., Decker, E. A., Hollender, R., McClements, D. J., Peterson, D. G., Roberts, R. F., & Coupland, J. N. (2007). Sensory properties of vanilla and strawberry flavored Ice cream supplemented with omega-3 fatty acids. *Milk Science International, 62,* 66-69.

Chee, C. P., Gallaher, J. J., Djordjevic, D., Faraji, H., McClements, D. J., Decker, E. A., Hollender, R., Peterson, D. G., Roberts, R. F., & Coupland, J. N. (2005). Chemical and sensory analysis of strawberry flavored yogurt supplemented with an algae oil emulsion. *Journal of Dairy Research, 72,* 311-316.

Chen, C., Han, D., Cai, C., & Tang, X. (2010). An overview of liposome lyophilization and its future potential. *Journal of Controlled Release, 142,* 299-311.

Cheong, J. N., Tan, C. P., Man, Y. B. C., & Misran, M. (2008). Alpha-Tocopherol nanodispersions: Preparation, characterization and stability evaluation. *Journal of Food Engineering, 89,* 204-209.

Ciftci, O. N., & Temelli, F. (2014). Melting point depression of solid lipids in pressurized carbon dioxide. *Journal of Supercritical Fluids, 92,* 208-214.

Constantinides, P. P., Chaubal, M. V., & Shorr, R. (2008). Advances in lipid nanodispersions for parenteral drug delivery and targeting. *Advanced Drug Delivery Reviews, 60,* 757-767.

Cooper, A. I. (2000). Polymer synthesis and processing using supercritical carbon dioxide. *Journal of Materials Chemistry, 10,* 207-234.

Coupland, J. N., & McClements, D. J. (1996). Lipid oxidation in food emulsions. *Trends in Food Science & Technology, 7,* 83-91.

De Paz, E., Martín, Á., & Cocero, M. J. (2012a). Formulation of β-carotene with soybean lecithin by PGSS (Particles from Gas Saturated Solutions)-drying. *Journal of Supercritical Fluids, 72,* 125-133.

De Paz, E., Martín, Á., Duarte, C. M. M., & Cocero, M. J. (2012b). Formulation of β-carotene with poly-(ε-caprolactones) by PGSS process. *Powder Technology, 217,* 77-83.

De Vos, P., Faas, M. M., Spasojevic, M., & Sikkema, J. (2010). Review: encapsulation for preservation of functionality and targeted delivery of bioactive food components. *International Dairy Journal, 20,* 292-302.

Del Valle, J. M., & Aguilera, J. M. (1988). An improved equation for predicting the solubility of vegetable oils in supercritical $CO_2$. *Industrial & Engineering Chemistry Research, 27,* 1551-1553.

Desai, K. G. H., & Park, H. J. (2005). Recent developments in microencapsulation of food ingredients. *Drying Technology, 23,* 1361-1394.

Dickinson, E. (2003). Hydrocolloids at interfaces and the influence on the properties of dispersed systems. *Food Hydrocolloids, 17,* 25-39.

Dolatabadi, J. E. N., Valizadeh, H., & Hamishehkar, H. (2015). Solid lipid nanoparticles as efficient drug and gene delivery systems: Recent breakthroughs. *Advanced Pharmaceutical Bulletin, 5,* 151-159.

Đorđević, V., Balanč, B., Belščak-Cvitanovič, A., Lević, S., Trifković, K., Kalušević, A., Kostić, I., Komes, D., Bugarski, B., & Nedović, V. (2015). Trends in encapsulation technologies for delivery of food bioactive compounds. *Food Engineering Reviews, 7,* 452-490.

Dos Santos, I. R., Richard, J., Pech, B., Thies, C., & Benoit, J. P. (2002). Microencapsulation of protein particles within lipids using a novel supercritical fluid process. *International Journal of Pharmaceutics, 242,* 69-78.

Drusch, S. (2007). Sugar beet pectin: A novel emulsifying wall component for microencapsulation of lipophilic good ingredients by spray-drying. *Food Hydrocolloids, 21,* 1223-1228.

Ekambaram, P., Sathali, A. A. H., & Priyanka, K. (2012). Solid lipid nanoparticles: A review. *Scientific Reviews & Chemical Communications, 2,* 80-102.

Evens, R., Schamphelaere, K. A. C., Balcaen, L., Wang, Z., Roy, K., Resano, M., Flórez, M., Boon, N., Vanhaecke, F., & Janssen, C. R. (2012). The use of liposomes to differentiate between the effects of nickel accumulation and altered food quality in Daphnia magna exposed to dietary nickel. *Aquatic Toxicology, 109,* 80-89.

Fahim, T. K., Zaidul, I. S. M., Abu Bakar, M. R., Salim, U. M., Awang, M. B., Sahena, F., Jalal, K. C. A., Sharif, K. M., & Sohrab, M. H. (2014). Particle formation and micronization using non-conventional techniques - review. *Chemical Engineering and Processing: Process Intensification, 86,* 47-52.

Falk, R., Randolph, T. W., Meyer, J. D., Kelly, R. M., & Manning, M. C. (1997). Controlled release of ionic compounds from poly(L-lactide) microspheres produced

by precipitation with a compressed anti-solvent. *Journal of Controlled Release, 44,* 77-85.

Fang, M., Jin, Y., Bao, W., Gao, H., Xu, M., Wang, D., Wang, X., Yao, P., & Liu, L. (2012). *In vitro* characterization and *in vivo* evaluation of nanostructured lipid curcumin carriers for intragastric administration. *International Journal of Nanomedicine, 7,* 5395-5404.

Fang, J. Y., Fang, C. L., Liu, C. H., & Su, Y. H. (2008). Lipid nanoparticles as vehicles for topical psoralen delivery: solid lipid nanoparticles (SLN) versus nanostructured lipid carriers (NLC). *European Journal of Pharmaceutics and Biopharmaceutics, 70,* 633-640.

Fathi, M., Mozafari, M. R., & Mohebbi, M. (2012). Nanoencapsulation of food ingredients using lipid based delivery system. *Trends in Food Science and Technology, 23,* 13-27.

Fidler, N., Sauerwald, T., Pohl, A., Demmelmair, H., & Koletzko, B. (2000). Docosahexaenoic acid transfer into human milk after dietary supplementation: a randomized clinical trial. *Journal of Lipid Research, 41,* 1376-1383.

Flanagan, J., & Singh, H. (2006). Microemulsions: a potential delivery system for bioactives in food. *Critical Reviews in Food Science and Nutrition, 46,* 221-237.

Franceschi, E., De Cesaro, A. M., Feiten, M., Ferreira, S. R. S., Dariva, C., Kunita, M. H., Rubira, A. F., Muniz, E. C., Corazza, M. L., & Oliveira, J. V. (2008). Precipitation of β-carotene and PHBV and co-precipitation from SEDS technique using supercritical $CO_2$. *Journal of Supercritical Fluids, 47,* 259-269.

Gallarate, M., Trotta, M., Battaglia, L., & Chirio, D. (2009). Preparation of solid lipid nanoparticles from W/O/W emulsions: preliminary studies on insulin encapsulation. Journal of Microencapsulation: *Micro and Nano Carriers, 26,* 394-402.

García-González, C. A., Argemí, A., Sampaio de Sousa, A. R., Duarte, C. M. M., Saurina, J., & Domingo, C. (2010). Encapsulation efficiency of solid lipid hybrid particles prepared using the PGSS technique and loaded with different polarity active agents. *Journal of Supercritical Fluids, 54,* 342-347.

Gasco, M. R. (1997). Solid lipid nanospheres from warm microemulsions. *Pharmaceutical Technology Europe, 9,* 52-58.

Gasco, M. R. (1993). Method for producing solid lipid microspheres having a narrow size distribution. United States Patent 5, 250, 236.

Gitin, L., Varona, S., & Cocero, M. J. (2011). Encapsulation of garlic essential oil by batch PGSS process. *Innovative Romanian Food Biotechnology, 9,* 60-67.

Gohla, S. H., & Dingler, A. (2001) Scaling up feasibility of the production of solid lipid nanoparticles (SLN). *Pharmazie, 56,* 61-63.

Gonnet, M., Lethuaut, L., & Boury, F. (2010). New trends in encapsulation of liposoluble vitamins. *Journal of Controlled Release, 146,* 276-290.

Gosselin, P. M., Thibert, R., Preda, M., & McMullen, J. N. (2003). Polymorphic properties of micronized carbamazepine produced by RESS. *International Journal of Pharmaceutic, 252,* 225-233.

Goyal, P., Goyal, K., Kumar, S. G. Y., Singh, A., Ktare, O. P., & Mishra, D. N. (2005). Liposomal drug delivery systems e clinical applications. *Acta pharmaceutica, 55,* 1-25.

Hakuta, Y., Hayashi, H., & Arai, K. (2003). Fine particle formation using supercritical fluids. *Current Opinion in Solid State and Materials Science, 7,* 341-351.

Hibbeln, J. R., Nieminen, L. R. G., Blasbalg, T. L., Riggs, J. A., & Lands, W. E. M. (2006). Healthy intakes of *n*-3 and *n*-6 fatty acids: estimations considering worldwide diversity. *American Journal of Clinical Nutrition, 83,* 1483S-1493S.

Hu, J., Johnston, K. P., & Williams III, R. O. (2004). Nanoparticle engineering processes for enhancing the dissolution rates of poorly water soluble drugs. *Drug Development and Industrial Pharmacy, 30,* 233-245.

Illing, A., & Unruh, T. (2004). Investigation on the flow behaviour of dispersions of solid triglyceride nanoparticles. *International Journal of Pharmaceutics, 284,* 123-131.

Isailović, B., Kostić, I., Zvonar, A., Đorđević, V., Gašperlin, M., Nedović, V., & Bugarski, B. (2013). Resveratrol loaded liposomes produced by different techniques. *Innovative Food Science and Emerging Technologies, 19,* 181-189.

Jahadi, M., Khosravi-Darani, K., Ehsani, M. R., Mozafari, M. R., Saboury, A. A., Seydahmadia, F., & Vafabakhsh, Z. (2012). Evaluating the effects of process variables on protease-loaded nano-liposome production by placket-burman design for utilizing in cheese ripening acceleration. *Asian Journal of Chemistry, 24,* 3891-3894.

Jaiswal, J., Gupta, S. K., & Kreuter, J. (2004). Preparation of biodegradable cyclosporinenanoparticles by high-pressure emulsification-solvent evaporation process. *Journal of Controlled Release, 96,* 169-178.

Jaspart, S., Piel, G., Delattre, L., & Evrard, B. (2005). Solid lipid microparticles: Formulation, preparation, characterization, drug release and applications. *Expert Opinion on Drug Delivery, 2,* 75-87.

Jenab, E., & Temelli, F. (2012). Density and volumetric expansion of carbon dioxide-expanded canola oil and its blend with fully-hydrogenated canola oil. *Journal of Supercritical Fluids, 70,* 57-65.

Jenning, V., Thünemann, A. F., & Gohla, S. H. (2000). Characterization of a novel solid lipid nanoparticle carrier system based on binary mixtures of liquid and solid lipids. *International Journal of Pharmaceutic, 199,* 167-177.

Jensen, C. L. (2006). Effects of *n*-3 fatty acids during pregnancy and lactation. *American Journal of Clinical Nutrition, 83,* 1452S-1457S.

Jesorka, A., & Orwar, O. (2008). Liposomes: technologies and analytical applications. *Annual Review of Analytical Chemistry, 1,* 801-832.

Jiang, S. Y., Chen, M., & Zhao, Y. P. (2003). A study on micronization of phytosterol by the RESS technique with supercritical $CO_2$. *6th International Symposium on Supercritical Fluids, 3,* 1653-1658.

Jung, J., & Perrut, M. (2001). Particle design using supercritical fluids: Literature and patent survey. *Journal of Supercritical Fluids, 20,* 179-219.

Kasongo, K. W., Pardeike, J., Müller, R. H., & Walker, R. B. (2011). Selection and characterization of suitable lipid excipients for use in the manufacture of Didanosine-loaded solid lipid nanoparticles and nanostructured lipid carriers. *Journal of Pharmaceutical Sciences, 100,* 5185-5196.

Kayrak, D., Akman, U., & Hortacsu, O. (2003). Micronization of ibuprofen by RESS. *Journal of Supercritical Fluids, 26,* 17-31.

Kerdudo, A., Dingas, A., Fernandez, X., & Faure, C. (2014). Encapsulation of rutin and naringenin in multilamellar vesicles for optimum antioxidant activity. *Food Chemistry, 159,* 12-19.

Kim, S.-J., Lee, B.-M., Lee, B.-C., Kim, H.-S., Kim, H., & Lee, Y.-W. (2011). Recrystallization of cyclotetramethylenetetranitramine (HMX) using gas anti-solvent (GAS) process. *Journal of Supercritical Fluids, 59,* 108-116.

Klinkesorn, U., Sophanodora, P., Chinachoti, P., McClements, D. J., & Decker, E. A. (2005). Stability of spray-dried tuna oil emulsions encapsulated with two-layered interfacial membranes. *Journal of Agricultural and Food Chemistry, 53,* 8365-8371.

Knez, Z., & Weidner, E. (2003). Particles formation and particle design using supercritical fluids. *Current Opinion in Solid State and Materials Science, 7,* 353-361.

Kris-Etherton, P. M., Hecker, K. D., Bonanome, A., Coval, S. M., Binkoski, A. E., Hilpert, K. F., Griel, A. E., & Etherton, T. D. (2002). Bioactive compounds in foods: their role in the prevention of cardiovascular disease and cancer. *American Journal of Medicine, 113,* 71S-88S.

Kunastitchai, S., Pichert, L., Sarisuta, N., & Müller, B. W. (2006). Application of aerosol solvent extraction system (ASES) process for preparation of liposomes in a dry and reconstitutable form. *International Journal of Pharmaceutics, 316,* 93-101.

Lacatusu, I., Badea, N., Ovidiu, O., Bojin, D., & Meghea, A. (2012). Highly antioxidant carotene-lipid nanocarriers: synthesis and antibacterial activity. *Journal of Nanoparticle Research, 14,* 1-16.

Lasch, J., Weissig, V., & Brandl, M. (2003). Preparation of liposomes. In: Torchilin V.P, Weissig V (eds) liposomes. Oxford University Press, New York.

Lee, S., Faustman, C., Djordjevic, D., Faraji, H. & Decker, E. A. (2006). Effect of antioxidants on stabilization of meat products fortified with *n*-3 fatty acids. *Meat Science, 72,* 18-24.

Leong, W. F., Lai, O. M., Long, K., Yaakob, B., Mana, C., Misran, M., & Tan, C. P. (2011). Preparation and characterization of water-soluble phytosterol nanodispersions. *Food Chemistry, 129,* 77-83.

Lim, S. J., & Kim, C. K. (2002). Formulation parameters determining the physicochemical characteristics of solid lipid nanoparticles loaded with all-trans retinoic acid. *International Journal of Pharmaceutics, 243,* 135-146.

Losso, J. N., Khachatryan, A., Ogawa, M., Godber, J. S., & Shih, F. (2005). Random centroid optimization of phosphatidylglycerol stabilized lutein-enriched oil-in-water emulsions at acidic pH. *Food Chemistry, 92,* 737-744.

Lubary, M., De Loos, T. W., Ter Horst, J. H., & Hofland, G. W. (2011). Production of microparticles from milk fat products using the Supercritical Melt Micronization (ScMM) process. *Journal of Supercritical Fluids, 55,* 1079-1088.

Maa, Y. F., & Hsu, C. C. (1999). Performance of sonication and microfluidization for liquid-liquid emulsification. *Pharmaceutical Development and Technology, 4,* 233-240.

Mainardes, R. M., & Evangelista, R. C. (2005). PLGA nanoparticles containing praziquantel: effect of formulation variables on size distribution. *International Journal of Pharmaceutics, 290,* 137-144.

Makrides, M., & Gibson, R. A. (2000). Long-chain polyunsaturated fatty acid requirements during pregnancy and lactation. *American Journal of Clinical Nutrition, 71,* 307S-311S.

Malheiros, P. S., Sant'Anna, V., Barbosa, M. S., Brandelli, A., & Franco, B. D. G. M. (2012). Effect of liposome-encapsulated nisin and bacteriocin-like substance P34 on Listeria monocytogenes growth in Minas frescal cheese. *International Journal of Food Microbiology, 156,* 272-277.

Mandžuka, Z., & Knez, Ž. (2008). Influence of temperature and pressure during PGSS micronization and storage time on degree of crystallinity and crystal forms of monostearate and tristearate. *Journal of Supercritical Fluids, 45,* 102-111.

Martín, Á., & Weidner, E. (2010). PGSS-drying: Mechanisms and modeling. *Journal of Supercritical Fluids, 55,* 271-281.

Martín, A., & Cocero, M. J. (2008). Micronization processes with supercritical fluids: Fundamentals and mechanisms. *Advanced Drug Delivery Reviews, 60,* 339-350.

Maulucci, G., De Spirito, M., Arcovito, G., Boffi, F., Castellano, A. C., & Briganti, G. (2005). Particle size distribution in DMPC vesicle solutions undergoing different sonication times. *Biophysical Journal, 88,* 3545-3550.

McClements, D. J., Decker, E. A., Park, Y., & Weiss, J. (2009). Structural design principles for delivery of bioactive components in nutraceuticals and functional foods. *Critical Review in Food Science and Nutrition, 49,* 577-606.

McClements, D. J., Decker, E. A., & Weiss, J. (2007). Emulsion-based delivery systems for lipophilic bioactive components. *Journal of Food Science, 72,* R109-R124.

McClements, D. J. (2005). Food Emulsions: Principles, Practice, and Techniques (2nd edn). Boca Raton, FL: CRC Press.

McClements, D. J., & Decker, E. A. (2000). Lipid oxidation in oil-in-water emulsions: Impact of molecular environment on chemical reactions in heterogeneous food systems. *Journal of Food Science, 65,* 1270-1282.

Mehnert, W., & Mader, K. (2001). Solid lipid nanoparticles production, characterization and applications. *Advanced Drug Delivery Reviews, 47,* 165-196.

Mishima, K. (2008). Biodegradable particle formation for drug and gene delivery using supercritical fluid and dense gas. *Advance in Drug Delivery Reviews, 60,* 411-432.

Mishima, K., Matsuyama, K., Tanabe, D., Yamauchi, S., Young, T. J., & Johnston, K. P. (2000). Microencapsulation of proteins by rapid expansion of supercritical solution with a non-solvent. *AIChE Journal, 46,* 857-865.

Montes, A., Gordillo, M. D., Pereyra, C., & Martinez de la Ossa, E. J. (2011). Particles formation using supercritical fluids. In: H. Nakajima (Ed.), *Mass transfer - Advanced aspects* (pp. 836). InTech.

Moran, C., Ross, J., Cunningham, C., Butler, M., Anderson, T., Newby, D., Fox, K. A., & McDicken, W. N. (2006). Manufacture and acoustical characterization of a high-frequency contrast agent for targeting applications. *Ultrasound in Medicine and Biology, 32,* 421-428.

Mozafari, M. R., & Khosravi-Darani, K. (2007). An overview of liposome-derived nanocarrier technologies. In M. R. Mozafari (Ed.), *Nanomaterials and nanosystems for biomedical applications* (pp. 113-123). Dordrecht: Springer.

Müller, R. H., Radtke, M., & Wissing, S. A. (2002). Nanostructured lipid matrices for improved microencapsulation of drugs. *International Journal of Pharmaceutics, 242,* 121-128.

Müller, R. H., Mäder, K., & Gohla, S. (2000). Solid lipid nanoparticles (SLN) for controlled drug delivery - a review of the state of the art. *European Journal of Pharmaceutics and Biopharmaceutics, 50,* 161-177.

Müller, R. H., Mehnert, W., Lucks, J. S., Schwarz, C., Zur Mühlen, A., Weyhers, H., Freitas, C., & Rühl, D. (1995). Solid lipid nanoparticles (SLN) - An alternative colloidal carrier system for controlled drug delivery. *European Journal of Pharmaceutics and Biopharmaceutics, 41,* 62-69.

Münüklü, P. (2005). Particle formation of ductile materials using the PGSS technology with supercritical carbon dioxide, PhD thesis, University of Delft.

Nalawade, S. P., Picchioni, F., & Janssen, L. P. B. M. (2006). Supercritical carbon dioxide as a green solvent for processing polymer melts: Processing aspects and applications. *Progress in Polymer Science, 31,* 19-43.

Naseri, N., Valizadeh, H., & Zakeri-Milani, P. (2015). Solid lipid nanoparticles and nanostructured lipid carriers: structure, preparation and application. *Advanced Pharmaceutical Bulletin, 5,* 305-313.

Nayak, A. P., Tiyaboonchai, W., Patankar, S., Madhusudhan, B., & Souto, E. B. (2010). Curcuminoids-loaded lipid nanoparticles: Novel approach towards malaria treatment. *Colloids and Surfaces. B, Biointerfaces, 81,* 263-273.

Nedovic, V., Kalusevic, A., Manojlović, V., Petrovic, T., & Bugarski, B. (2013). Encapsulation systems in the food industry. In: Yanniotis et al. (Eds.), *Advances in food process engineering research.* Springer Science + Business Media, New York.

Oehlke, K., Adamiuk, M., Behsnilian, D., Gräf, V., Mayer-Miebach, E., Walz, E., & Greiner, R. (2014). Potential bioavailability enhancement of bioactive compounds using food-grade engineered nanomaterials: a review of the existing evidence. *Food & Function, 5,* 1341-1359.

Oliveira, J. V., Pinto, J. C., & Dariva, C. (2005). Application of a modified RESS process for polypropylene microparticle production. *Fluid Phase Equilibria, 228-229,* 381-388.

Ostlund, R. E. (2004). Phytosterols and cholesterol metabolism. *Current Opinion in Lipidology, 15,* 37-41.

Pardeshi, C., Rajput, P., Belgamwar, V., Tekade, A., Patil, G., Chaudhary, K., & Sonje, A. (2012). Solid lipid based nanocarriers: an overview. *Acta Pharmaceutica, 62,* 433-472.

Pasquali, I., Bettini, R., & Giordano, F. (2008). Supercritical fluid technologies: An innovative approach for manipulating the solid-state of pharmaceuticals. *Advanced Drug Delivery Reviews, 60,* 399-410.

Patel, M. R., & San Martin-Gonzalez, M. F. (2011). Characterization of ergocalciferol loaded solid lipid nanoparticles. *Journal of Food Science, 71,* N8-N13.

Patil, M. N., & Pandit, A. B. (2007). Cavitation - a novel technique for making stable nano-suspensions. *Ultrasonics Sonochemistry, 14,* 519-530.

Pedro, A. S., Villa, S. D., Caliceti, P., Vieira de Melo, S. A. B., Albuquerquea, E. C., Bertucco, A., & Salmaso, S. (2016). Curcumin-loaded solid lipid particles by PGSS technology. *Journal of Supercritical Fluids, 107,* 535-541.

Priamo, W. L., Dalmolin, I., Boschetto, D. L., Mezzomo, N., Ferreira, S. R. S., & Oliveira, J. V. (2013). Micronization processes by supercritical fluid technologies: a short review on process design (2008-2012). *Acta Scientiarum Technology, 35,* 695-709.

Pravilović, R. N., Radunović, V. S., Bošković-Vragolović, N. M., Bugarski, B. M., & Pjanović, R. V. (2014). The influence of membrane composition on the release of polyphenols from liposomes. *Hemijska industrija, 69,* 347-353.

Qian, C., Decker, E. A., Xiao, H., & McClements, D. J. (2012). Physical and chemical stability of beta-carotene-enriched nanoemulsions: Influence of pH, ionic strength, temperature, and emulsifier type. *Food Chemistry, 132,* 1221-1229.

Quintanar-Guerrero, D., Allémann, E., Fessi, H., & Doelker, E. (1999). Pseudolatex preparation using a novel emulsion–diffusion process involving direct displacement of partially water-miscible solvents by distillation. *International Journal of Pharmaceutics, 188,* 155-164.

Radtke, M., & Müller, R. H. (2001). Nanostructured lipid carriers: the new generation of lipid drug carriers. *New Drugs, 2,* 48-52.

Rantakylä, M. (2004). Particle production by supercritical antisolvent processing techniques, PhD thesis, University of Technology, Helsinki.

Rashidinejad, A., Birch, E. J., Sun-Waterhouse, D., & Everett, D. W. (2014). Delivery of green tea catechin and epigallocatechin gallate in liposomes incorporated into low-fat hard cheese. *Food Chemistry, 156,* 176-183.

Reverchon, E., Adami, R., Caputo, G., & De Marco, I. (2008). Spherical microparticles production by supercritical antisolvent precipitation: Interpretation of results. *Journal of Supercritical Fluids, 47,* 70-84.

Reverchon, E., & Adami, R. (2006). Nanomaterials and supercritical fluids. *Journal of Supercritical Fluids, 37,* 1-22.

Reverchon, E. (1999). Supercritical anti-solvent precipitation of micro- and nano-particles. *Journal of Supercritical Fluids, 15,* 1-21.

Ribeiro, H. S., Guerrero, J. M. M., Briviba, K., Rechkemmer, G., Schuchmann, H. P., & Schubert, H. (2006). Cellular uptake of carotenoid-loaded oil-in-water emulsions in colon carcinoma cells *in vitro*. *Journal of Agricultural and Food Chemistry, 54,* 9366-9369.

Ribeiro, H. S., Ax, K., & Schubert, H. (2003). Stability of lycopene emulsions in food systems. *Journal of Food Science, 68,* 2730-2734.

Salmaso, S., Elvassore, N., Bertucco, A., & Caliceti, P. (2009). Production of solid lipid submicron particles for protein delivery using a novel supercritical gas-assisted melting atomization process. *Journal of Pharmaceutical Sciences, 98,* 640-650.

Sampaio de Sousa, A. R., Simplício, A. L., De Sousa, H. C., & Duarte, C. M. M. (2007). Preparation of glyceryl monostearate-based particles by PGSS - Application to caffeine. *Journal of Supercritical Fluids, 43,* 120-125.

Santipanichwong, R., & Suphantharika, M. (2007). Carotenoids as colorants in reduced-fat mayonnaise containing spent brewer's yeast beta-glucan as a fat replacer. *Food Hydrocolloids, 21,* 565-574.

Scalia, S., Young, P. M., & Traini, D. (2015). Solid lipid microparticles as an approach to drug delivery. *Expert Opinion on Drug Delivery, 12,* 583-599.

Schroeder, A., Kost, J., & Barenholz, Y. (2009). Ultrasound, liposomes, and drug delivery: principles for using ultrasound to control the release of drugs from liposomes. *Chemistry and Physics of Lipids, 162,* 1-16.

Schubert, M. A., & Müller-Goymann, C. C. (2005). Characterization of surface-modified solid lipid nanoparticles (SLN): influence of lecithin and nonionic emulsifier. *European Journal of Pharmaceutics and Biopharmaceutics, 61,* 77-86.

Severino, P., Andreani, T., Macedo A. S., Fangueiro, J. F., Santana, M. H. A., Silva, A. M., & Souto, E. B. (2012). Current state-of-art and new trends on lipid nanoparticles (SLN and NLC) for oral drug delivery. *Journal of Drug Delivery, 10,* 1-10.

Sharma, R. (2005). Market trends and opportunities for functional dairy beverages. *Australian Journal of Dairy Technology, 60,* 195-198.

Shin, G. H., Kim, J. T., & Park, H. J. (2015). Recent developments in nanoformulations of lipophilic functional foods. *Trends in Food Science & Technology, 46,* 144-157.

Silva, E. K., & Meireles, M. A. A. (2014). Encapsulation of food compounds using supercritical technologies: Applications of supercritical carbon dioxide as an antisolvent. *Food and Public Health, 4,* 247-258.

Smith, A., Jaime-Fonseca, M., Grover, L. M., & Bakalis, S. (2010). Alginate-loaded liposomes can protect encapsulated alkaline phosphatase functionality when exposed to gastric pH. *Journal of Agricultural and Food Chemistry, 58,* 4719-4724.

Soottitantawat, A., Yoshii, H., Furuta, T., Ohkawara, M., & Linko, P. (2003). Microencapsulation by spray drying: influence of emulsion size on the retention of volatile compounds. *Journal of Food Science, 68,* 2256-2262.

Stewart, B. H., & Kleihues, P. (2003). World Cancer Report - International Agency for Research on Cancer. World Health Organization, New York.

Stringham, J, M., & Hammond, B. R. (2005). Dietary lutein and zeaxanthin: possible effects on visual function. *Nutrition Reviews, 63,* 59-64.

Subramaniam, B., Rajewski, R. A., & Snavely, K. (1997). Pharmaceutical processing with supercritical carbon dioxide. *Journal of Pharmaceutical Sciences, 86,* 885-890.

Sun, J., Bi, C., Chan, H. M., Sun, S., Zhang, Q., & Zheng, Y. (2013). Curcumin-loaded solid lipid nanoparticles have prolonged *in vitro* antitumour activity, cellular uptake and improved *in vivo* bioavailability. *Colloids and Surfaces B: Biointerfaces, 111,* 367-375.

Sun-Waterhouse. D., & Wadhwa, S. S. (2013). Industry-relevant approaches for minimizing the bitterness of bioactive compounds in functional foods: a review. *Food and Bioprocess Technology, 6,* 607-627.

Tabatt, K., Sameti, M., Olbrich, C., Müller, R. H., & Lehr, C. M. (2004). Effect of cationic lipid and matrix lipid composition on solid lipid nanoparticle-mediated gene transfer. *European Journal of Pharmaceutics and Biopharmaceutics, 57,* 155-162.

Tabernero, A., Del Valle, E. M. M., & Galán, M. A. (2012). Precipitation of tretinoin and acetaminophen with solution enhanced dispersion by supercritical fluids (SEDS). Role of phase equilibria to optimize particle diameter. *Powder Technology, 217,* 177-188.

Tadros, T., Izquierdo, R., Esquena, J., & Solans, C. (2004). Formation and stability of nanoemulsions. *Advances in Colloid and Interface Science, 108-109,* 303-318.

Tamjidi, F., Shahedi, M., Varshosaz, J., & Nasirpour, A. (2013). Nanostructured lipid carriers (NLC): A potential delivery system for bioactive food molecules. *Innovative Food Science and Emerging Technologies, 19,* 29-43.

Taylor, T. M., Bruce, B. D., Weiss, J., & Davidson, P. M. (2008). Listeria monocytogenes and Escherichia coli O157:H7 inhibition *in vitro* by liposome-encapsulated nisin and ethylene diaminetetraacetic acid. *Journal of Food Safety, 28,* 183-197.

Taylor, T. M., Gaysinsky, S., Davidson, P. M., Bruce, B. D., & Weiss, J. (2007). Characterization of antimicrobial-bearing liposomes by z-potential, vesicle size, and encapsulation efficiency. *Food Biophysics, 2,* 1-9.

Temelli, F. (2009). Perspectives on supercritical fluid processing of fats and oils. *Journal of Supercritical Fluids, 47,* 583-590.

Thereza, M., Gomes, M. S., Santos, D. T., & Meireles, M. A. A. (2012). Trends in particle formation of bioactive compounds using supercritical fluids and nanoemulsions. *Food Public Health, 2,* 142-152.

Thiering, R., Dehghani, F., & Foster, N. R. (2001). Current issues relating to anti-solvent micronization techniques and their extension to industrial scales. *Journal of Supercritical Fluids, 21,* 159-177.

Ting, Y., Jiang, Y., Ho, C., & Huang, Q. (2014). Common delivery systems for enhancing *in vivo* bioavailability and biological efficacy of nutraceuticals. *Journal of Functional Foods, 7,* 112-128.

Tiyaboonchai, W., Tungpradit, W., & Plianbangchang, P. (2007). Formulation and characterization of curcuminoids loaded solid lipid nanoparticles. *International Journal of Pharmaceutics, 337,* 299-306.

Tomasko, D. L., Li, H., Lui, D., Han, X., Wingert, M. J., Lee, L. J., & Koelling, K. W. (2003). A Review of $CO_2$ applications in the processing of polymers. *Industrial & Engineering Chemistry Research, 42,* 6431-6456.

Trotta, M., Debernardi, F., & Caputo, O. (2003). Preparation of solid lipid nanoparticles by a solvent emulsification-diffusion technique. *International Journal of Pharmaceutic, 257,* 153-160.

Türk, M., & Lietzow, R. (2004). Stabilized nanoparticles of phytosterol by Rapid Expansion from Supercritical Solution into aqueous solution. *AAPS PharmSciTech, 5,* 1-10.

Türk, M., & Bolten, D. (2010). Formation of submicron poorly water-soluble drugs by rapid expansion of supercritical solution (RESS): results for Naproxen. *Journal of Supercritical Fluids, 55,* 778-785.

Üner, M. (2006). Preparation, characterization and physicochemical properties of solid lipid nanoparticles (SLN) and nanostructured lipid carriers (NLC): Their benefits as colloidal drug carrier systems. *Die Pharmazie, 61,* 375-386.

Unger, E. C., Porter, T., Culp, W., Labell, R., Matsunaga, T., & Zutshi, R. (2004). Therapeutic applications of lipid-coated microbubbles. *Advanced Drug Delivery Reviews, 56,* 1291-1314.

Varona, S., Kareth, S., Martín, Á., & Cocero Alonso, M. J. (2010). Formulation of lavandin essential oil with biopolymers by PGSS for application as biocide in ecological agriculture. *Journal of Supercritical Fluids, 54,* 369-377.

Varshosaz, J., Ghaffari, S., Khoshayand, M. R., Atyabi, F., Azarmi, S., & Kobarfard, F. (2010). Development and optimization of solid lipid nanoparticles of amikacin by central composite design. *Journal of Liposome Research, 20,* 97-104.

Vega, C., & Roos, Y. H. (2006). Invited review: spray-dried dairy and dairy-like emulsions compositional considerations. *Journal of Dairy Science, 89,* 383-401.

Vemavarapu, C., Mollan, M. J., Lodaya, M., & Needham, T. E. (2005). Design and process aspects of laboratory scale SCF particle formation systems. *International Journal of Pharmaceutics, 292,* 1-16.

Vezzù, K., Borin, D., Bertucco, A., Bersani, S., Salmaso, S., & Caliceti, P. (2010). Production of lipid microparticles containing bioactive molecules functionalized with PEG. *Journal of Supercritical Fluids, 54,* 328-334.

Walstra, P. (2003). *Physical chemistry of foods.* New York, NY: Marcel Dekker.

Wang, X., Jiang, Y., Wang, Y. W., Huang, M. T., Hoa, C. T., & Huang, Q. (2008). Enhancing anti-inflammation activity of curcumin through O/W nanoemulsions. *Food Chemistry, 108,* 419-424.

Weber, A., Beutin, M., Tschernjaew, J., & Kummel, R. (1997). Compressed fluid antisolvent crystallization for controlled particle design. *Crystal Growth Organization Matter 4, International Workshop,* 214-221.

Weidner, E. (2009). High pressure micronization for food applications. *Journal of Supercritical Fluids, 47,* 556-565.

Weiss, J., Decker, E. A., McClements, D. J., Kristbergsson, K., Helgason, T., & Awad, T. (2008). Solid lipid nanoparticles as delivery systems for bioactive food components. *Food Biophysics, 3,* 146-154.

Westesen, K., & Siekmann, B. (1997). Investigation of the gel formation of phospholipid-stabilized solid lipid nanoparticles. *International Journal of Pharmaceutic, 151,* 35-45.

Westesen, K., Siekmann, B., & Koch, M. H. J. (1993). Investigations on the physical state of lipid nanoparticles by synchrotron radiation X-ray diffraction. *International Journal of Pharmaceutics, 93,* 189-199.

Wissing, S. A., Kayser, O., & Müller, R. H. (2004). Solid lipid nanoparticles for parental drug delivery. *Advanced Drug Delivery Review, 56,* 1257-1272.

Wong, N. C. W. (2001). The beneficial effects of plant sterols on serum cholesterol. *Canadian Journal of Cardiology, 17,* 715-721.

Yasuji, T., Takeuchi, H., & Kawashima, Y. (2008). Particle design of poorly water-soluble drug substances using supercritical fluid technologies. *Advanced Drug Delivery Reviews, 60,* 388-398.

Yeo, S. D., & Kiran, E. (2005). Formation of polymer particles with supercritical fluids: A review. *Journal of Supercritical Fluids, 34,* 287-308.

Yoshida, P. A., Yokota, D., Foglio, M. A., Rodrigues, R. A. F., & Pinho, S. C. (2010). Liposomes incorporating essential oil of Brazilian cherry (*Eugenia uniflora* L.): characterization of aqueous dispersions and lyophilized formulations. *Journal of Microencapsulation, 27,* 416-425.

Young, T. J., Johnston, K. P., Mishima, K., & Tanaka, H. (1999). Encapsulation of lysozyme in a biodegradable polymer by precipitation with a vapor-over-liquid antisolvent. *Journal of Pharmaceutical Sciences, 88,* 640-650.

Yuan, Y., Gao, Y., Mao, L., & Zhao, J. (2008). Optimization of conditions for the preparation of β-carotene nanoemulsions using response surface methodology. *Food Chemistry, 107,* 1300-1306.

Yun, J.-H., Lee, H.-Y., Asaduzzaman, A. K. M., & Chun, B.-S. (2013). Micronization and characterization of squid lecithin/polyethylene glycol composite using particles from gas saturated solutions (PGSS) process. *Journal of Industrial and Engineering Chemistry, 19,* 686-691.

Željko, K. (2006). Particle formation using supercritical fluids - A short review. *Chemical Industry and Chemical Engineering Quarterly, 12,* 141-146.

Zimmermann, E., & Müller, R. H. (2001). Electrolyte-and pH-stabilities of aqueous solid lipid nanoparticle (SLN) dispersions in artificial gastrointestinal media. *European Journal of Pharmaceutics and Biopharmaceutics, 52,* 203-210.

# CHAPTER 3. FORMATION OF HOLLOW SOLID LIPID MICRO- AND NANOPARTICLES USING SUPERCITICAL CARBON DIOXIDE*

## 3.1. Abstract

Hollow solid lipid micro- and nanoparticles were formed from FHSO using atomization of the carbon dioxide ($CO_2$)-expanded lipid. Melting point of FHSO decreased from 68.5 °C to 57 °C (0.096 °C/bar) above 120 bar in pressurized $CO_2$. Processing conditions of 50 μm nozzle diameter and 200 bar $CO_2$ pressure yielded smaller ($d_{50\%}$ = 278 nm) hollow solid lipid particles. Increasing nozzle diameter and pressure affected the particle morphology and size negatively. Shell thickness of the particles decreased with increasing pressure at the same nozzle diameter. Decreasing the nozzle diameter yielded the polymorphism of the particles from β to α. Melting point of the particles shifted to a lower melting range and broadened the melting range compared to FHSO. The results showed that the reported supercritical $CO_2$-assisted atomization process is a promising method to form hollow solid lipid micro- and nanoparticles to develop bioactive delivery systems.

Keywords: Nanoparticle; Supercritical carbon dioxide; Lipid; Melting; Oil

## 3.2. Introduction

The growing demand for “natural” and “clean” products along with the increase in the prevalence of diet-related illnesses such as obesity, type-2 diabetes, cardiovascular disease and cancer have led the food industry prioritize the development of health and

* This chapter has been published. Yang, J., & Ciftci, O. N. (2016). Formation of hollow solid lipid micro- and nanoparticles using supercritical carbon dioxide. *Food and Bioproducts Processing, 98,* 151-160.

wellness promoting foods by incorporating bioactive components into foods and beverages. Many researches have verified that by incorporating functional ingredients into consumers' daily diet could have a significant positive effect on health promotion as well as relief of the above-mentioned illnesses (Qin et al., 2004; Shu et al., 2009; Bradford & Awad, 2007). However, many bioactives are lipophilic, resulting in poor water solubility that requires extra processes such as emulsification to make their addition into water possible, and result in poor absorption through gastrointestinal tract and limited bioavailability due to various physiochemical transformations during digestion (Ting et al., 2014). In addition, many of these bioactives are chemically sensitive, prone to degrade or decompose when exposed to light, oxygen, and heat during processing and storage. Therefore, inclusion of lipophilic bioactives in foods and beverages to produce functional foods and beverages has been a main challenge in the food industry.

Lipids are promising delivery vehicles for lipophilic bioactives due to their biocompatibility and enhanced absorption (Dolatabadi et al., 2015; Severino et al., 2012). The utilization of solid lipids rather than liquid oils has the advantages of achieving controlled bioactive release and bioactive stability against thermal and mechanical stress (Dolatabadi et al., 2015; Scalia et al., 2015), thus solid lipid nanoparticles (SLN) have become one promising lipid-based delivery system for bioactives and drugs. Nevertheless, to some extent, drawbacks of the SLN and their conventional production methods have restricted the full potential of developing an efficient delivery system. Safety concerns due to solvent use in solvent emulsification/evaporation method; bioactive instability in hot homogenization and high shear homogenization methods, and potential metal contamination and particle physical instability in ultrasonication method

are the limitations of the current methods (Beh et al., 2012; Ekambaram et al., 2012). Moreover, SLN possess poor loading capacity, and also may expel the loaded bioactive during crystallization, because it is a full solid lipid particle (Mukherjee, Ray, & Thakur, 2009).

A promising strategy to overcome above-mentioned problems in manufacturing fine solid lipid particles can be realized by using supercritical fluid technology, which has been considered as an effective and green alternative to process materials in the pharmaceutical, chemical and food industries (Subramaniam et al., 1997; Fahim et al., 2014; Campardelli et al., 2013). Among many substances that can be used as supercritical fluid, $CO_2$ is the most common one since it has a relatively mild critical temperature and pressure (31 °C, 74 bar), and also it is nontoxic, nonflammable, environmental friendly, cheap, and safe. SC-$CO_2$ has a substantial impact on the properties of components with which they are mixed, including increasing solubility, affecting phase behavior, drastically decreasing the viscosity of condensed phases and surface tension of liquid (Brunner, 2010), thus serving as the most important phenomenon used to optimize process parameters to generate ideal particles with preferred size and morphology (Hakuta et al., 2003; Knez & Weidner, 2003; Nalawade et al., 2006; Mishima, 2008).

Though have been recognized as an efficient alternative to liquid oils and/or colloidal systems, the potential of solid lipid carrier systems for food applications has not yet been fully explored. In this study, we investigated the formation hollow solid lipid micro- and nanoparticles that can be used as bioactive-carrier systems using SC-$CO_2$ technology. The hollow structure can increase the loading efficiency significantly compared to SLN, and solve the bioactive expelling problem. There are few reports on

the formation of solid lipid particles using supercritical fluid technology reporting formation of only microsize particles using the Particles from Gas-saturated Solutions (PGSS) technique (Sampaio de Sousa et al., 2007; Mandžuka & Knez, 2008; García-González et al., 2010; Lubary et al., 2011). Previously, Bertucco et al. (2007) reported a similar process for the formation of SLN using a similar process Gas-assisted Melting Atomization (GAMA). In their process, molten mixture was pressurized with $CO_2$, and then a semisolid or liquid mixture was created with a second gas (air) which did not completely dissolve into the mixture, and then the mixture was expanded with evaporation of $CO_2$ to form solid lipid micro- and nanoparticles (Bertucco et al., 2007). Production of solid lipid submicron particles for protein delivery (Salmaso et al., 2009) and bioactive-containing solid lipid microparticles (Vezzù et al., 2010) were also reported. To the best of our knowledge, there is no report on the formation of hollow solid lipid particles at both micro- and nanosize using SC-$CO_2$.

The main objective of this study was to form hollow solid lipid micro- and nanoparticles (nanospheres) from fully hydrogenated soybean oil (FHSO) that will be used as biocompatible lipophilic bioactive delivery systems using SC-$CO_2$. The specific objectives were to investigate the effects of pressure and nozzle diameter on the particle morphology, size and size distribution, melting properties, and polymorphism.

## 3.3. Materials and methods

### 3.3.1. Materials

FHSO was kindly provided by ConAgra Foods Inc. (Omaha, NE, USA). $CO_2$ (99.99% purity) was purchased from Matheson (Lincoln, NE, USA).

### 3.3.2. Determination of melting behavior of the FHSO in pressurized $CO_2$

Melting behavior of the FHSO in pressurized $CO_2$ was studied according to Ciftci and Temelli (2014) in a jacketed high pressure vessel equipped with two sapphire windows, microscope and camera systems, refrigerated circulator (model 1162A, VWR Inc., Radnor, PA, USA). The temperature of the vessel was controlled by circulating water through the jacket of the vessel. The molten FHSO was placed into a glass gas chromatograph vial insert (200 µL) between two windows, then the vessel with $CO_2$ pressurized using a syringe pump (Model 250D, Teledyne Isco Inc., Lincoln, NE, USA). After 1 h stabilization time, the temperature of the vessel was decreased to 5 °C below the solidification temperature of the FHSO that was observed via the microscope-camera system. Then, the temperature of the vessel was increased at a rate of 0.3 °C/min until first melting of the sample was observed. The melting temperature and pressure of the lipid under pressurized $CO_2$ was recorded as the pressure and temperature at which the first melting was observed.

### 3.3.3. Production of hollow solid lipid micro- and nanoparticles using SC-$CO_2$

The hollow solid lipid particles were produced from FHSO using the particle formation system shown in Figure 3.1. The system consisted of a high-pressure syringe pump, pre-heating section, 100 mL high-pressure expansion vessel, magnetic drive, magnetic drive controller, pressure gauge, thermocouple, sampling port, rupture disk, depressurization valve, and nozzle. The expansion vessel, depressurization valve, and nozzle were heated with heating tapes, and digital temperature controllers were used to control temperature of the heating tapes. Temperature of the expansion vessel was

maintained at 57 °C that is the melting point of FHSO under $CO_2$ at 120 bar. Temperature of the depressurization valve and nozzle was set to 5 °C above the melting point of the FHSO under atmospheric conditions.

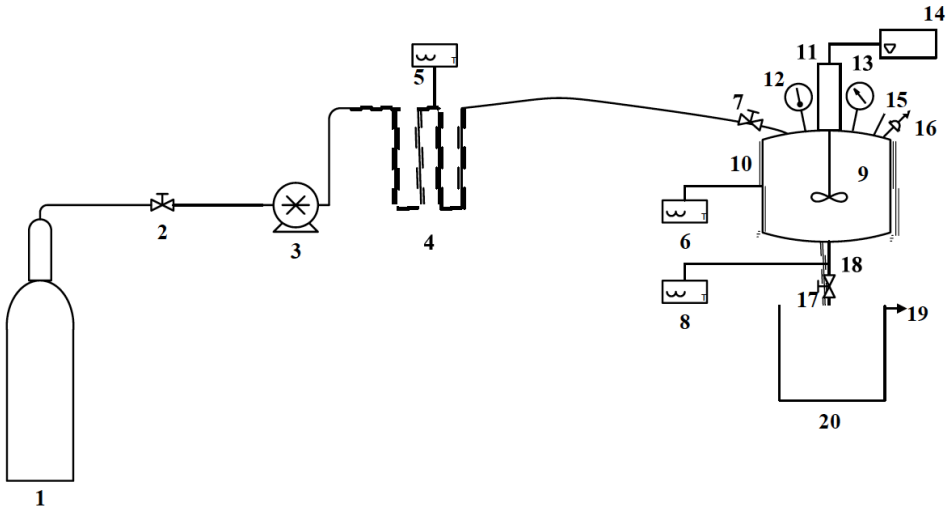


**Figure 3.1.** Schematic diagram of the particle formation unit. (1) $CO_2$ cylinder; (2) needle valve; (3) high pressure syringe pump; (4) pre-heating section; (5), (6), (8) temperature controller; (7) $CO_2$ inlet valve; (9) 100 mL high pressure expansion vessel; (10), (18) heating tape; (11) magnetic drive; (12) thermocouple; (13) pressure gauge; (14) magnetic drive controller; (15) sample inlet port; (16) rupture disc; (17) depressurization valve; (19) $CO_2$ exhaust; (20) sample collection vessel.

The FHSO sample was firstly melted on a heater at 130 °C and then 20 mL of molten FHSO was injected into the expansion vessel through the sampling port. Then, the $CO_2$ inlet valve was slowly opened, and the expansion vessel was pressurized with $CO_2$ with the syringe pump until the set pressure was reached. The magnetic drive was turned on at 1000 rpm to mix the pressurized $CO_2$ and the FHSO to obtain the maximum expansion of SC-$CO_2$-dissolved solid lipid for 1 h. Then, the magnetic drive was turned off and waited for 10 min for stabilization of the SC-$CO_2$-expanded solid lipid. The

pressure of the syringe pump was set to 10 bar above the pressure of the expansion vessel, and $CO_2$ inlet valve was opened, then depressurization valve was opened. Upon opening depressurization valve, $CO_2$-expanded lipid was atomized through the nozzle, solid lipid particles were formed and collected in the sample collection vessel, and $CO_2$ left the system in the gas form. During atomization, the pressure in the expansion vessel stayed constant due to continuous feeding $CO_2$ into the vessel.

### 3.3.4. Determination of the particle size and size distribution

Particle size and size distribution of the samples were measured using a laser diffraction particle size analyzer (Mastersizer 3000, Malvern Instruments Ltd., Worcestershire, UK). Samples (30 mg) were dispersed in 25 mL distilled water containing 0.4% (w/w) of Tween 80. Suspensions were sonicated in an ultrasonic water bath (3510 R-MTH, Branson Ultrasonics Corporation, Danbury, CT, USA) for 30 min before each analysis. The refractive index (RI) of the material was set as 1.46 with distilled water (RI = 1.33) as dispersant. The obscuration value was in the range of 5% - 7% for each analysis.

### 3.3.5. Determination of the particle morphology

Morphology of the obtained particles was analyzed by using a Field Emission-Scanning Electron Microscope (FE-SEM) (S4700, Hitachi High-Technologies Corporation, Japan). A thin layer of the sample was placed onto a sample mount using double-sided carbon tape and sputter coated with chromium using a HiPace 80 (Pfeiffer Vacuum, Germany) in argon atmosphere.

Morphology of the filtered nanoparticles obtained at 50 μm nozzle diameter and 200 bar was analyzed using a Transmission Electron Microscopy (TEM) (H7500, Hitachi High-Technologies Corporation, Japan). Drops of 2% (w/w) suspension dispersed in water after filtration were deposited on a carbon-coated copper grid (200 mesh) and negatively stained with 2% uranyl acetate solution, and waited to dry before examination.

### 3.3.6. Separation of the nanoparticles from microparticles

Samples (30 mg) were dispersed in 25 mL distilled water containing 0.4% (w/w) of polyoxyethylene sorbitan monooleate (Tween 80). Suspensions were sonicated in an ultrasonic water bath (3510 R-MTH, Branson Ultrasonics Corporation, Danbury, CT, USA) for 30 min. Then, the suspension was filtered through 0.45 μm pore size syringe filter. The filtrate was analyzed for the particle size and size distribution and morphology as described in Sections 3.3.3. and 3.3.4., respectively.

### 3.3.7. Determination of the melting profile

Melting profile of the obtained particles was determined using a Differential Scanning Calorimeter (DSC) (Pyris 1, Perkin Elmer, Waltham, Massachusetts, USA). The samples (5-7 mg) were placed and hermetically sealed in a stainless steel pan with an O-ring attached. An empty sealed pan was used to serve as a reference. The pans were placed in the calorimeter and equilibrated at 25 °C for 1 min. The samples were heated from 25 °C to 100 °C at a heating rate of 5 °C/min to observe the fusion of the particles.

### 3.3.8. Determination of the polymorphism

The polymorphism of the obtained lipid particles was determined using PANalytical Empyrean Diffractometer (XRD) unit (Empyrean, PANalytical, Westborough, MA, USA), operated with Cu Kα radiation at a voltage of 40 kV and intensity of 45 mA. A mask of 20 mm and a divergence slit of 1/4 degree were used on the incident beam path. Before XRD analysis, the powder samples were filled in 27 mm diameter, 2 mm deep pockets of stainless steel holders and the surface was levelled. A 15-position, automatic sample exchanger was used to measure the batch of samples. The sample holders were continuously spun at the rate of 22.5 deg/s during the measurement. Samples were run from 2 to 50 degrees under continuous scan at $2\theta\ min^{-1}$ with a step size of 0.026, and a diffracted beam monochromator for the PIXcel detector was utilized to improve the signal to noise ratio.

## 3.4. Results and discussion

Expansion of the lipids under pressurized $CO_2$ due to the solubility of the $CO_2$ in the lipids is the key to the formation of micro- and nanoparticles using atomization of $CO_2$-expanded lipid mixtures. Previously, it was shown that solid lipids expand when mixed with pressurized $CO_2$, and melting point of the lipids decrease significantly in pressurized $CO_2$ (Ciftci & Temelli, 2014). Therefore, it is crucial to conduct a separate study to determine the melting point of the lipid that will be used for particle formation using the atomization of $CO_2$-expanded lipid method. Melting point of the FHSO in pressurized $CO_2$ was determined (Fig. 3.2), and the obtained melting temperature of the FHSO in the pressurized $CO_2$ was used as the temperature in the particle formation

experiments. Melting point of FHSO at atmospheric conditions was 68.5 °C; however, it decreased to 57 °C above 120 bar under pressurized $CO_2$ (Fig. 3.2). Melting temperature of 57 °C was the lowest temperature that FHSO will melt under pressurized $CO_2$; therefore, 57 °C was used for all particle formation experiments. Pressure range used in the particle formation experiments started from the lowest pressure (120 bar) where the lowest melting point of the FHSO (57 °C) was obtained (Fig. 3.2). Melting point depression in pressurized $CO_2$ is important; a lower temperature will be used to keep the lipid and bioactive mixture in the liquid state, and lower process temperatures will enable us to minimize the degradation of the heat sensitive bioactives when lipid and bioactive are mixed to obtain bioactive-loaded lipid particles.

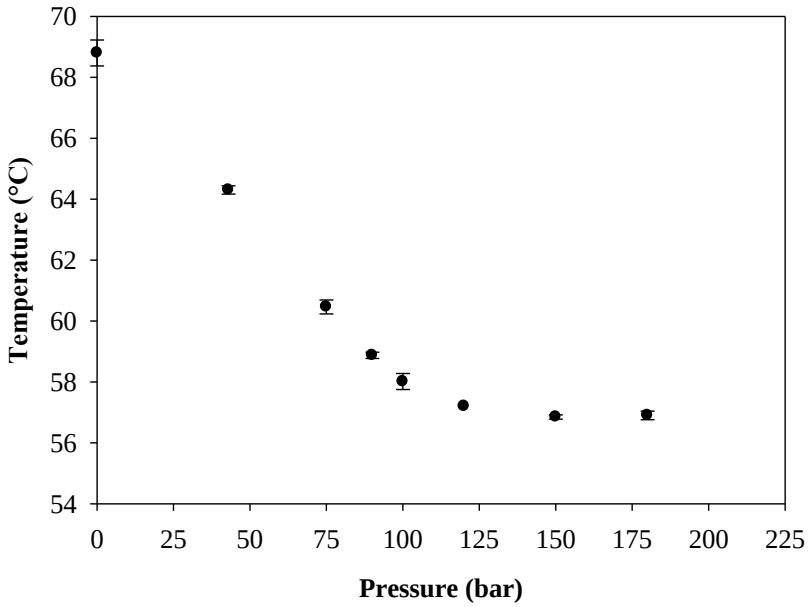


**Figure 3.2.** Melting point depression of fully hydrogenated soybean oil (FHSO) in pressurized $CO_2$.

### 3.4.1. Effect of particle formation conditions on the particle morphology

Figure 3.3 shows the effect of particle formation conditions (nozzle diameter and pressure) on the morphology of the lipid particles. Nozzle diameter and pressure was critical to control the morphology of the lipid particles. Hollow solid lipid particles were successfully obtained with 50 μm nozzle diameter at all studied pressures (120, 200, and 300 bar). Increasing nozzle diameter affected the particle morphology negatively; particles lost their spherical shape and smooth surface at 75 and 100 μm nozzle diameters at all studied pressures. It was targeted to obtain spherical particles because spherical shape provides homogenous mixing during product formulation, and more controlled release of the bioactives (Mu & Feng, 2003). Solubility of $CO_2$ in the molten lipid was the key phenomena for the particle formation by atomization of the SC-$CO_2$-expanded FHSO. Upon pressurization with SC-$CO_2$, liquid FHSO expanded due to dissolution of the $CO_2$ in the lipid phase. Volumetric expansion of the lipids is a function of $CO_2$ solubility in the lipid phase (Jenab & Temelli, 2012), and recently Ciftci and Temelli (2014) reported the volumetric expansion of various solid lipids (fully hydrogenated canola oil, cocoa butter, coconut oil, tristearin, trilaurin, monostearin, stearic acid, lauric acid) in pressurized $CO_2$.

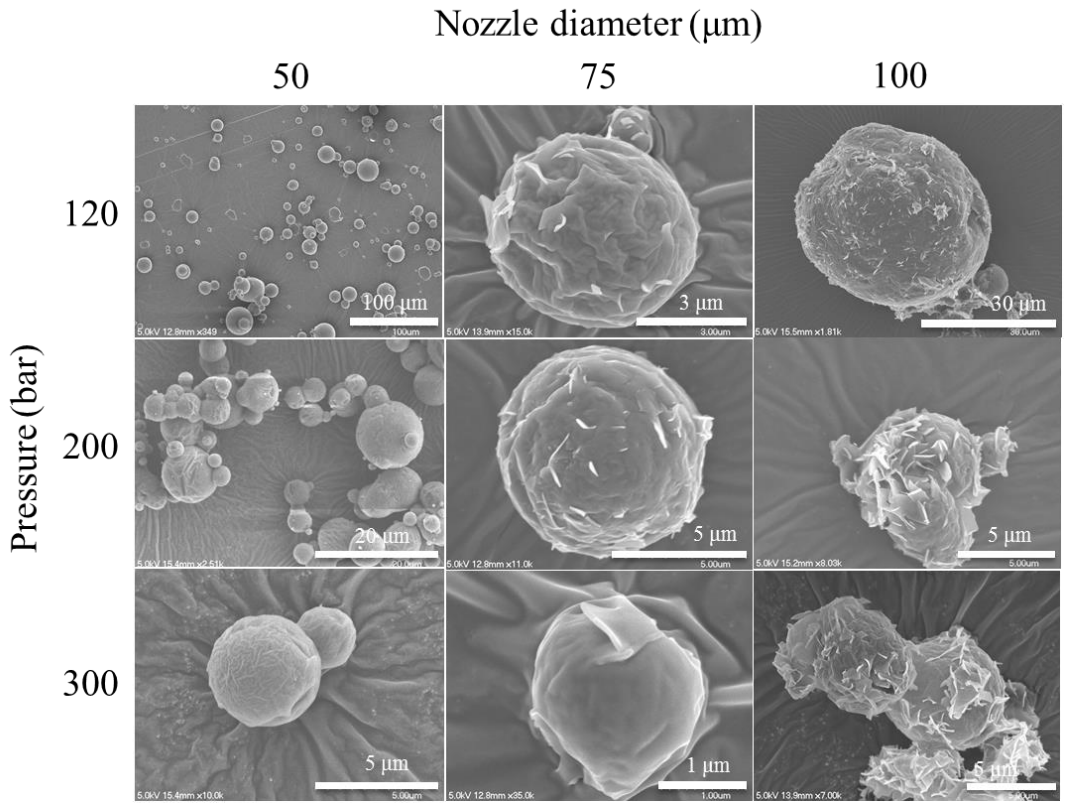


**Figure 3.3.** Scanning electron microscopy (SEM) images showing the effect of the particle formation conditions on the particle morphology.

Ciftci and Temelli (2014) showed that degree of the volumetric expansion of the solid lipids due to dissolution of the $CO_2$ in the lipid phase depends of the fatty acid composition (chain length) of the lipid; it increases up to a certain level with increasing pressure but then reaches a plateau. They reported that fully hydrogenated canola oil, which is very similar to FHSO in terms of fatty acid composition (88% stearic acid) expands by 9.7%, reaches plateau at 122 bar, and further increase in the pressure does not increase the volumetric expansion further, meaning the concentration of the $CO_2$ in the lipid phase does not change after 122 bar. Based on the findings of Ciftci and Temelli (2014), the amount of the $CO_2$ in the expanded FHSO above 120 bar was constant, and

this was supported by the decrease in the melting point of the FHSO in pressurized $CO_2$ up to 120 bar and staying constant above 120 bar (Fig. 3.2). The proposed mechanism of hollow solid lipid particle formation using the atomization of the $CO_2$-expanded lipid is presented in Figure 3.4. Upon atomization of the $CO_2$-expanded lipid through the nozzle, small droplets of lipid and $CO_2$ mixture were formed. Due to pressure drop, $CO_2$ in the atomized liquid lipid expanded, and the atomized lipid formed a spherical denser shell. During $CO_2$ expansion, cooling at the nozzle and surrounding area took place due to Joule-Thompson effect. The dense lipid shell formed by the expansion of $CO_2$ solidified when contacted with the cold environment, and formed the hollow spherical solid lipid particles. Both pressure and nozzle diameter played critical role in the formation of spherical hollow lipid particles. At higher pressures and bigger nozzle diameters (100 μm), the size of the atomized lipid + $CO_2$ droplet was bigger and there was more $CO_2$ dissolved in the lipid droplet, and this caused a more powerful $CO_2$ expansion that broke the particles. However, nozzle with 50 μm diameter formed smaller droplets of lipid and $CO_2$ mixture; smaller droplets contained smaller amount of $CO_2$; therefore, expansion of the $CO_2$ was less powerful, which resulted in unbroken spherical hollow solid lipid particles. Pressure was critical to control the shell thickness of the particles. SEM images showed that the shell thickness of the lipid particles decreased with increasing pressure (Fig. 3.5). At higher pressure (300 bar), a bigger force was exerted onto the forming liquid lipid shell during $CO_2$ expansion in all directions; therefore, the diameter of the lipid shell was bigger and the thickness of the liquid shell was smaller when the solidification took place.

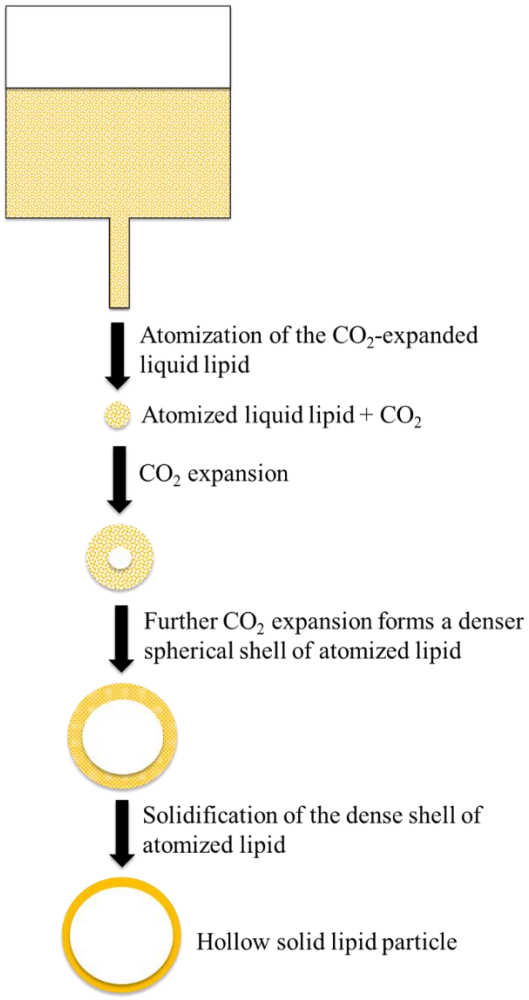


**Figure 3.4.** Proposed mechanism of the hollow solid lipid particle formation using atomization of $CO_2$-expanded lipid.

Shell thickness determines the volume in the hollow particle, in turn loading capacity, and also the strength of the particles. Moreover, shell thickness is important for the protection of the loaded bioactive and its release properties. Thinner shells will result in bigger inner volume; however, the particles may be fragile. Figure 3.5 shows the SEM images of the selected particles that were broken to show the hollow structure. As shown in Figures 3.5a and 3.5b, increasing the pressure from 120 to 300 bar using the 50 μm

nozzle diameter decreased the shell thickness and made the particles fragile. Similarly, increasing the pressure from 120 to 200 bar using 75 μm nozzle diameter decreased the shell thickness; however, the particles were not fragile due to presence of more lipid to form the shell (Figs. 3.5c and 3.5d). The particles obtained with 50 μm nozzle diameter at 200 bar were intact hollow solid lipid particles and they were not damaged during handling.

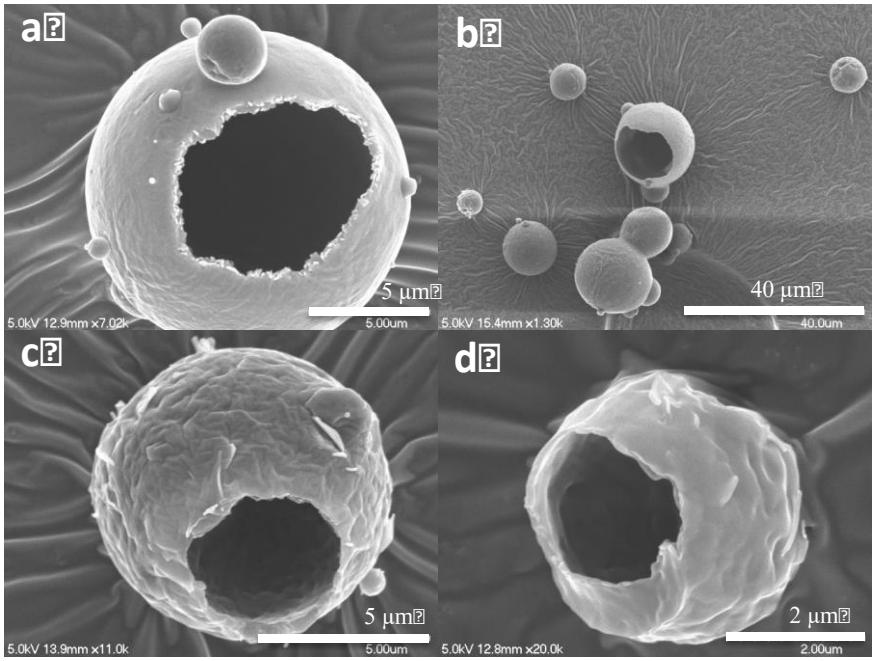


**Figure 3.5.** Scanning electron microscopy (SEM) images of the broken hollow solid lipid particles. (a) 120 bar, 50 μm nozzle; (b) 300 bar, 50 μm nozzle; (c) 120 bar, 75 μm nozzle; (d) 200 bar, 75 μm nozzle.

### 3.4.2. Effect of processing conditions on the particle size

Figure 3.6 presents the size distribution of the lipid particles obtained with different nozzle diameters (100, 75 and 50 μm) and pressures (120, 200, and 300 bar). Nozzle diameters of 75 and 100 μm formed particles with similar size; whereas, 50 μm

nozzle diameter formed smaller particles at 200 and 300 bar because smaller nozzle diameters generated smaller lipid droplets containing smaller amount of lipid and compressed $CO_2$. Size distribution of the particles obtained using nozzle diameters of 75 and 100 µm was unimodal at 120 bar, whereas they were bimodal at 200 and 300 bar.

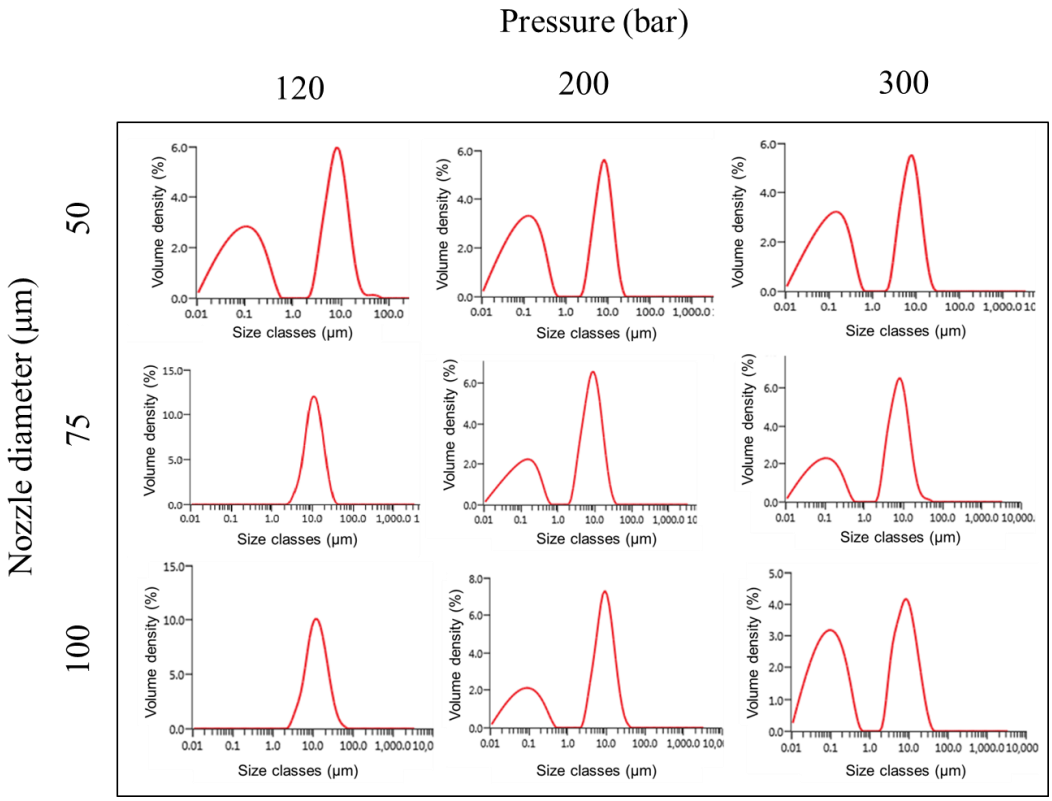


**Figure 3.6.** Effect of the particle formation conditions on the size distribution of the hollow solid lipid particles.

Size distribution of the particles obtained using nozzle diameters of 50 µm was bimodal at all pressures. It should be noted that the pieces of the broken particles may cause smaller particle size resulting at high pressures; therefore, it is important to evaluate the morphology of the particles with SEM. Figure 3.6 shows that fifty percent

($d_{50\%}$) of the particles obtained with 100 µm at 300 bar was smaller than 28.6 nm; however, SEM images showed that the small size distribution was primarily due to the presence of the pieces of the broken particles. Based on the particle size data and morphology of the particles, processing conditions of 50 µm and 200 bar was found to be the optimum processing conditions to obtain spherical hollow lipid particles. Ten percent ($d_{10\%}$) and fifty percent of the particles ($d_{50\%}$) obtained with 50 µm and 200 bar were smaller than 35.7 nm and 278 nm, respectively. Previously, Mandžuka and Knez (2008) reported particle sizes of 10 to 40 µm for the tristearin particles obtained with a similar process, but they did not report a hollow structure for their particles. Presence of nanoparticles in the particles formed at 50 µm and 200 bar was further confirmed by separation of the nanoparticles by filtration, and the morphology of the particles investigated by TEM which showed the presence of spherical nanoparticles (Fig. 3.7).

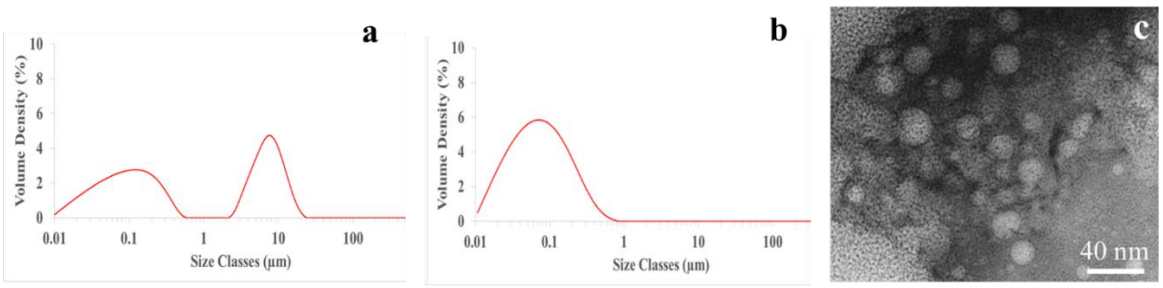


**Figure 3.7.** a) Size distribution of the particles formed at 50 µm nozzle diameter and 200 bar; b) Size distribution of the nanoparticles obtained from the particles formed at 50 µm nozzle diameter and 200 bar through filtration using 0.45 µm syringe filter; and c) Transmission electron microscopy (TEM) image of the nanoparticles obtained from particles formed at 50 µm nozzle diameter and 200 bar through filtration using 0.45 µm syringe filter.

### 3.4.3. Effect of processing conditions on the polymorphism

Polymorphism of the bioactive-loaded solid lipid particles affects the melting properties of the particles and release profile of the bioactives. Figure 3.8 reveals the effects of nozzle diameter and pressure on the polymorphism of the hollow solid particles obtained from FHSO. Fats can crystallize in three main polymorphic forms, namey, α, β', and β. Polymorphic form α is the unstable form, β is the most stable form, and the β' is the metastable form (Rousseau, Marangoni, & Jeffrey, 1998). The polymorphic forms are characterized by short spacings (d) obtained from XRD patterns, which is the distance due to lateral packing of the fatty acid chains on the triacylglycerol molecules (Ten Grotenhuis, Van Aken, Van Malssen, & Schenk, 1999). The short spacing at d=0.37 nm and d= 0.46 nm indicated that the predominant polymorphic forms of bulk FHSO were β and β', respectively. The main polymorphic form in all particles changed to α (d= 0.41 nm) with decreasing nozzle diameter and pressure. The shift from β to α form was observed as a main XRD peak at d=0.41 for the particles obtained with 75 and 50 μm nozzle diameters. Main polymorphic form of the particles obtained with 100 μm was β at 300 bar; however, α form became more pronounced with decreasing nozzle diameter to 50 μm. The particles obtained with 100 μm and 120 bar had a major peak for α and a small β peak. The nozzle diameter of 75 μm yielded a main polymorphic form of α and a less pronounced form of β at 200 and 300 bar; however, 120 bar yielded particles with only α polymorphic form. Different from nozzles with 75 and 100 μm diameter, nozzle with 50 μm diameter formed particles with a single polymorphic form of α at all studied pressures.

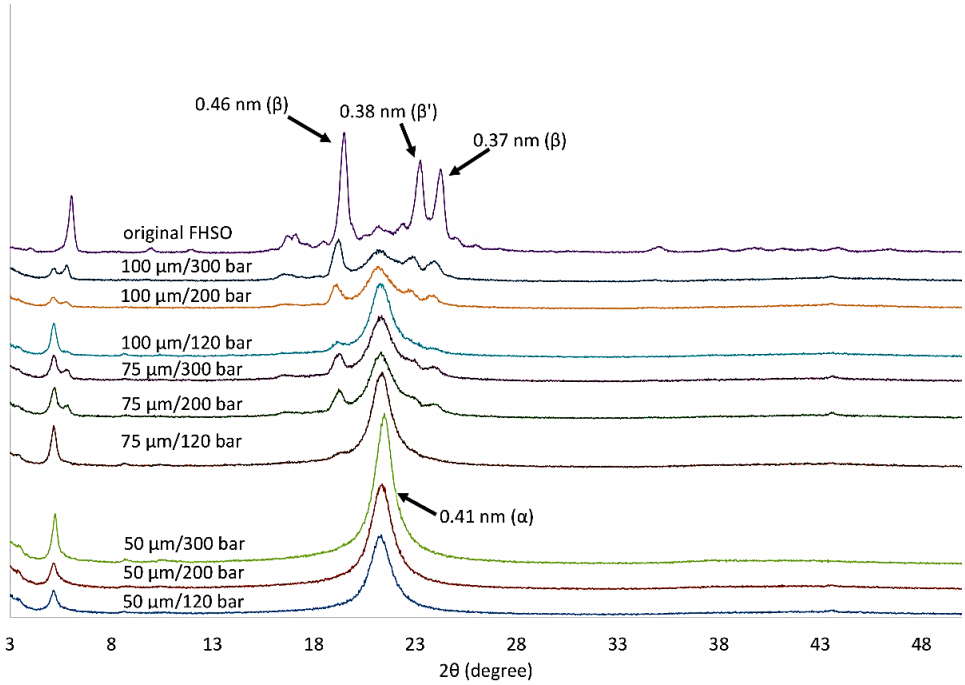


**Figure 3.8.** X-ray powder diffraction (XRD) patterns showing the effect of the particle formation conditions on the polymorphism of the hollow solid lipid particles.

The more stable the crystal structure (β), the more organized the molecules packing within the lattice and could make expelling of the entrapped compounds out of the particle possible (Lawler & Dimick, 2008; Helgason et al., 2009). This kind of expelling is not expected for the particles obtained in this study because the particles are hollow, which can be an advantageous over SLN which are full solid lipid particles. The dense packing of the β form may also prevent the release of the loaded bioactives (Heurtault, Saulnier, Pech, Proust, & Benoit, 2003).

### 3.4.4. Melting properties

Melting properties of the lipid particles are of great importance for achieving ideal and controlled release of lipid micro and nanoparticles loaded with bioactives or/and

drugs. Figure 3.9 presents the DSC melting curves of FHSO and the lipid particles obtained from FHSO using different nozzle diameters and pressures. Understanding the melting behavior of the particles was complicated due to the presence of different polymorphic forms and particle size in the same sample.

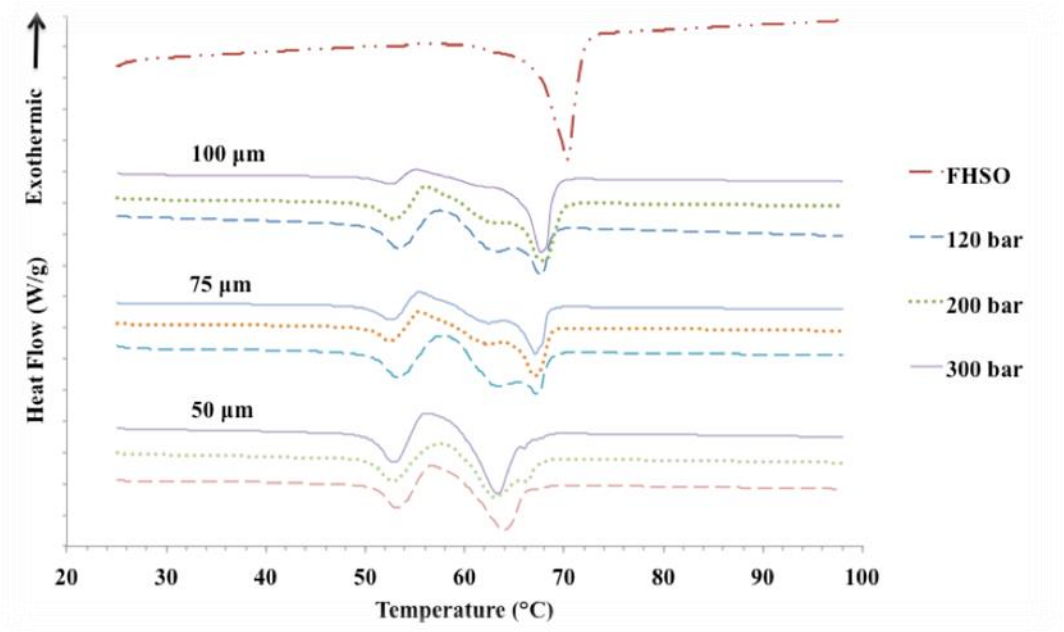


**Figure 3.9.** Differential scanning calorimetry (DSC) curves showing the effect of the particle formation conditions on the melting profile of the hollow solid lipid particles.

Lipid particles presented a different melting profile compared to the FHSO. FHSO exhibited a single endothermic peak, whereas lipid particles exhibited a stepwise melting and a broader melting range, and also melting temperature of the particles decreased compared to the FHSO. Even though the fatty acid composition of the lipid particles did not change, they had two major melting peaks as opposed to single melting peak in FHSO. The differences in the melting profiles of the particles obtained with

different processing conditions were attributed to the particle size differences and the presence of different polymorphic forms. The main reason for the lower melting point of the particles was attributed to particle size. From thermodynamics point of view, melting temperature of colloidal substances decreases with decreasing particle size (Defay, Prigogine, Bellemans, & Everett, 1966). This behavior has been observed for both inorganic (Lai, Guo, Petrova, Ramanath, & Allen, 1996) and organic nanoparticles (Westesen et al., 1997). Bunjes et al. (2000) reported that the melting behavior of triacylglycerol nanoparticles strongly depended on particle size irrespective of the matrix material. Lipid particles obtained in this study had a broader melting range and lower onset temperatures compared to the single sharp melting peak of FHSO. Melting point depression of the triacylglycerol nanoparticles compared to their bulk phase has also been explained using the Gibbs-Thompson equation previously (Siekmann & Westesen, 1994). The broading in the melting range and shift in the onset temperature to lower temperatures were due to the small size of the particles. In a good agreement with our findings, Bunjes et al. (2000) reported that the coarser dispersions of monoacid triacylglycerols melt in a single transition at a slightly lower temperature that of the bulk one; however, the melting range broadens and shifts to lower temperatures with decreasing particle size. They also reported that the melting of both monoacid and complex very fine triacylglycerols is stepwise rather than a continuous melting. Particles obtained with 75 and 100 μm nozzle diameters at all pressures had similar melting profiles except the one obtained with 100 μm and 300 bar; it had a melting curve similar to that of FHSO due to the main polymorphic form of β and presence of very weak α form. Particles obtained with 75 and 100 μm nozzle had three melting peaks (53 °C,

63 °C, and 67 °C); whereas particles obtained with 50 µm nozzle exhibited two melting peaks (53 °C and 63 °C). The presence of the peak at 53 °C became more pronounced with increasing intensity of the α peak on the XRD graph, and the peak at 63 °C was attributed to the β form. The α form was less pronounced in the particles obtained with 100 µm and 300 bar; therefore, their melting peak at 63 °C was smaller. Similarly, particles obtained with 75 µm nozzle and 120 bar had a more intense α peak (Fig. 3.8); therefore, it had a bigger melting peak at 63 °C (Fig. 3.9). All particles had a lower melting point peak at 53 °C, which was not available in the FHSO regardless the nozzle diameter, pressure, and the XRD peaks. The XRD patterns showed that the particles obtained with 50 µm had a single α peak; however, they exhibited two DSC melting peaks. The melting peak of the particles from 50 µm nozzle diameter at 63 °C was due to the α form, whereas the lower melting point melting peaks at 53 °C was attributed to the small size of the particles from all nozzle diameters.

### 3.5. Conclusions

Hollow solid lipid micro- and nanoparticles were successfully formed from FHSO by the atomization of the SC-$CO_2$-expanded molten FHSO. Hollow solid lipid microparticles were obtained using 75 and 100 µm nozzle diameters between the pressure range of 120 and 300 bar; whereas, a mixture of micro- and nanoparticles were obtained using 50 µm nozzle diameter. Processing conditions of 50 µm and 200 bar was found to be the optimum conditions to yield intact smaller hollow solid lipid particles. The size of the 50% of the particles obtained with 50 µm nozzle diameter was smaller than 278 nm. Increasing nozzle diameter and pressure affected the particle morphology and size

negatively. Shell thickness of the particles decreased with increasing pressure at the same nozzle diameter. Decreasing the nozzle diameter changed the polymorphism of the particles from β to α. Particles obtained with 50 μm nozzle diameter had only α form. Melting behavior of the FHSO particles strongly depended on the particle size; decreasing particle size broadened the DSC melting range and shifted the melting range to lower temperatures. Hollow solid lipid micro- and nanoparticles are promising carriers for bioactives that can be used as food ingredients to develop health and wellness promoting foods and beverages. They are more advantageous over SLN because the hollow particles have higher loading capacity, and the dry free-flowing powder form makes it easy to use, transport, and store.

### 3.6. References

Beh, C. C., Mammucari, R., & Foster, N. R. (2012). Lipid-based drug carrier systems by dense gas technology: A review. *Chemical Engineering Journal, 188,* 1-14.

Bertucco, A., Caliceti, P., & Elvassore, N. (2007). Patent No. WO2007028421 A1.

Bradford, P. G., & Awad, A. B. (2007). Phytosterols as anticancer compounds. *Molecular Nutrition & Food Research, 51,* 161-170.

Brunner, G. (2010). Applications of supercritical fluids. *Annual Review of Chemical Biomolecular Engineering, 1,* 321-342.

Bunjes, H., Koch, M. H. J., & Westesen, K. (2000). Effect of particle size on colloidal solid triglycerides. *American Chemical Society, 16,* 5234-5241.

Campardelli, R., Cherain, M., Perfetti, C., Iorio, C., Scognamiglio, M., Reverchon E., & Porta, F. D. (2013). Lipid nanoparticles production by supercritical fluid assisted emulsion-diffusion. *Journal of Supercritical Fluids, 82,* 34-40.

Ciftci, O. N., & Temelli, F. (2014). Melting point depression of solid lipids in pressurized carbon dioxide. *Journal of Supercritical Fluids, 92,* 208-214.

Defay, R., Prigogine, I., Bellemans, A., & Everett, D. H. (1966). *Surface Tension and Adsorption*. New York: Wiley.

Dolatabadi, J. E. N., Valizadeh, H., & Hamishehkar, H. (2015). Solid lipid nanoparticles as efficient drug and gene delivery systems: Recent breakthroughs. *Advanced Pharmaceutical Bulletin, 5,* 151-159.

Ekambaram, P., Sathali, A. A. H., & Priyanka, K. (2012). Solid lipid nanoparticles: A review. *Scientific Reviews & Chemical Communications, 2,* 80-102.

Fahim, T. K., Zaidul, I. S. M., Abu Bakar, M. R., Salim, U. M., Awang, M. B., Sahena, F., Jalal, K. C. A., Sharif, K. M., & Sohrab, M. H. (2014). Particle formation and micronization using non-conventional techniques - review. *Chemical Engineering and Processing, 86,* 47-52.

García-González, C. A., Argemí, A., Sampaio de Sousa, A. R. S., Duarte, C. M. M., Saurina, J. & Domingo, C. (2010). Encapsulation efficiency of solid lipid hybrid particles prepared using the PGSS technique and loaded with different polarity active agents. *Journal of Supercritical Fluids, 54,* 342-347.

Hakuta, Y., Hayashi, H., & Arai, K. (2003). Fine particle formation using supercritical fluids. *Current Opinion in Solid State & Materials Science, 7,* 341-351.

Helgason, T., Awad, T. S., Kristbergsson, K., Decker, E. A., McClements, D. J., & Weiss, J. (2009). Impact of surfactant properties on oxidative stability of β-carotene encapsulated within solid lipid nanoparticles. *Journal of Agricultural and Food Chemistry, 7,* 8033-8040.

Heurtault, B., Saulnier, P., Pech, B., Proust, J. E., & Benoit, J. P. (2003). Physicochemical stability of colloidal lipid particles. *Biomaterials, 24,* 4283-4300.

Jenab, E., & Temelli, F. (2012). Density and volumetric expansion of carbon dioxide-expanded canola oil and its blend with fully-hydrogenated canola oil. *Journal of Supercritical Fluids, 70,* 57-65.

Knez, Z., & Weidner, E. (2003). Particles formation and particle design using supercritical fluids. *Current Opinion in Solid State & Materials Science, 7,* 353-361.

Lawler, P. J., & Dimick, P. S. (2008). Crystallization and polymorphism of fats. In C. C. Akoh, & D. B. Min, (Eds.), *Food Lipids: chemistry, nutrition and biotechnology.* (pp. 253). Boca Raton, Fla.: CRC Press.

Lai, S. L., Guo, J. Y., Petrova, V. V., Ramanath, G., & Allen, L. H. (1996). Size-dependent melting properties of small tin particles: nanocalorimetric measurements. *Physical Review Letters, 77,* 99-102.

Lubary, M., De Loos, T. W., Ter Horst, J. H., & Hofland, G. W. (2011). Production of microparticles from milk fat products using the Supercritical Melt Micronization (ScMM) process. *Journal of Supercritical Fluids, 55,* 1079-1088.

Mandžuka, Z., & Knez, Ž. (2008). Influence of temperature and pressure during PGSS micronization and storage time on degree of crystallinity and crystal forms of monostearate and tristearate. *Journal of Supercritical Fluids, 45,* 102-111.

Mishima, K. (2008). Biodegradable particle formation for drug and gene delivery using supercritical fluid and dense gas. *Advanced Drug Delivery Reviews, 60,* 411-432.

Mu, L., & Feng, S. S. (2003). A novel controlled release formulation for the anticancer drug paclitaxel (Taxol): PLGA nanoparticles containing vitamin E TPGS. *Journal of Controlled Release, 86,* 33-48.

Mukherjee, S., Ray, S., & Thakur, R. S. (2009). Solid lipid nanoparticles: A modern formulation approach in drug delivery system. *Indian Journal of Pharmaceutical Sciences, 71,* 349-358.

Nalawade, S. P., Picchioni, F., & Janssen, L. P. B. M. (2006). Supercritical carbon dioxide as a green solvent for processing polymer melts: Processing aspects and applications. *Progress in Polymer Science, 31,* 19-43.

Qin, B., Nagasaki, M., Ren, M., Bajotto, G., Oshida, Y., & Sato, Y. (2004). Cinnamon extract prevents the insulin resistance induced by a high-fructose diet. *Hormone Metabolism Research, 36,* 119-125.

Rousseau, D., Marangoni, A. G., & Jeffrey, K. R. (1998). The influence of chemical interesterification on the physicochemical properties of complex fat systems: 2. Morphology and polymorphism. *Journal of the American Oil Chemists' Society, 75,* 1833-1839.

Salmaso, S., Elvassore, N., Bertucco, A., & Caliceti, P. (2009). Production of solid lipid submicron particles for protein delivery using a novel supercritical gas-assisted melting atomization process. *Journal of Pharmaceutical Sciences, 98,* 640-650.

Sampaio de Sousa, A. R., Simplício, A. L., De Sousa, H. C., & Duarte, C. M. M. (2007). Preparation of glyceryl monostearate-based particles by PGSS - Application to caffeine. *Journal of Supercritical Fluids, 43,* 120-125.

Scalia, S., Young, P. M., & Traini, D. (2015). Solid lipid microparticles as an approach to drug delivery. *Expert Opinion on Drug Delivery, 12,* 583-599.

Severino, P., Andreani, T., Macedo A. S., Fangueiro, J. F., Santana, M. H. A., Silva, A. M., & Souto, E. B. (2012). Current state-of-art and new trends on lipid nanoparticles (SLN and NLC) for oral drug delivery. *Journal of Drug Delivery, 10,* 1-10.

Shu, X. O., Zheng, Y., Cai, H., Gu, K., Chen, Z., Zheng, W., & Lu, W. (2009). Soy food intake and breast cancel survival. *American Medical Association, 302,* 2437-2443.

Siekmann, B., & Westesen, K. (1994). Thermoanalysis of the recrystallization process of melt-homogenized glyceride nanoparticles. *Colloids and Surfaces B: Biointerfaces, 3,* 159-175.

Subramaniam, B., Rajewski, R. A., & Snavely, K. (1997). Pharmaceutical processing with supercritical carbon dioxide. *Journal of Pharmaceutical Sciences, 86,* 885-890.

Ting, Y., Jiang, Y., Ho, C., & Huang, Q. (2014). Common delivery systems for enhancing *in vivo* bioavailability and biological efficacy of nutraceuticals. *Journal of Functional Foods, 7,* 112-128.

Ten Grotenhuis, E., Van Aken, G. A., Van Malssen, K. F., & Schenk, H. (1999). Polymorphism of Milk Fat Studied by Differential Scanning Calorimetry and Real-Time X-ray Powder Diffraction. *Journal of the American Oil Chemists' Society, 76,* 1031-1039.

Vezzù, K., Borin, D., Bertucco, A., Bersani, S., Salmaso, S., & Caliceti, P. (2010). Production of lipid microparticles containing bioactive molecules functionalized with PEG. *Journal of Supercritical Fluids, 54*, 328-334.

Westesen, K., Bunjes, H., & Koch, M. H. J. (1997). Physicochemical characterization of lipid nanoparticles and evaluation of their drug loading capacity and sustained release potential. *Journal of Controlled Release, 48,* 189-197.

# CHAPTER 4. DEVELOPMENT OF ANTIBACTERIAL FREE-FLOWING PEPPERMINT ESSENTIAL OIL-LOADED HOLLOW SOLID LIPID MICRO- AND NANOPARTICLES USING SUPERCRTIAL CARBON DIOXIDE*

## 4.1. Abstract

The main objective of this study was to overcome the issues related to the volatility and strong smell of essential oils that limit their utilization as "natural" antimicrobials in the food industry. Peppermint essential oil-loaded hollow solid lipid micro- and nanoparticles were formed using a novel "green" method based on atomization of $CO_2$-expanded lipid mixture. The highest essential oil loading efficiency (47.5%) was achieved at 50% initial essential oil concentration at 200 bar expansion pressure and 50 μm nozzle diameter. After 4 weeks of storage, 61.2%, 42.5%, 0.2%, and 2.0% of the loaded essential oil was released from the particles formed at 5%, 10%, 20%, and 50% (v/v) initial essential oil concentrations, respectively. Moreover, essential oil-loaded particles obtained at 50% initial essential oil concentration caused 3 log decrease in the growth of *Pseudomonas fluorescens*, which was significant higher than only 2 log decrease at free essential oil ($p<0.05$). This innovative simple and clean process can form spherical hollow micro- and nanoparticles loaded with essential oil that can be used as food grade antibacterials.

Keywords: Essential oil; Microparticle; Nanoparticle; Lipid; Supercritical carbon dioxide; Encapsulation.

* A version of this chapter has been published. Yang, J., & Ciftci, O. N. (2016). Development of free-flowing peppermint essential oil-loaded hollow solid lipid micro- and nanoparticles via atomization with carbon dioxide. *Food Research International, 87,* 83-91.

## 4.2. Introduction

In recent years, there is a growing demand for foods prepared using "natural" antimicrobials and antioxidants. However, many of those "natural" compounds that can be used as antimicrobials and antioxidants are lipophilic, meaning water-insoluble, and degrade easily during storage when exposed to oxygen and light. Therefore, addition of the lipophilic compounds into foods and beverages has been a major challenge in the food industry and remained as a barrier in front of the utilization of many "natural" compounds to be used as antimicrobials and antioxidants. The need for efficient, simple, and clean methods to incorporate lipophilic bioactive compounds in food systems has urged the development of new delivery systems. Lipids could play a key role in the delivery systems due to their physiological composition well tolerated by the human body (Davis, 2004; Heurtault et al., 2003; Severino et al., 2012). Among lipid based carrier systems, solid lipid nanoparticles (SLN) have advantages over other colloidal carriers such as liposomes and nanoemulsions regarding the better stability and protection of the incorporated bioactive compounds (Müller et al., 2002; Scalia et al., 2015). Nevertheless, as mentioned in Chapter 3, current SLN production methods are either multi-steps, or some of them involve organic solvents, or have severe processing conditions damaging sensitive bioactives (Sampaio de Sousa et al., 2007). Moreover, SLN have low loading capacity, and may expel the loaded bioactive during crystallization and storage due to solid lipid core (Mukherjee et al., 2009).

As presented in Chapter 3, formation of free-flowing hollow solid lipid micro- and nanoparticles using SC-$CO_2$ can overcome the limitations of the current SLN. In that process, SC-$CO_2$ was used as an expander and atomizer to form hollow solid lipid micro-

and nanoparticles. The process is also able to decrease the melting point of the solid lipids, which allows us to decrease the energy consumption and also protect the heat sensitive compounds during processing. Single step process without the use of any organic solvent, need for moderate pressurization, and need for low amount of $CO_2$ make it feasible to scale up.

In this study, the process developed in Chapter 3 was used to load the hollow solid lipid micro- and nanoparticles with a lipophilic bioactive oil, namely essential oil, to develop food grade antibacterials, and also to test the performance of the hollow solid lipid particles as liquid oil carrier. Peppermint essential oil is a "natural" antimicrobial, but its high volatility, vulnerability to heat, light and oxygen, and strong smell make it difficult to use as antimicrobials in foods (Varona et al., 2010). In this work, essential oil was loaded into the hollow solid lipid micro- and nanoparticles using the developed hollow solid lipid micro- and nanoparticle formation process to overcome the above-mentioned limitations associated with the use of essential oils in foods.

Previously, Varona et al. (2010) formed lavandin essential oil with biopolymers by a similar process called Particles from Gas Saturated Solutions (PGSS) and PGSS-drying processes, respectively, and found out that encapsulation efficiency of lavandin oil was between 14-66% in polyethylene glycol (PEG) microcapsules. Varona et al. (2013) further explored the antimicrobial activity of the same lavandin essential oil formulations against pathogenic foodborne bacteria. They showed that lavandin oil's antibacterial activity could be enhanced by encapsulation, and encapsulation might present an opportunity to facilitate the action of essential oil as antimicrobial agent penetrating inside the outer membrane.

The main objective of this study was to load the hollow solid lipid micro- and nanoparticles with essential oil to develop food grade free-flowing powder antibacterials using the process developed in Chapter 3. The specific objectives were to: i) load peppermint essential oil into the hollow solid lipid micro- and nanoparticles made of FHSO, ii) determine the essential oil loading efficiency, particle morphology, particle size and size distribution, and melting properties, iii) determine the release profile of the loaded essential oil, iv) investigate the storage stability of the essential oil-loaded particles in terms of particle morphology and size, and v) evaluate the antibacterial activity of the essential oil-loaded hollow particles on *Pseudomonas fluorescens*.

## 4.3. Materials and methods

### 4.3.1. Materials

FHSO was kindly provided by ConAgra Foods Inc. (Omaha, NE, USA). $CO_2$ (99.99% purity) was purchased from Matheson (Lincoln, NE, USA). Peppermint essential oil (100% purity) was purchased from Nature's (Streetsboro, OH, USA). *Pseudomonas fluorescens* was obtained from American Type Culture Collection (ATCC®), Manassas, VA. Tryptone Soya Broth (TSB) and Tryptone Soy agar (TSA) were purchased from Becton, Dickinson and Company (Franklin Lakes, NJ, USA).

### 4.3.2. Production of the essential oil-loaded hollow solid lipid micro- and nanoparticles using supercritical carbon dioxide

Essential oil-loaded hollow solid lipid micro- and nanoparticles were produced using particle formation system described in Section 3.3.3. Temperature of the expansion

vessel was maintained at 57 °C which is the melting point of FHSO at 120 bar $CO_2$ pressure, and at this temperature the mixture of the FHSO and the essential oil is in the liquid state. Temperature of the depressurization valve and nozzle was set to 20 °C above the melting point of the FHSO under atmospheric conditions. Molten FHSO was placed into the expansion vessel and then predetermined volumes of essential oil was injected into the expansion vessel through the sampling port to obtain initial essential oil concentrations of 5, 7, 10, 20, and 50% (v/v) in the FHSO. For each run, the total volume of the FHSO and essential oil mixture in the vessel was kept constant at 20 mL; therefore, the volumes of the essential oil injected into the vessel were 1, 1.4, 2, 4, and 10 mL for initial essential oil concentrations of 5, 7, 10, 20 and 50% (v/v), respectively. The sampling port was closed immediately after injecting the essential oil to prevent evaporation of the essential oil. Then, the expansion vessel was pressurized with $CO_2$ at 200 bar and the mixture in the vessel was mixed at 1000 rpm using the magnetic drive. Upon mixing, the lipid mixture expanded due to dissolution of the SC-$CO_2$ in the lipid mixture. Then, the magnetic drive was turned off and the expanded lipid mixture was stabilized for 10 min. The pressure of the syringe pump was set to 10 bar above the pressure of the expansion vessel, and the $CO_2$ inlet valve was opened, then depressurization valve was opened and the mixture was atomized through a 50 µm diameter nozzle. Upon depressurization, particles were formed and collected in the sample collection vessel. Particle formation conditions (200 bar expansion pressure and 50 µm nozzle diameter) were based on the optimized conditions that yielded smallest ($d_{50\%}$ = 278 nm) hollow solid lipid micro- and nanoparticles in Chapter 3.

### 4.3.3. Determination of the essential oil loading capacity and efficiency

Essential oil-loaded lipid particles (1 g) were spread on a light aluminum dish as a thin layer and heated at 150 °C for 30 min to evaporate the essential oil. Essential oil loading capacity (LC) and loading efficiency (LE) were calculated according to Eq. (4.1) and Eq. (4.2), respectively:

$$LC\ (\%) = \frac{(m_i - m_f)}{m_f} \times 100 \quad (4.1)$$

where $m_i$ is the initial mass of the sample, and $m_f$ is the mass of the sample after heating.

$$LE\ (\%) = \frac{LC_e}{LC_t} \times 100 \quad (4.2)$$

where LE is the loading efficiency, $LC_e$ is the experimental loading capacity obtained from Eq. (4.1), and $LC_t$ is the theoretical loading capacity, which is the initial weight concentration of the essential oil in the lipid mixture used for particle formation. Weight concentrations were calculated by weighing the amounts of the FHSO and the essential oil used for each particle formation.

### 4.3.4. Determination of the particle size and size distribution

Particle size and size distribution of the essential oil-loaded lipid particles were measured using a laser diffraction particle size analyzer (Mastersizer 3000, Malvern Instruments Ltd., Worcestershire, UK) as described in Section 3.3.4.

### 4.3.5. Scanning Electron Microscopy analysis

Morphology of the particles was analyzed using a Field Emission-Scanning Electron Microscope (FE-SEM) (S4700, Hitachi High-Technologies Corporation, Japan) as described in Section 3.3.5.

### 4.3.6. Transmission Electron Microscopy analysis

Hollow structure of the nanoparticles was examined using a Transmission Electron Microscope (TEM) (H7500, Hitachi High-Technologies Corporation, Japan) as described in Section 3.3.5.

### 4.3.7. Confocal fluorescence microscopy analysis

Essential oil-loaded lipid particles obtained at 10, 20 and 50% (v/v) initial essential oil concentration were analyzed using a confocal fluorescence microscope (A1, Nikon Instruments Inc., Japan) to investigate the loading of the essential oil in the hollow solid lipid micro- and nanoparticles since peppermint essential oil exhibits visible florescence. Essential oil-loaded lipid particles were dispersed in distilled water without the addition of Tween 80. The dispersions were then vortexed and sonicated using an ultrasonic water bath (3510 R-MTH, Branson Ultrasonics Corporation, Danbury, CT, USA) for 30 min before each analysis. The confocal images were recorded by a fluorescence microscope (90i, Nikon Instruments Inc., Japan) using z series scanning at each distance of 0.5 µm. Analyses were conducted at the excitation wavelengths of 405 nm and 488 nm and emission wavelengths of 450 nm and 525 nm.

### 4.3.8. Determination of the melting profile

Melting profile of the essential oil-loaded lipid particles was determined using a differential scanning calorimeter (DSC) (Pyris 1, Perkin Elmer, Waltham, Massachusetts, USA) as described in Section 3.3.7.

### 4.3.9. Release profile of the essential oil loaded in the hollow solid lipid micro- and nanoparticles

Four grams of essential oil-loaded particles with 5, 10, 20 and 50% (v/v) initial essential oil concentration were stored in closed containers at room temperature (22 °C) for 6 weeks and the amount of released essential oil was determined from the weight difference weekly over 6 weeks.

### 4.3.10. Storage stability of the essential oil-loaded hollow solid lipid micro- and nanoparticles

The storage stability of the essential oil-loaded hollow solid lipid micro- and nanoparticles (5, 10, 20 and 50%, v/v, initial essential oil concentration) was investigated in terms of changes in particle size and size distribution and particle morphology over 6 weeks of storage at room temperature (22 °C) in closed containers. Samples were analyzed every week with particle size analyzer and FE-SEM as described in Sections 3.3.4 and 3.3.5, respectively.

### 4.3.11. Antibacterial assays

#### 4.3.11.1. Bacterial strain and culture media

The strain studied in evaluating the antibacterial activity of the essential oil-loaded hollow solid lipid micro- and nanoparticles was a Gram-negative bacterium, *Pseudomonas fluorescens*. The culture media used for the strain was Tryptone Soya Broth (TSB).

#### 4.3.11.2. Plate count assay

The plate count assay was performed to determine the antibacterial activity of free peppermint essential oil and peppermint essential oil loaded into the hollow solid lipid micro- and nanoparticles. Briefly, a predetermined quantity of free essential oil (111 µL), particles obtained at 50% (v/v) initial essential oil concentration (0.5 g) to achieve essential oil concentration of 10 mg/mL or empty unloaded particles alone (0.2 g) was dissolved in 10 mL bacteria suspension ($10^6$ CFU/mL) in TSB medium and incubated at 25 °C during 24 h with a gentle agitation (100 rpm). Control was performed with only bacteria suspension in TSB medium. After incubation, appropriate serial dilutions of each culture in physiologic solution were conducted and spread on the surface of the solidified agar plates (TSA medium). Microorganism colonies were counted after 24 h of incubation at 25 °C to calculate the percentage of log inhibition of each system according to the following equation (Pettit et al., 2005), where C is the bacterial colonies counted for the negative control (bacteria free growth without addition of essential oil) and samples (bacteria growth in the presence of free or loaded essential oil).

$$\%\, log\ inhibition = \frac{C\ (negative\ control) - C\ (sample)}{C\ (negative\ control)} \times 100 \quad (4.3)$$

### 4.3.12. Statistical analysis

Data are presented as mean ± standard deviation based on triplicate experiments and analyses. Statistical analysis of the data was performed by using SAS (version 9.3) software package (SAS Institute Inc., NC, USA) at 95% confidence interval.

## 4.4. Results and discussion

### 4.4.1. Essential oil loading efficiency

Figure 4.1 presents the essential oil loading efficiency obtained at different initial essential oil concentrations. There was no significant difference between the loading efficiencies at 5, 7, 10, and 20% initial essential oil concentrations ($p>0.05$); however, it was significantly higher at 50% initial essential oil concentration ($p<0.05$). The essential oil loading efficiency increased from 39.0 to 47.5% when the initial essential oil concentration increased from 20 to 50%. During particle formation, the amount of essential oil available for loading is lower than the initial amount of essential oil introduced into the expansion vessel. Two phases were formed in the expansion vessel; the bottom phase was $CO_2$-expanded liquid phase that consisted of mixture of FHSO, essential oil, and $CO_2$, and the upper gas phase consisted of SC-$CO_2$. Upon mixing, the essential oil was equilibrated between the two phases by diffusing into the upper SC-$CO_2$ phase. Because the amount of total lipid mixture was kept constant in each

run, the amount of the SC-$CO_2$ in the upper phase was constant. At higher essential oil concentration, there was more essential oil in the liquid phase after the upper phase was saturated by the essential oil; therefore, there was more essential oil in the $CO_2$-expanded lipid phase. As a result, more essential oil was loaded into the lipid particles during depressurization of the $CO_2$-expanded lipid mixture. A similar phenomenon was reported for enzymatic synthesis of fatty acid methyl esters from methanol and corn oil (Ciftci & Temelli, 2011). It was reported that the substrate molar ratio of methanol to oil changed in the reaction mixture due to diffusion of methanol into the upper SC-$CO_2$ phase which resulted in less methanol in the $CO_2$-expanded liquid phase where the reaction took place (Ciftci & Temelli, 2011). These results suggested that the amount of essential oil loaded into the particles will be different than the initial concentration depending on the particle formation conditions, namely, pressure, temperature, ratio of lipid mixture to the SC-$CO_2$ phase, and expansion time.

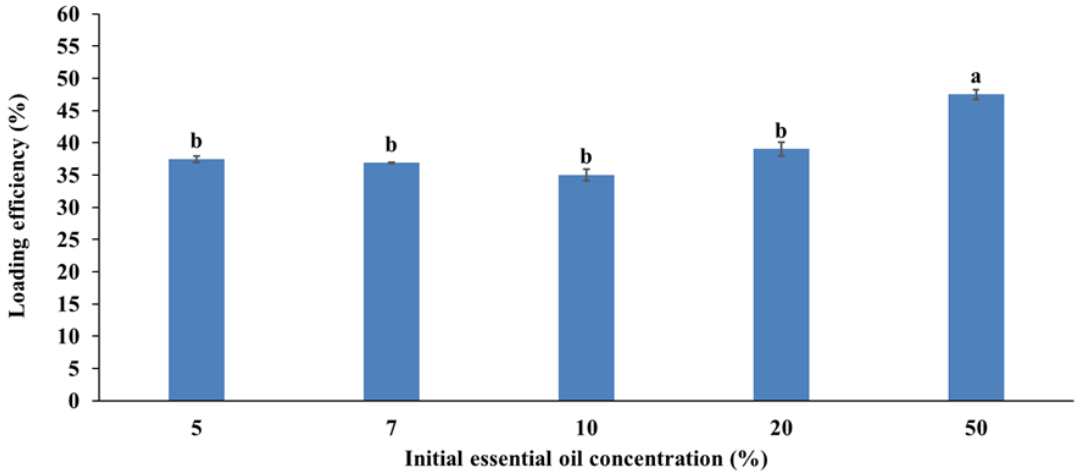


**Figure 4.1.** Loading efficiency at varying initial peppermint essential oil concentrations.

### 4.4.2. Particle morphology

Figure 4.2 shows the morphology of the essential oil-loaded lipid particles obtained at different initial essential oil concentrations. In Chapter 3, it has been found that increasing nozzle diameter affected the particle morphology negatively; particles lost their spherical shape and smooth surface at bigger nozzle diameters (75 and 100 μm) at all studied pressures (120, 200 and 300 bar). Essential oil-loaded spherical particles were successfully generated, which could provide homogenous mixing during formulation, and achieve more controlled release of the loaded essential oil (Mu & Feng, 2003). As explained in Chapter 3, the $CO_2$-expanded lipid was atomized through the nozzle, and formed small liquid lipid droplets containing pressurized $CO_2$. Upon atomization, the compressed $CO_2$ in the lipid droplets expanded and formed a liquid lipid bubble. At the same time, the temperature decreased below the solidification temperature of the solid lipid due to Joule-Thompson effect and the lipid bubble solidified and formed a spherical hollow solid lipid particle. During solidification, the FHSO encapsulated the liquid essential oil in the inner cavity.

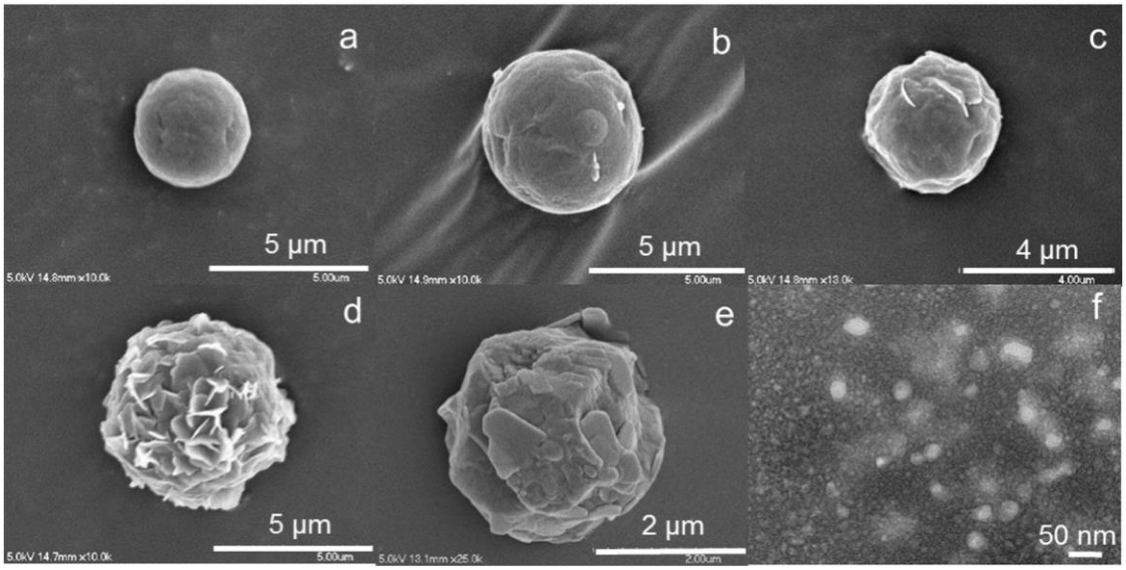


**Figure 4.2.** (a)-(e) Scanning electron microscopy (SEM) images of the essential oil loaded hollow solid lipid microparticles obtained at varying initial essential oil concentrations (v/v): (a) 5%, (b) 7%, (c) 10%, (d) 20%, and (e) 50%; (f) Transmission electron microscopy (TEM) image of the essential oil-loaded lipid nanoparticles obtained at 50% initial essential oil concentration after filtration using 0.45 µm filter.

SEM images shown in Figure 4.2 indicated that the initial essential oil concentration affected the morphology of the essential oil-loaded lipid particles. At lower initial essential oil concentrations (5-7%), the essential oil-loaded lipid particles had a smooth surface; however, increasing initial essential oil concentration to 20-50% resulted in formation of particles with wrinkled-like surface. During particle formation, higher amount of essential oil evaporated from the lipid bubble due to high volatility and therefore particles had an irregular surface during sudden solidification. The agglomeration of the lipid particles became more pronounced with increasing initial essential oil concentration, suggesting that there was essential oil on the surface of the particles which made the final product sticky. A similar agglomeration was observed by Varona et al. (2010) for the production of lavandin essential oil-loaded biopolymer

polyethylene glycol (PEG) particularly with increasing the oil to PEG ratio from 0.25 to 0.37.

Figure 4.3 presents the cross-sectional images of the essential oil-loaded hollow solid lipid particles obtained by z series scanning by confocal fluorescence microscopy. Figure 4.3 reveals that the peppermint essential oil, shown in dark blue color, was loaded mainly in the cavity and some in the shell of the particles. When a laser z series scanning was applied, the fluorescence gradually appeared and became more predominant in the cavity, as well as in the particle shell. Presence of the essential oil in the solid lipid shell was due to entrapment of the essential oil in the shell during sudden solidification of the lipid mixture and also release of the essential oil through the solid lipid shell after particle formation for some particles.

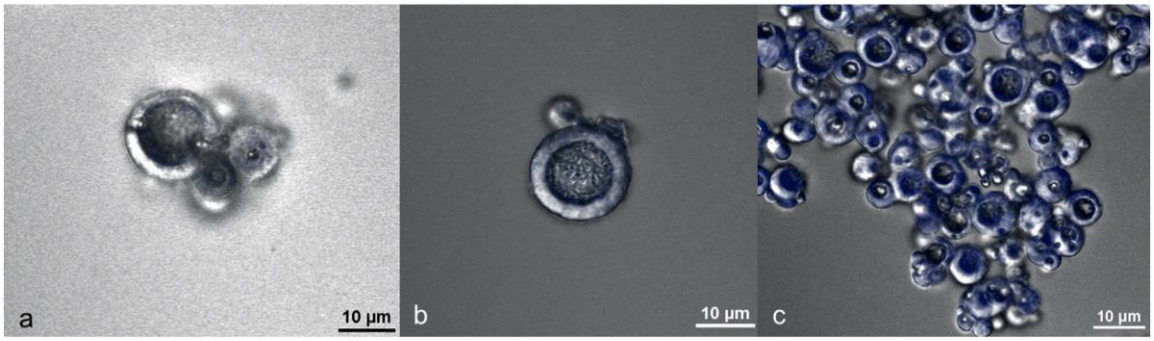


**Figure 4.3.** Confocal fluorescence microscopy z-series scanning images of the essential oil-loaded hollow solid lipid micro- and nanoparticles obtained at varying initial essential oil concentrations (v/v): (a) 10%, (b) 20%, and (c) 50%.

### 4.4.3. Particle size and size distribution

Particles obtained at all initial essential oil concentrations exhibited a bimodal size distribution (Fig. 4.4). Powder solid lipid particles consisted of both nanoparticles

and microparticles. The smallest particles were obtained at 5% initial essential oil concentration ($d_{10\%}$= 0.0809 µm, $d_{50\%}$= 6.06 µm, and $d_{90\%}$= 13.1 µm). Ten percent ($d_{10\%}$), fifty percent ($d_{50\%}$) and ninety percent ($d_{90\%}$) of the particles formed at 50% initial essential oil concentration were smaller than 0.0811 µm, 7.24 µm, and 18.3 µm, respectively. During particle formation, essential oil exerted pressure from inside of the liquid lipid bubble in addition to $CO_2$ and expanded the bubble. At lower essential oil concentration, there was lower force acting from inside of the lipid bubble which resulted in smaller particles.

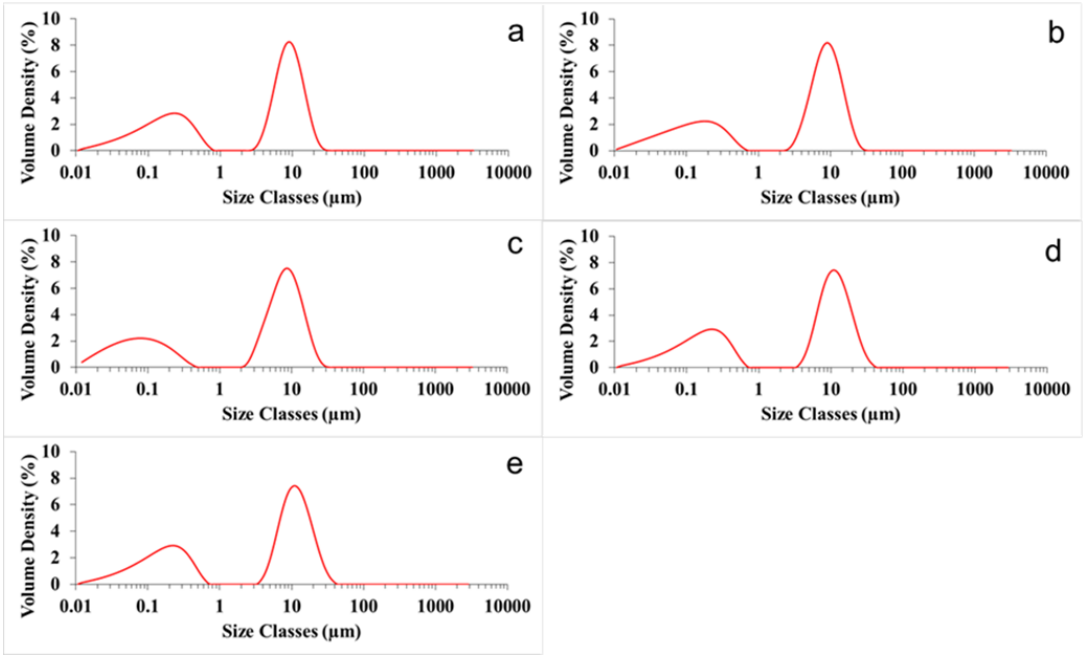


**Figure 4.4.** Particle size and size distribution of the essential oil-loaded hollow solid lipid micro- and nanoparticles obtained at varying initial essential oil concentrations: (a) 5%, (b) 7%, (c) 10%, (d) 20%, and (e) 50%.

The particle size and size distribution were similar among the particles obtained at all initial essential oil concentrations; however, the size of the essential oil-loaded lipid

particles increased compared to empty particles ($d_{10\%}$= 0.0357 µm, $d_{50\%}$= 0.278 µm, $d_{90\%}$= 11.2 µm). It should be noted that the particle size results may be affected by the agglomeration of the particles; therefore, it must be compared with the SEM analyses. When SEM images of the empty and loaded particles were compared, it was observed that the particles agglomerated due to the presence of smaller amounts of essential oil on the particle surface which made the particles sticky (Fig. 4.5).

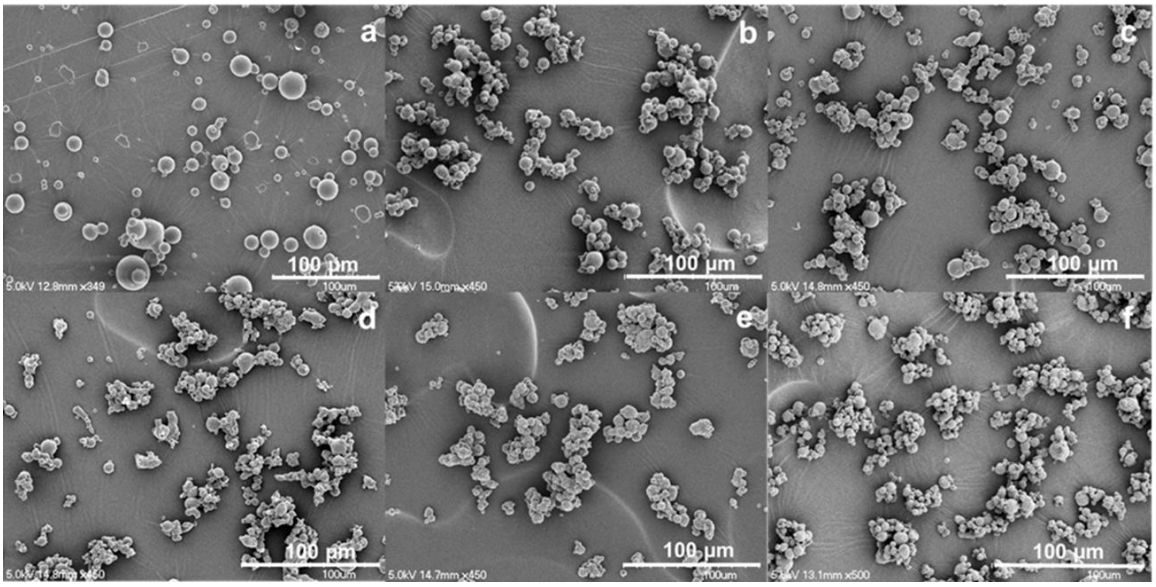


**Figure 4.5.** Scanning electron microscopy (SEM) images of the empty and essential oil-loaded hollow solid lipid micro- and nanoparticles obtained at varying initial essential oil concentrations (v/v): (a) 0, (b) 5%, (c) 7%, (d) 10%, (e) 20%, and (f) 50%.

Previously, Leimann, Gonçalves, Machado, and Bolzan (2009) reported that when the essential oil volume fraction increased from 3.4 to 7.4%, the size distribution tended to be bimodal, particle diameter increased, and particle size distribution became broader during microencapsulation of lemongrass essential oil by simple coacervation. Similarly, Varona et al. (2010) reported that the mean particle size ($d_{50\%}$) of the lavandin oil-loaded

polymer obtained with PGSS increased with increasing encapsulated lavandin oil content ($d_{10\%}$ = 10 µm, $d_{90\%}$= 500 µm). In another study, encapsulation of essential oil using PGSS generated larger garlic essential oil-loaded PEG 6000 particles with a particle size ranging from 71 to 206 µm (Gitin et al., 2011). However, those studies did not report a hollow structure, and the particle sizes were only in the micron range.

### 4.4.4. Melting properties

Melting behavior of the essential oil-loaded solid lipid particles plays an important role in the storage and release properties of the loaded essential oil. Figure 4.6 presents the DSC melting curves of the hollow solid lipid particles loaded with peppermint essential oil. The original FHSO melted between 69.4 °C and 73.1 °C with a single endothermic melting peak at 71.7 °C. Even though the fatty acid composition of the hollow solid lipid particles obtained from FHSO and the original FHSO is the same, the major melting peak of the lipid particles obtained at 5, 7, 10, 20 and 50% initial essential oil concentrations gradually shifted to relatively lower onset melting temperatures compared to the original FHSO, and this trend became more pronounced when initial essential oil concentration was increased to 50%. The major melting peak of the particles with 5% initial essential oil concentration was 70 °C, whereas it was 65 °C for the ones with 50% initial essential oil concentration. In Chapter 3, it was shown that the presence of lower melting peaks at 53 °C for the empty hollow solid lipid particles was due to presence of nanoparticles; however, no pronounced melting peak was observed at 53 °C at the initial essential oil concentrations above 7% in this study. This

was attributed to the agglomeration of the particles at increased initial essential oil concentrations.

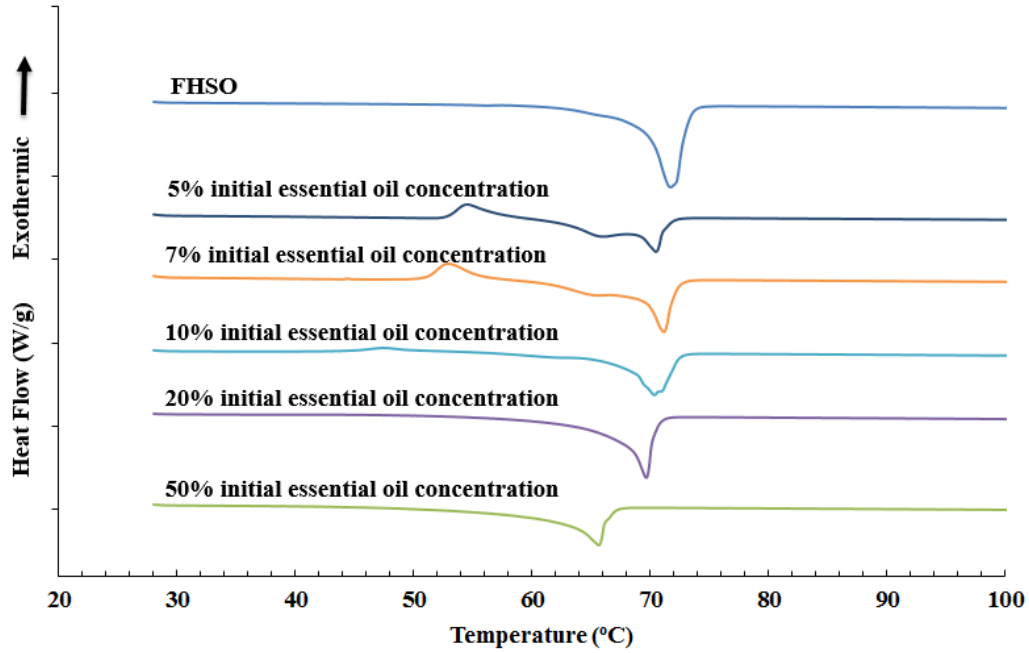


**Figure 4.6.** Differential scanning calorimetry (DSC) melting curves of the essential oil-loaded hollow solid lipid micro- and nanoparticles obtained at varying initial essential oil concentrations.

### 4.4.5. Release profile of the essential oil

Release profile of the essential oil from the lipid particles during storage is presented in Figure 4.7. The results indicated that the release of the loaded essential oil varied with its initial concentration used for particle formation. Although the lipid particles obtained at 5, 10 and 20% initial essential oil concentration had comparable essential oil loading efficiencies, they exhibited different release profiles during storage.

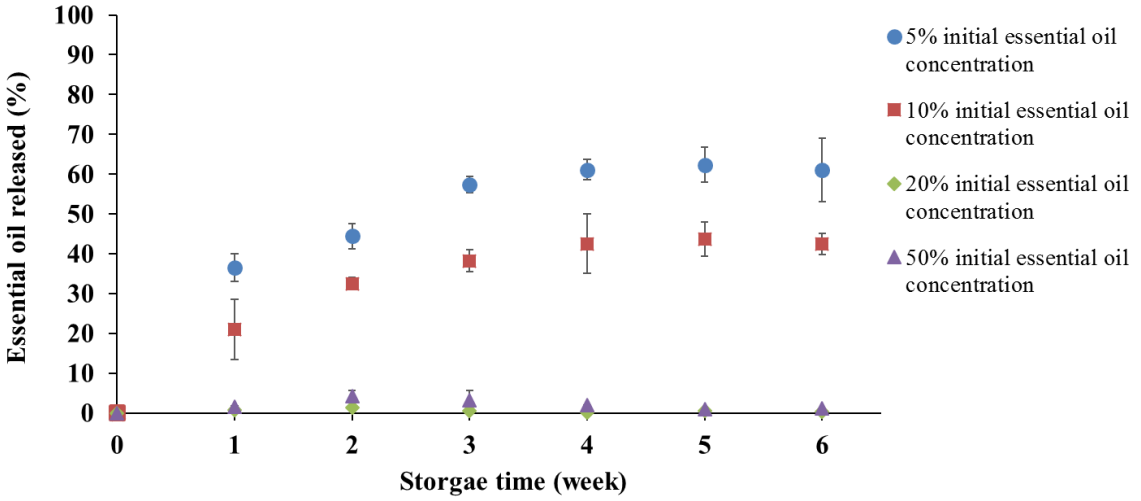


**Figure 4.7.** Release profile of the essential oil from the hollow solid lipid micro- and nanoparticles during 6 weeks of storage at room temperature (22 °C).

Particles obtained at 5 and 10% initial essential oil concentration exhibited higher release of the loaded essential oil than that of the lipid particles obtained at 20 and 50% initial essential oil concentration. The amount of essential oil released at 5, 10, 20 and 50% initial essential oil concentration after 1 week of storage was 36.5, 20.9, 0.7, and 1.6%, respectively. With increasing storage time, the amount of released essential oil increased for the lipid particles obtained at 5 and 10% initial essential oil concentration, whereas stayed almost constant for the particles obtained at 20 and 50% initial essential oil concentration. After 4 weeks of storage, the released essential oil in lipid particles at 5, 10, 20 and 50% initial essential oil concentration reached 61.2, 42.5, 0.2, and 2.0%, respectively, and then stayed constant until week 6. Lower release from the particles obtained at higher initial essential oil concentrations was attributed to the stronger shell of the lipid particles obtained at high initial essential oil concentrations. During particle formation, there was more essential oil in the lipid mixture at higher initial essential oil

concentrations which formed a viscous lipid mixture and in turn formed a stronger lipid shell consisted of FHSO and essential oil compared to particles obtained at lower initial essential oil concentrations. Presence of more essential oil in the lipid shell, observed by confocal fluorescence microscopy, but no release of the essential oil from those particles confirmed this finding. Unchanged morphology of the particles obtained at 20 and 50% initial essential oil concentration during storage also showed that there was no release of the essential oil from those particles at the studied storage conditions (Fig. 4.8). The study of Varona et al. (2010) also suggested the amount of released essential oil mainly related to the initial amount of essential oil in the initial emulsion and the amount of oil in the final product where lavandin essential oil was encapsulated in starch in their study. However, it should be noted that the release profile does not only depend on the initial concentration of the loaded compound but also the encapsulation matrix as observed in this study. In another study, the release of the fragrances from a polymer matrix was dominated by the interaction between the fragrance and polymer matrix rather than vapor pressure and boiling point of the fragrance (Sansukcharearnpon, Wanichwecharungruang, Leepipatpaiboon, Kerdcharoen, & Arayachukeat, 2010).

We also tested the release of the essential oil from the particles obtained at 50% initial essential oil concentration stored at 25 °C after 24 h, which was the condition used for the further determination of antibacterial effect against *Pseudomonas fluorescens*. There was 2.77% essential oil released and was higher than that of the particles stored at room temperature (22 °C) releasing only 2.0% after 4 weeks (Fig. 4.7), which was due to the difference in storage temperature; relatively higher temperature prompted the release.

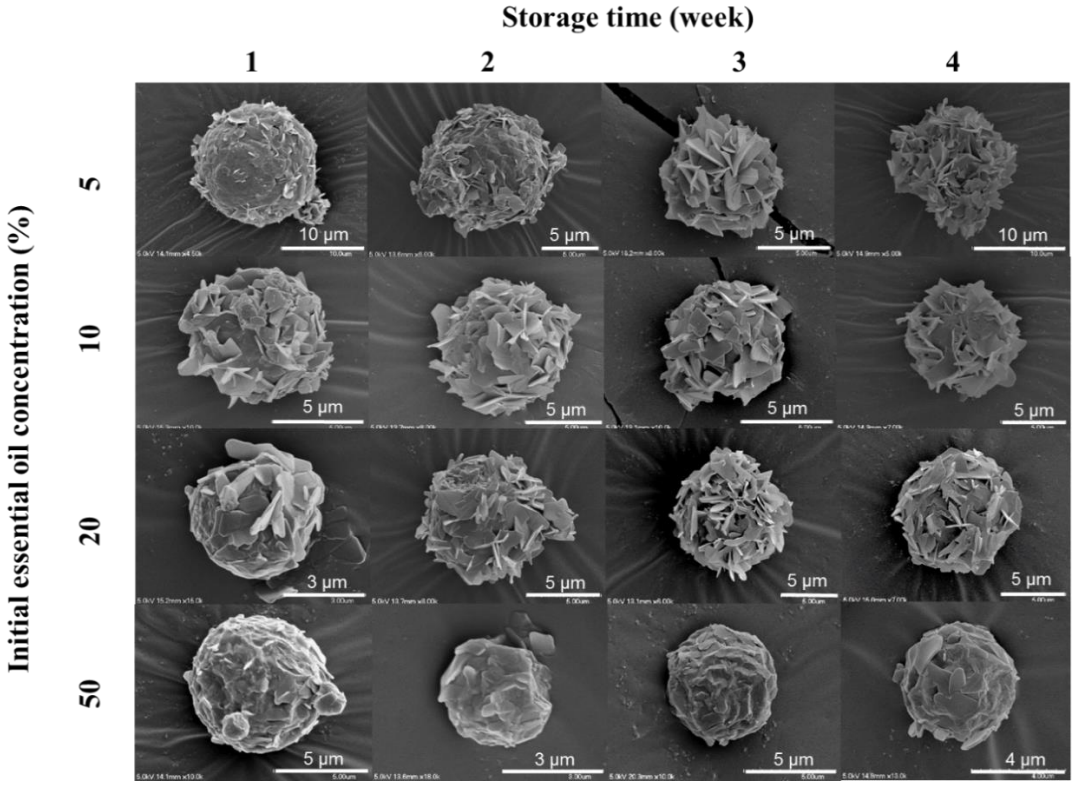


**Figure 4.8.** Scanning electron microscopy (SEM) images of the essential oil-loaded hollow solid lipid micro- and nanoparticles during 4 weeks of storage at room temperature (22 °C).

### 4.4.6. Storage stability of the essential oil-loaded hollow solid lipid micro- and nanoparticles

Storage stability is an important parameter that must be studied for such products intended to be used in food preparations that will be stored. Change in the morphology of the particles loaded with essential oil is one of the most important studies that needs to be conducted. Integrity of the particles is needed to keep the essential oil in the lipid particles. Change in the morphology of the particles will also give information about the release properties of the loaded essential oil. Figure 4.8 presents the change in the morphology of the essential oil-loaded lipid particles over 4 weeks of storage at room

conditions. Morphology of the particles changed at 5% and 10% initial essential oil concentration due to release of the loaded essential oil through the solid lipid shell. Particles with 5 and 10% initial essential oil concentration lost their smooth surface but the particles preserved their spherical shape. The flaky surface structure was due to the evaporation of the essential oil through the solid lipid shell. Even though no major changes in the morphology of the particles obtained at 20 and 50% initial essential oil concentration were observed during storage, the change in the particles with 20% initial essential oil concentration was more pronounced compared to that of 50%. This was due to very low release of the loaded essential oil, which was also supported by the very low release of the essential oil from these particles shown in Figure 4.7. Even though morphology of the individual particle is important to understand the storage stability of the particles in terms of particle morphology, it is also important to understand the behavior of bulk particles. Figure 4.9 presents that the particles that exhibited change in the surface morphology during storage tended to stick to each other and form non-spherical bigger agglomerates. During storage, essential oil released from the particles and formed a sticky surface; therefore, particles agglomerated. However, even though an agglomeration was observed for the particles obtained at 50% initial essential oil concentration, those particles stayed intact and spherical due to very low release of the essential oil.

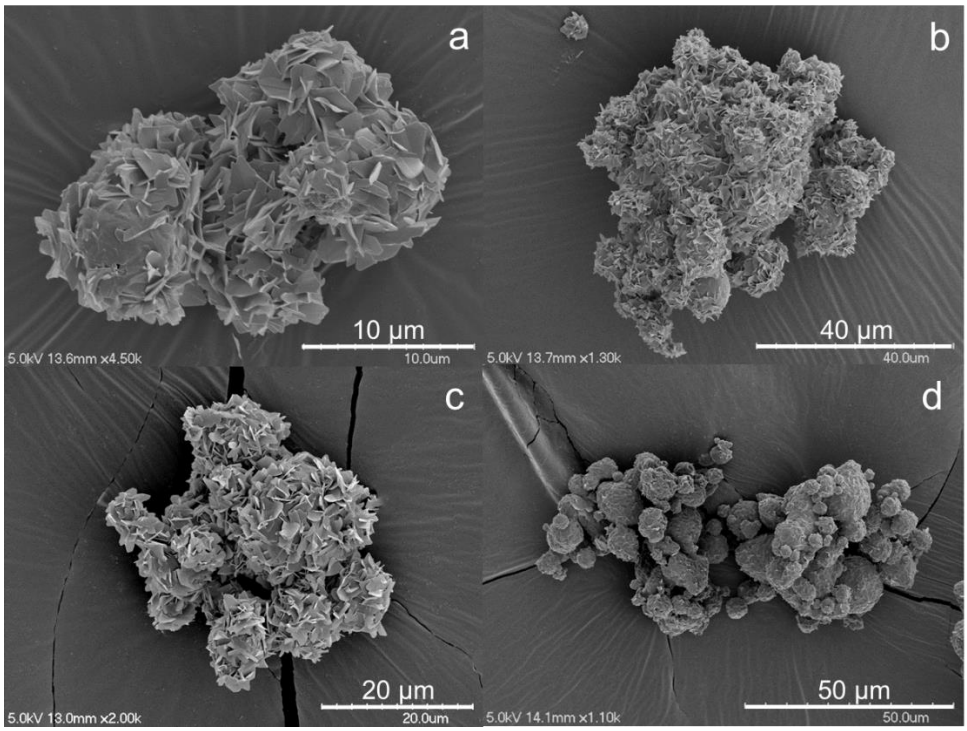


**Figure 4.9.** Scanning electron microscopy (SEM) images of the essential oil-loaded hollow solid lipid micro- and nanoparticles in the third week of the storage at room temperature (22 °C): (a) 5%, (b) 10%, (c) 20%, and (d) 50%.

Change in the morphology of the essential oil-loaded lipid particles was also studied at refrigeration condition, which is another storage temperature for food products in addition to room temperature. It was found that the change in the morphology was greatly affected by the storage temperature. Particles stored at refrigeration temperature (4 °C) did not exhibit the morphological changes observed at room temperature (Fig. 4.10). The surface of the particles obtained at 5% initial essential oil concentration became flaky at room temperature, whereas there was no change in the same particles at refrigeration temperature because of very low release of the essential at low temperature due to lower evaporation of the essential oil.

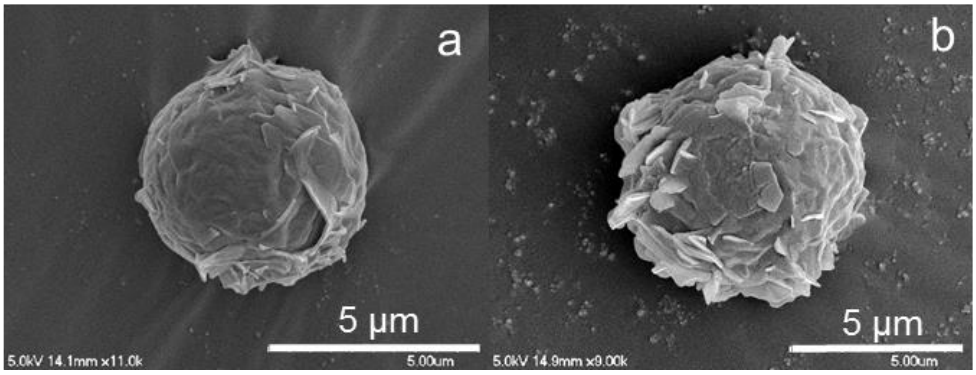


**Figure 4.10.** Scanning electron microscopy (SEM) images of the morphology of the essential oil-loaded hollow solid lipid micro- and nanoparticles stored at 4 °C: (a) particles obtained at 5% initial essential oil concentration stored at 4 °C for 2 months, and (b) particles obtained at 20% initial essential oil concentration stored at 4 °C for 2 months.

Storage stability was also investigated in terms of particle size. Figure 4.11 presents the change in the particle size of the essential oil-loaded particles during storage at room temperature. Particle size increased after 1 week of storage for all particles due to agglomeration caused by the released essential oil. The agglomeration was more pronounced after first week due to more released essential oil. The mean particles size increase during the 6 weeks of storage was from 5.9 to 37.5 µm, 6.0 to 37.1 µm, 7.8 to 32.3 µm, and 6.7 to 32.1 µm for essential oil-loaded lipid particles obtained at 5, 10, 20 and 50% initial essential oil concentration, respectively. This agglomeration was also observed by SEM imaging as mentioned before (Fig. 4.9). It should be noted that the particle size analysis and SEM analysis should be carried out together to understand if the differences in the size are due to agglomeration or broken pieces of the particles. The changes in particle morphology and size could help to explain release profile of the loaded essential oil. The release of the loaded essential oil not only depends on the shell

strength and the amount of essential oil trapped in the particle shell, but also on the particle size; smaller particles have higher surface-to-volume ratio which could result in a greater release of the essential oil (Pedro, Santo, Silva, Detoni, & Albuquerque, 2013). The mean particles size of essential oil-loaded lipid particles was 10.3 µm, 16.4 µm, 22.6 µm and 25.9 µm at 5, 10, 20 and 50% initial essential oil concentration after the first week of storage, respectively. Initial essential oil concentration of 5% produced the smallest particles, whereas 20 and 50% produced the largest particles, and 10% was in between, suggesting that the release of essential oil was easier from the particles with 5 and 10% initial essential oil concentrations, which agreed with the release profile results. Similar agglomeration was observed by Hill, Gomes, and Taylor (2013) for their essential oil-$\beta$-cyclodextrin complexes. In another study, this agglomeration was attributed to the binding of oil together with spheres via capillary forces (Wendt, Brandin, Kilzer, Weidner, & Peterman, 2007).

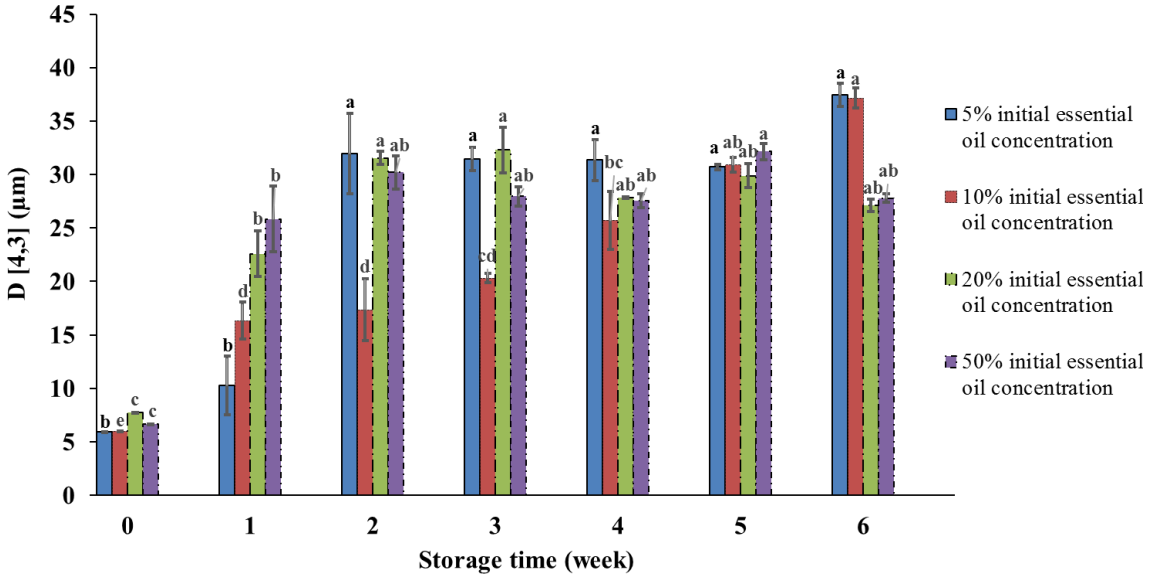


**Figure 4.11.** Mean particle size of the essential oil-loaded hollow solid lipid micro- and nanoparticles stored for 6 weeks at room temperature (22 °C).

### 4.4.7. Antibacterial effect of the essential oil in lipid particles on *Pseudomonas fluorescens*

The antibacterial activity of the essential oil in both lipid particles obtained at 50% initial essential oil concentration and free formulation tested against Gram-negative strain *Pseudomonas fluorescens* is presented in Fig. 4.12. It is more difficult to treat Gram-negative bacteria than Gram-positive bacteria due to the presence of an outer membrane, porin channels, antibiotics resistance, and both exotoxins and endotoxins. Therefore, *Pseudomonas fluorescens*, one of the major food spoilage Gram-negative bacteria, was selected in this study. The concentration of the essential oil in both loaded and free form was set at 10 mg/mL. This concentration was chosen to have sensitivity to detect differences of antibacterial activity among the samples, along with the fact that higher concentrations of essential oil lead to strong inhibition effect, and therefore, the

same result could be obtained with all formulations studied. *Pseudomonas fluorescens* tested in this study demonstrated some degrees of sensitivity of free and loaded essential oil. Both free essential oil and loaded essential oil in lipid particles exhibited interesting antibacterial activity against *Pseudomonas fluorescens* after 24 h of incubation in TSB medium at 25 °C. Moreover, loading of the essential oil in the hollow solid lipid micro- and nanoparticles significantly improved the efficiency of antibacterial activity of essential oil. It showed 3 log decrease in the bacterial growth compared to the empty particles and negative control, and achieved the maximal log inhibition of 75%. However, the inhibition caused by the free essential oil was significantly lower than the inhibition caused by the same concentration of loaded essential oil in lipid particles ($p<0.05$). Only 2 log decrease in the bacterial growth and 50% log inhibition was observed for the free essential oil treatment. The improvement in efficiency against bacterial growth of the essential oil in lipid particles could be due to the increment of the active compounds given by a decrease of the other ingredients, which may have a low volatile point (Arana-Sánchez et al., 2010). This improvement could also be related to the increased solubility of the oil in water, improving the stabilization and bioavailability of the guest molecule in broth mixture (Polyakov, Leshina, Konovalova, Hand, & Kispert, 2004). Consequently, the physical, chemical and biological properties of the loaded molecules were modified (Mourtzinos, Kalogeropoulos, Papadakis, Konstantinou, & Karathanos, 2008), enabling the loaded essential oil to achieve a controlled release with higher potency. Previously, Varona et al. (2013) evaluated the antimicrobial activity of encapsulated lavandin essential oil particles using PGSS, PGSS-drying, and spray-drying against three pathogenic bacteria. They reported that lavandin oil antibacterial activity

could be enhanced by encapsulation since it provided the protection and controlled release of the oil.

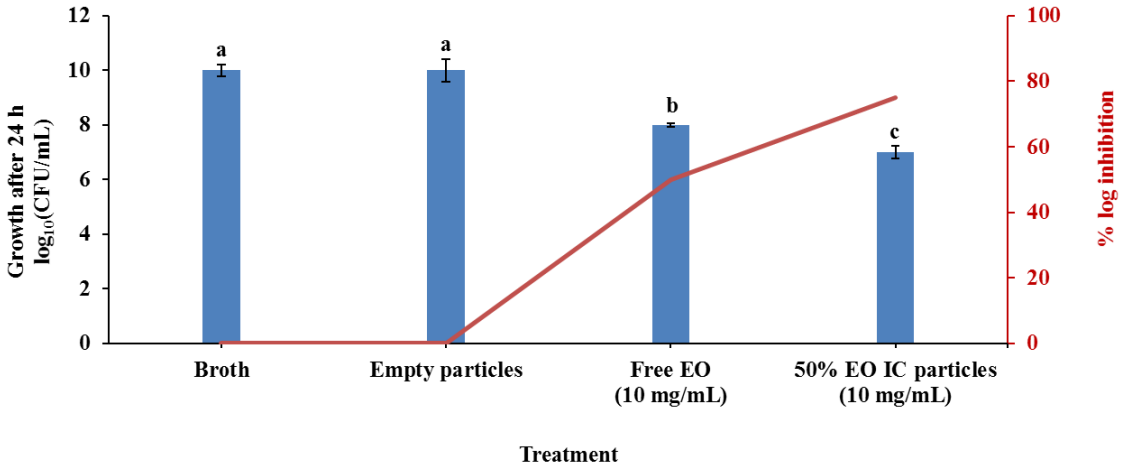


**Figure 4.12.** Antibacterial inhibitory effect of essential oil-loaded hollow solid lipid particles of 50% initial concentration at 10 mg/mL content.

### 4.5. Conclusions

Peppermint essential oil-loaded hollow solid lipid micro- and nanoparticles were successfully formed from FHSO by a novel process based on atomization of the $CO_2$-expanded lipid mixture. The study generated important information on the essential oil-loaded hollow solid lipid micro- and nanoparticle formation, storage stability of the loaded particles, and the release properties of the essential oil from particles. The highest loading efficiency (47.5%) was obtained at 50% initial essential oil concentration. Storage stability studies showed that the release properties of the loaded essential oil depended on the initial essential oil concentration, which affected the physical strength of the solid lipid shell. During the 6 weeks of storage time at room temperature (22 °C), particles generated at 5 and 10% initial essential oil concentration released 61.0 and

42.5% of the loaded essential oil. Process could form spherical intact particles loaded with essential oil at all studied conditions. Another unique advantage of the process is our control over the shell thickness of the particles by changing the process pressure; thicker shells can be obtained at lower pressures.

This innovative process to encapsulate essential oil in solid lipids under mild, simple, and clean processing conditions allowed us to slow down the release of the essential oil and minimize the strong smell that will be important for their use as natural antimicrobials in foods. Study showed that the hollow solid lipid micro- and nanoparticles are promising novel "natural" carrier systems for various bioactives. Nano size allows us to prepare transparent beverages that contain lipophilic bioactives, which is a challenge in food industry. The novel hollow solid lipid micro- and nanoparticles are alternatives to the SLN, and overcome the issues associated with the SLN. The solid lipid shell provides protection for the loaded compound while the hollow structure increases the loading capacities. The dry free-flowing products also make the handling and storage more convenient, and the simple and clean process makes the scaling up more feasible. There is a growing demand for foods prepared using "natural" ingredients and therefore food industry is in a constant search for "natural" food grade antimicrobials to eliminate the artificial preservatives from foods. Developed peppermint essential oil-loaded hollow solid lipid particles have the potential to be used as "natural" food antimicrobials. Using a "clean" process is another advantage for food industry.

## 4.6. References

Arana-Sánchez, A., Estarrón-Espinosa, M., Obledo-Vázquez, E. N., Padilla-Camberos, E., Silva-Vázquez, R., & Lugo-Cervantes, E. (2010). Antimicrobial and antioxidant activities of Mexican oregano essential oils (*Lippia graveolens* H. B. K.) with different composition when microencapsulated in β-cyclodextrin. *Letters in Applied Microbiology, 50,* 585-590.

Ciftci, O. N., & Temelli, F. (2011). Continuous production of fatty acid methyl esters from corn oil in a supercritical carbon dioxide bioreactor. *Journal of Supercritical Fluids, 58,* 79-87.

Davis, S. S. (2004). Coming of age of lipid-based drug delivery systems. *Advanced Drug Delivery Reviews, 56,* 1241-1242.

Gitin, L., Varona, S., & Alonso, M. J. C. (2011). Encapsulation of garlic essential oil by batch PGSS process. *Innovative Romanian Food Biotechnology, 9,* 60-67.

Heurtault, B., Saulnier, P., Pech, B., Proust, J. E., & Benoit, J. P. (2003). Physico-chemical stability of colloidal lipid particles. *Biomaterials, 24,* 4283-4300.

Hill, L. E., Gomes, C., & Taylor, T. M. (2013). Characterization of beta-cyclodextrin inclusion complexes containing essential oils (trans-cinnamaldehyde, eugenol, cinnamon bark, and clove bud extracts) for antimicrobial delivery applications. *LWT - Food Science and Technology, 51,* 86-93.

Leimann, F. V., Gonçalves, O. H., Machado, R. A. F., & Bolzan, A. (2009). Antimicrobial activity of microencapsulated lemon grass essential oil and the effect of experimental parameters on microcapsules size and morphology. *Materials Science and Engineering: C, 29,* 430-436.

Mourtzinos, I., Kalogeropoulos, N., Papadakis, S. E., Konstantinou, K., & Karathanos, V. T. (2008). Encapsulation of nutraceutical monoterpenes in β-cyclodextrin and modified starch. *Journal of Food Science, 73,* 89-94.

Mu, L., & Feng, S. S. (2003). A novel controlled release formulation for the anticancer drug paclitaxel (Taxol): PLGA nanoparticles containing vitamin E TPGS. *Journal of Controlled Release, 86,* 33-48.

Mukherjee, S., Ray, S., & Thakur, R. S. (2009). Solid lipid nanoparticles: a modern formulation approach in drug delivery system. *Indian Journal of Pharmaceutical Sciences, 71,* 349-358.

Müller, R. H., Radtke, M., & Wissing, S. A. (2002). Solid lipid nanoparticles (SLN) and nanostructured lipid carriers (NLC) in cosmetic and dermatological preparations. *Advanced Drug Delivery Review, 54,* S131-S155.

Pedro, A. S., Santo, I. E., Silva, C. V., Detoni, C., & Albuquerque, E. (2013). The use of nanotechnology as an approach for essential oil-based formulations with antimicrobial activity. In A. Méndez-Vilas (Ed.), *Microbial pathogens and strategies*

*for combating them: science, technology and education* (pp. 1364-1374). Badajoz, Spain: Formatex Research Center.

Pettit, R. K., Weber, C. A., Kean, M. J., Hoffmann, H., Pettit, G. R., Tan, R., Franks, K. S., & Horton, M. L. (2005). Microplate alamar blue assay for *Staphylococcus epidermidis* biofilm susceptibility testing. *Antimicrobial Agents and Chemotherapy,* 2612-2617.

Polyakov, N. E., Leshina, T. V., Konovalova, T. A., Hand, E. O., & Kispert, L. D. (2004) Inclusion complexes of carotenoids with cyclodextrins: $^{1}$H NMR, EPR, and optical studies. *Free Radical Biology & Medicine, 36,* 872-880.

Sampaio de Sousa, A. R., Simplício, A. L., De Sousa, H. C., & Duarte, C. M. M. (2007). Preparation of glyceryl monostearate-basedparticles by PGSS - Application to caffeine. *Journal of Supercritical Fluids, 43,* 120-125.

Sansukcharearnpon, A., Wanichwecharungruang, S., Leepipatpaiboon, N., Kerdcharoen, T., & Arayachukeat, S. (2010). High loading fragrance encapsulation based on a polymer-blend: Preparation and release behavior. *International Journal of Pharmaceutics, 391,* 267-273.

Scalia, S., Young, P. M., & Traini, D. (2015). Solid lipid microparticles as an approach to drug delivery. *Expert Opinion on Drug Delivery, 12,* 583-599.

Severino, P., Andreani, T., Macedo, A. S., Fangueiro, J. F., Santana, M. H. A., Silva, A. M., & Souto, E. B. (2012). Current state-of-art and new trends on lipid nanoparticles (SLN and NLC) for oral drug delivery. *Journal of Drug Delivery, 10,* 1-10.

Varona, S., Kareth, S., Martín, Á., & Cocero, M. J. (2010). Formulation of lavandin essential oil with biopolymers by PGSS for application as biocide in ecological agriculture. *Journal of Supercritical Fluids, 54,* 369-377.

Varona, S., Rojo, S. R., Martín, Á., Cocero, M. J., Serra, A. T., Crespo, T., & Duarte, C. M. M. (2013). Antimicrobial activity of lavandin essential oil formulations against three pathogenic food-borne bacteria. *Industrial Crops and Products, 42,* 243-250.

Wendt, T., Brandin, G., Kilzer, A., Weidner, E., & Peterman, M. (2007). Generation of fluid-filled micro particles using PGSS technology. In: *Proceedings of European Congress of Chemical Engineering (ECCE6).* Kongens Lyngby, Denmark: Technical University of Denmark.

# CHAPTER 5. SUMMARY, CONCLUSIONS AND RECOMMENDATIONS

## 5.1. Summary and conclusions

This thesis has reported that hollow solid lipid micro- and nanoparticles from FHSO can be used as promising bioactive-carriers using a green method based on atomization of $CO_2$-expanded lipids. Obtained hollow solid lipid particles were both in micro- and nanosize, with high loading capacity, minimized or no bioactive expelling, and provided bioactive protection and controlled release.

In Chapter 3, it has been found that pressure and nozzle diameter affected the particle morphology negatively. Shell thickness of the particles decreased with increasing pressure. Optimal processing condition was selected at 50 μm nozzle diameter and 200 bar expansion pressure, based on the particle morphology and size and distribution with the preference of intact spherical smaller particles. Fifty percent of the particles obtained under optimal condition was smaller than 278 nm. The major polymorphic form of the particles changed from β to α with decreasing pressure and nozzle diameter, with particles generated from 50 μm nozzle diameter had only α form. Decreasing particle size to nanosize broadened the melting range and shifted the melting to lower onset temperatures.

In Chapter 4, essential oil was successfully loaded in the hollow solid lipid micro- and nanoparticles at optimal particle formation conditions obtained in Chapter 3. The highest loading efficiency of 47.5% was achieved at 50% initial essential oil concentration. Initial essential oil concentration affected the particle morphology negatively. Loaded essential oil in the particles obtained at 5 and 10% initial essential oil

concentration released more than that of the particles obtained at 20 and 50% counterparts after four weeks of storage at room temperature, achieved 61.2, 42.5, 0.2, and 2.0%, respectively. Moreover, the particles obtained at 50% initial essential oil concentration showed significant antibacterial activity against *Pseudomonas fluorescens* than free essential oil, with 3 log decrease in bacterial growth after 24 h of incubation. The study suggested that the essential oil-loaded hollow solid lipid micro- and nanoparticles obtained by this simple and clean process can be used as food grade antibacterials.

The hollow structure can increase the loading capacity significantly compared to SLN, and solve the bioactive expelling problem of the SLN. This study explored hollow solid lipid micro- and nanoparticles for food applications, and introduced a novel production method with several advantages: 1) simple, energy efficient, and easy to scale-up process; 2) green technology (i.e., no organic solvent was used and no waste generated); 3) no degradation of bioactives due to mild processing temperature and absence of oxygen; 4) can generate a variety of bioactive-loaded hollow solid lipid micro- and nanoparticles to deliver omega-3 fatty acids, carotenoids, phytosterols and natural antioxidants; 6) particles can be added directly to clear liquids without affecting clarity; and 7) particles are free flowing dry powder which makes handling, transportation, and storage convenient.

## 5.2. Recommendations

Understanding the effect of triacylglycerol structure and distribution of fatty acids on the glycerol backbone on the melting and volumetric expansion of the solid lipids is

critical to obtain particles from a number of solid lipids and to better understanding the particle formation mechanism. In this thesis, we selected fully hydrogenated soybean oil as the model solid lipid to construct the hollow solid lipid micro- and nanoparticles as the bioactive-carrier. In the future planning, different solid lipid matrix should be studied to further optimize the physicochemical properties of the lipid particles, for example, release properties, solubility, and stability. Modifying the lipid shell my using mixtures of mono-, di-, and triacylglycerols to create imperfections in the lipid shell to control the release of the bioactive will help create particles designed for controlled release.

Even though we proposed a mechanism for the hollow particle formation in this process, it will be useful to use computational fluid dynamics to simulate the particle formation and temperature changes during atomization. In this thesis, it has been found that pressure and sudden cooling during atomization determine the particle size and shell thickness; however, such a simulation will help us better understand the effect of process parameters on particle size and morphology.

Another future research that should be conducted to further complete the study is the investigation of performance of the bioactive-loaded particles in real food systems, and the *in vitro* and *in vivo* bioavailability of the loaded bioactives in the hollow solid lipid micro- and nanoparticle. We should be able to know if the loaded bioactives can withstand processing, be released from the food matrix after digestion and be bioaccessible in the GI tract, undergo metabolism and reach the blood serum for action to exert health benefits. Using the particles in selected food formulations and investigating the effect of the particles on the quality and sensory properties of the end products will help us determine specific food applications.